Catalytic Hydrogenation and Dehydrogenation of Heterocyclic Compounds through sp^3-C–H Bond Activation

触媒的 sp^3-C–H 結合活性化によるヘテロ芳香族化合物の水素化と脱水素化反応

Deliang Zhang

2021

Contents

General Introduction

1. Traditional Methods for the Functionalization of Heterocycles

Heterocycles widely exist in bioactive natural products and pharmaceutical compounds (Figure 1). The development of efficient methods that enable rapid functionalization of *N*-adjacent C–H bonds in these heterocycles is very attractive from the standpoint of drug discovery. The most conventional method for the direct functionalization of *N*-heterocycles is α-lithiation with alkyllithium/diamine complexes, producing a dipole-stabilized carbanion, followed by electrophilic substitution (Scheme 1a) but the stoichiometric strong base was required for deprotonation of heterocycles and limited electrophiles were utilized in this method.[1] Recently, photoredox catalysis has emerged as a powerful tool for the functionalization of heterocycles. Under irradiation of visible light, amino radical cations were generated and subsequent H-atom abstraction or deprotonation followed by oxidation provided the electrophilic iminium ion intermediates (Scheme 1b).[2] The usefulness of this method is highlighted by the compatibility of a broad range of nucleophiles resulting in functionally diverse products, while the asymmetric version has not been well-established.

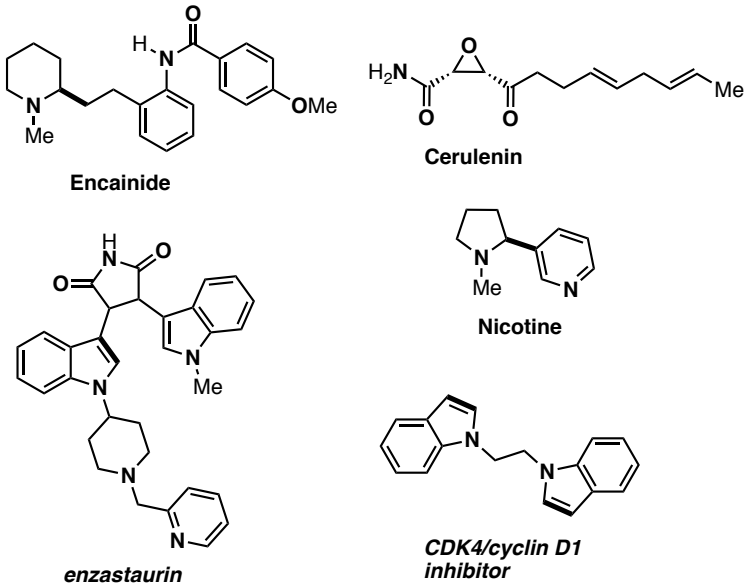

Figure 1. Some Biologically Significant Compounds Containing Heterocycles

Scheme 1. Traditional Methods for the Functionalization of Heterocycles

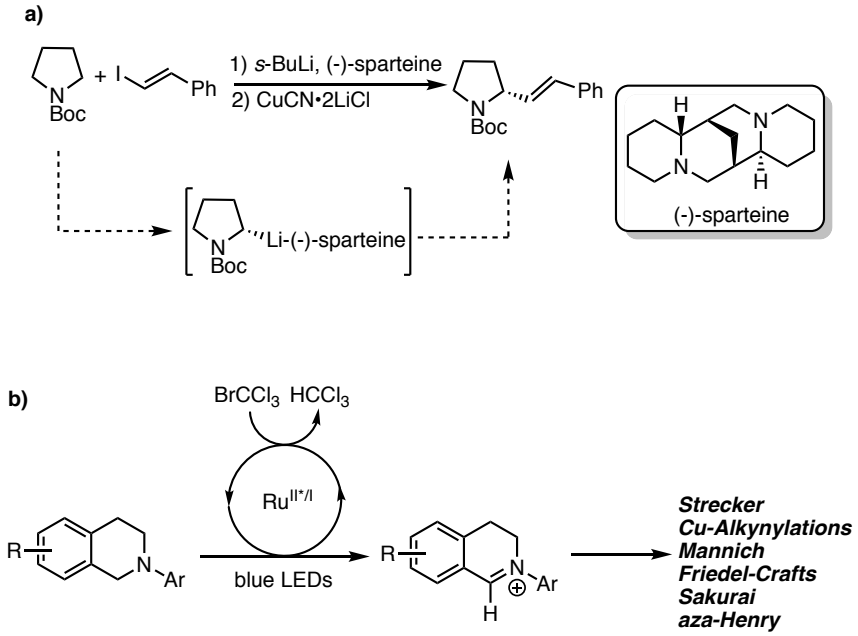

2. Transition Metal-Catalyzed α-C(sp^3)–H Bond Activation of Heterocycles

2.1 Introduction

Transition metal-catalyzed α-C(sp^3)–H bond activation of heterocycles has drawn much attention owing to its high efficiency and straightforwardness. This introduction outlines three sections, each describing a different strategy for the functionalization of heterocycles – the use of pincer ligands for the dehydrogenation of heterocycles to produce heteroarenes (section 1.2), α-C(sp^3)–H functionalization of heterocycles in the presence of directing groups (section 1.3), metal-catalyzed carbene insertions (section 1.4) .

Scheme 2. The Selective Strategies for the Functionalization of Heterocycles

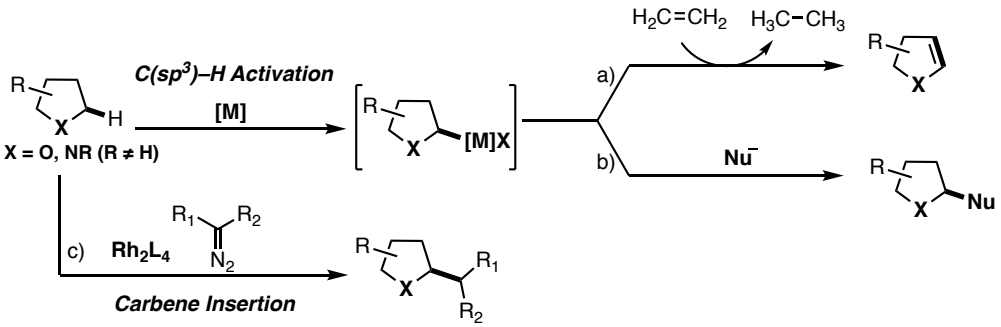

2.2 Use of Pincer Ligands for the Dehydrogenation of Heterocycles to Produce Heteroarenes

The selective dehydrogenation of inexpensive and abundant alkanes to produce higher value alkenes is an important task. Since the initial reports of alkane dehydrogenation by Grabtree and Felkin (Scheme 3),[3] numerous homogeneous alkane dehydrogenation catalysts have been developed allowing dehydrogenation under milder conditions (150–250 °C).[4] However, little work has been extended to heterocycles. In 2014, Huang group reported a new phosphinothious/phosphinite (*i*Pr$_4$PSCOP)Ir pincer complex. Upon activation with NaO*t*Bu, this complex exhibited exceptionally high activity for transfer dehydrogenation of alkanes with *tert*-butylethylene as a hydrogen acceptor. In addition, new catalytic systems were applied to the selective dehydrogenation of a wide variety of heterocycles to produce heteroarenes (Scheme 4).[5]

Scheme 3. Examples of Active Iridium Pincer Complexes for Alkane Dehydrogenation

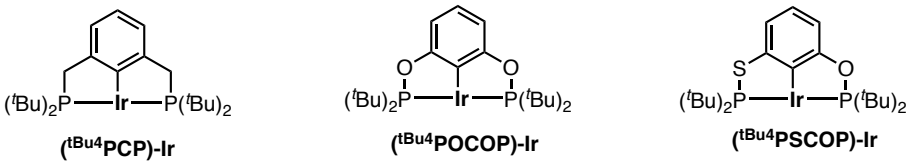

Scheme 4. Iridium Pincer-Catalyzed Dehydrogenation of *N*- and *O*-containing Heterocycles

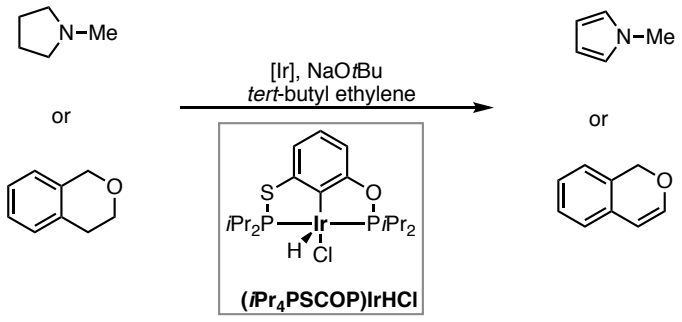

In 2015, Brookhart group reported a novel iridium pincer catalyst for the dehydrogenation of ethers using *tert*-butyl ethylene as a hydrogen acceptor. At 120 °C, cyclic ethers were dehydrogenated with high turnover numbers (over 400 in many

cases).[6] Acyclic ethers such as diethyl ether can also be dehydrogenated catalytically with TONs up to 90. The efficient dehydrogenation of cyclic and acyclic ethers using *tert*-butyl ethylene as a practical hydrogen acceptor has been demonstrated for the first time (Scheme 5).

Scheme 5. Iridium Pincer-Catalyzed Dehydrogenation of Ethers

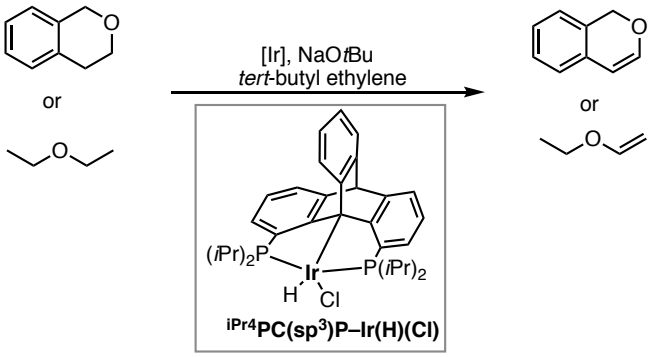

2.3 α-C(sp^3)–H Functionalization of Heterocycles in the Presence of Directing Groups

Murai has contributed extensively to the general area of transition metal-catalyzed C–H activation, and in 1997, first reported the rhodium-catalyzed carbonylation of *N*-(2-pyridinyl)piperazine via sp^3 C–H bond activation to produce desired product (Scheme 6).[7] Several factors were found to be critical to the success of the reaction. First, the 1,4-relationship of the amines in the piperazine core was essential for the reaction to proceed. Second, the reaction was strongly influenced by electronic perturbation of the substituents at both nitrogen termini: electronic donating groups were favored at the distal piperazine nitrogen, instead, electron-withdrawing groups on the pyridine improved reactivity. In addition, Murai and co-workers have also accomplished the same transformation on *N*-acylpiperazines, suggesting that other directing groups are also applicable for this reaction.

Mechanistic investigations revealed that ethylene was crucial for the conversion of **A** to the unsaturated tetrahydropyrazine **D**, which suggested that the process involved two steps: (a) Rh-catalyzed, pyridine-directed dehydrogenation of the piperazine via sp^3 C–H activation adjacent to nitrogen to form tetrahydropyrazine **D**, and (b) Rh-catalyzed, pyridine-directed carbonylation of **D** via sp^2 C–H activation adjacent to nitrogen to produce desired product **G** (Scheme 6).

Scheme 6. Rh-Catalyzed Carbonylative Coupling of Piperazines with Olefins

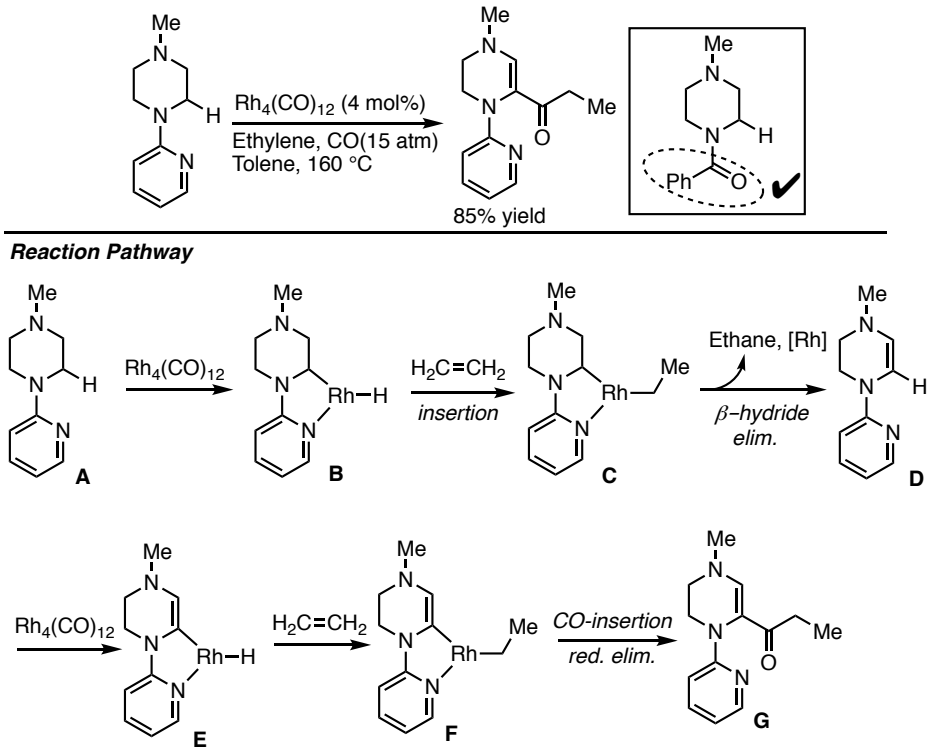

In 2001, Murai and co-workers described a catalytic reaction which involves the cleavage of an sp^3 C–H bond adjacent to a nitrogen atom in *N*-2-pyridynyl alkyamines (Scheme 7).[8] The use of $Ru_3(CO)_{12}$ as the catalyst resulted in the addition of the acyclic and cyclic alkenes to give the coupling products. The presence of directing groups such as pyridine, pyrimidine or an oxazoline ring on the nitrogen of the amine was critical for the reaction. In addition, the substitution of an electron-withdrawing group on the pyridine ring dramatically retards the reaction. Cyclic amines are more reactive than acyclic ones.

Scheme 7. $Ru(CO)_{12}$-Catalyzed $C(sp^3)$–H Functionalization of *N*-Heterocycles

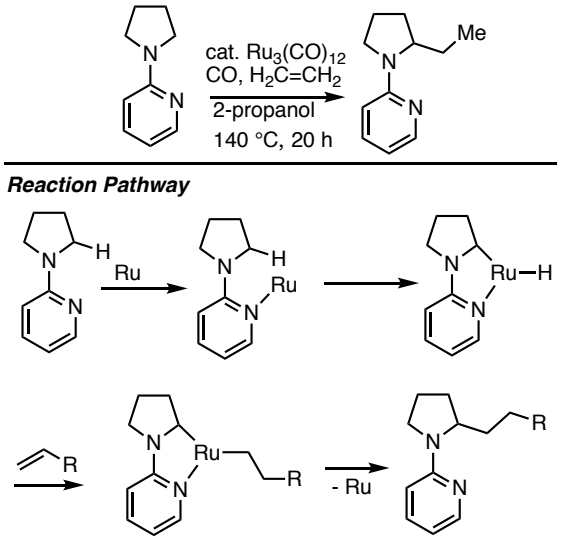

In 2004, Sames and co-workers reported the iridium-catalyzed formation of pyrrolizidinone from *N*-acylated pyrrolidine, which relied on directed sp^3 C–H insertion adjacent to nitrogen followed by intramolecular C–C bond formation with an olefin tether (Scheme 8).[9] Optimization studies of the iridium catalyst revealed that *N,N'*-bis-(2,6-diisopropylphenyl)imidazolyl carbene provided the best yield and selectivity for the 5-*exo* cyclized product over the 6-*endo* cyclized product. Addition of norbornene(NBE) to the reaction as a hydrogen acceptor further increased the yield by minimizing the formation of reduction side product.

Scheme 8. Iridium-Catalyzed $C(sp^3)$–H Functionalization of *N*-Heterocycles

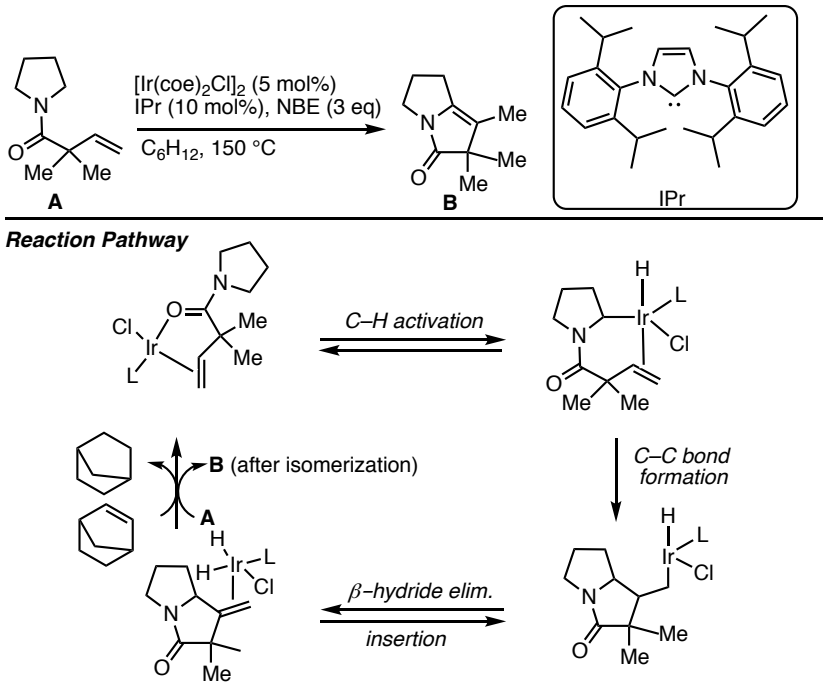

In 2012, Maes group reported a general directed Ru-catalyzed $C(sp^3)$–H α-alkylation protocol for piperidines (less-reactive substrates than the corresponding five-

membered cyclic amines) (Scheme 9).[10] The use of a hindered alcohol (2,4-dimethyl-3-pentanol) as the solvent and catalyst activator, and a catalytic amount of *trans*-1,2-cyclohexanedicarboxylic acid was necessary to achieve a high conversion to product. This protocol allowed to effectively synthesize a number of 2-hexyl- and 2,6-dihexyl piperidines, as well as the alkaloid (±)-solenopsin A. Kinetic studies revealed that the carboxylic acid additive has a significant effect on catalyst initiation, catalyst longevity, and reverses the reaction selectivity compared with the acid-free reaction.

Scheme 9. Ru-Catalyzed C(sp^3)–H Functionalization of *N*-Heterocycles

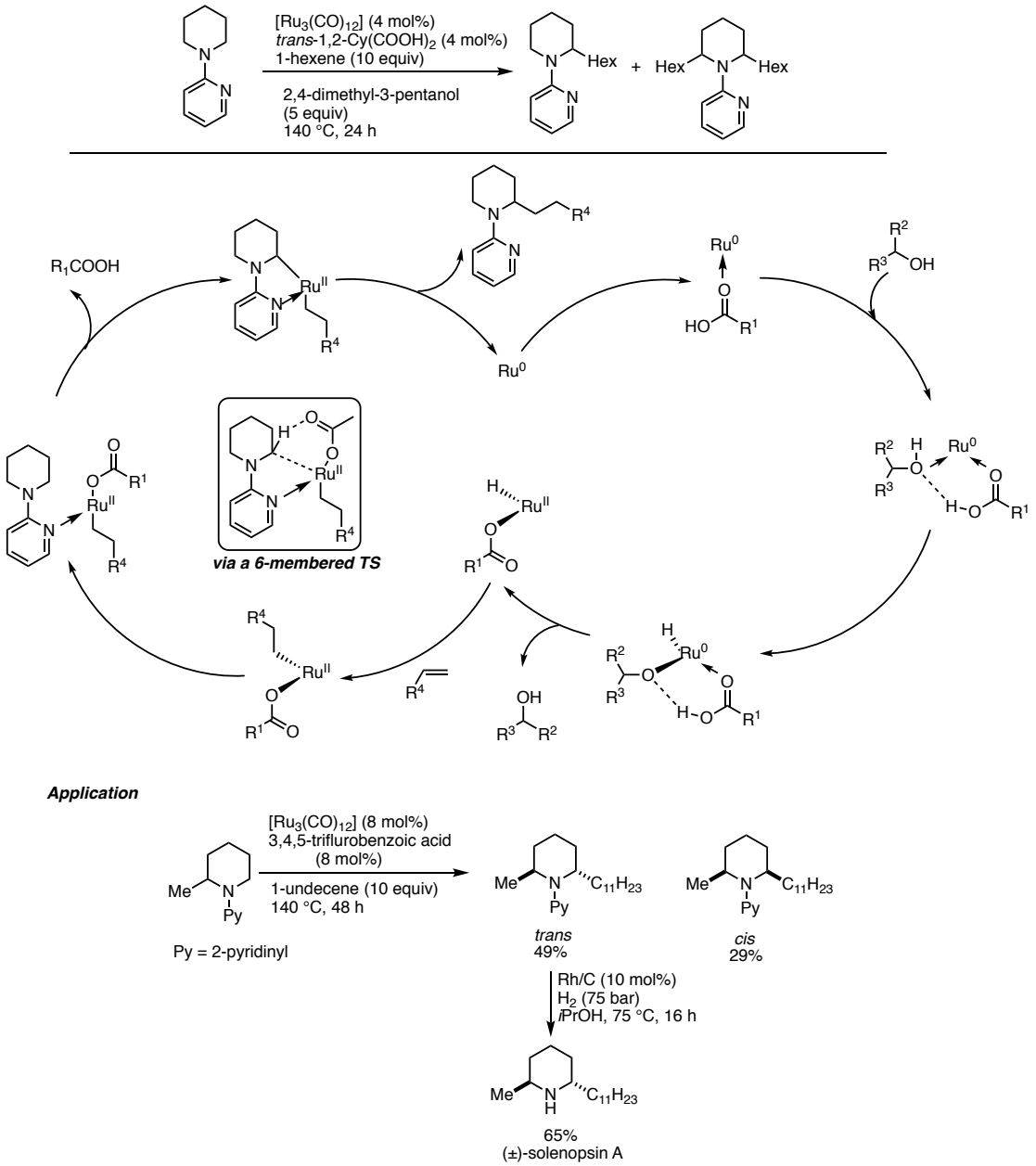

In 2012, Sawamura and co-workers reported a Rh-catalyzed C(sp^3)–H borylation of amides, ureas, and 2-aminopyridine derivatives at the position α to the N atom (*N*-adjacent position) that yields the corresponding α-aminoalkylboronic acid derivatives (Scheme 10).[11] The Rh catalysis occurs under mild conditions in the presence of the silica-supported triaryphosphine ligand Silica-TRIP, which contains an immobilized triptycene-type cage structure with a bridgehead P atom. The α-aminoalkylboronic acid derivatives underwent C−C bond formation reactions, such as Suzuki− Miyaura coupling with an aryl bromide and one-carbon homologation to a β-aminoalkylboronate. This novel transition-metal catalysis with an immobilized phosphine ligand offers a new method for the development of useful molecular transformations through heterogeneous approaches.

Moreover, in 2019, the same group reported a Rh-monophosphite chiral catalytic system that enables a highly efficient enantioselective borylation of *N*-adjacent C(sp^3)−H bonds for a range of substrate classes including 2-(*N*-alkylamino)heteroaryls and *N*-alkanoyl- or aroyl-based secondary or tertiary amides, some of which are pharmaceutical agents or related compounds (Scheme 11).[12] Various stereospecific transformations of the enantioenriched α-aminoboronates, including Suzuki−Miyaura coupling with aryl halides and the Rh-catalyzed reaction with an isocyanate derivative of α-amino acid, affording a new peptide chain elongation method, have been demonstrated. As a highlight of this work, the borylation protocol was successfully applied to the catalyst-controlled site-selective and stereoselective C(sp^3)−H borylation of an unprotected dipeptidic compound, allowing remarkably streamlined synthesis of the anti-cancer drug molecule bortezomib and offering a straightforward route for the synthesis of privileged molecular architectures.

Scheme 10. Rh-Catalyzed C(sp^3)–H Functionalization of *N*-Heterocycles

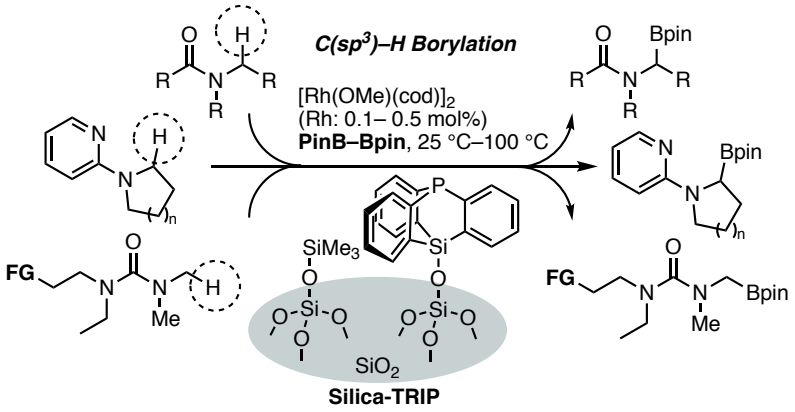

Scheme 11. Rh-Catalyzed Enantioselective C(sp^3)–H Functionalization of *N*-Heterocycles

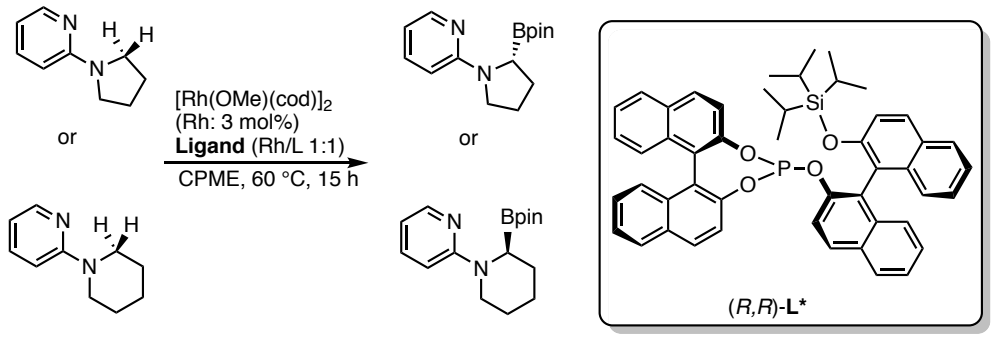

In 2017, Yu group reported an alkoxy-thiocarbonyl directing group for C(sp^3)–H alkylation of saturated azacycles using a cationic iridium(I) catalyst (Scheme 12a).[13] Although the one-step installation and removal of this directing group was advantageous over previous reports employing heterocyclic directing groups, the olefin coupling partner scope was limited to only mono-substituted olefins. In 2020, the same group reported a novel amidoxime directing groups for an iridium(I)-catalyzed α-C(sp^3)–H alkylation of saturated azacycles (Scheme 12b).[14] They observed an unprecedented selectivity for branched C(sp^3)–H alkylation products with ethyl acrylate as the olefin coupling partner. The first step involves the directed α-C−H activation of the pyrrolidine substrate via an oxidative addition mechanism, leading to the formation of a cationic Ir(III) intermediate. Next, a molecule of acrylate may react reversibly with this iridium-hydride species in two different ways–Pathways L and B. In Pathway L, acrylate undergoes a sterically controlled 1,2-migratory insertion into the Ir–H bond, leading to a linear Ir-alkyl species, which upon a C−C reductive elimination gives the linearly α-alkylated product. In Pathway B, acrylate undergoes an electronically controlled 2,1-migratory insertion into the Ir–H bond leading to a branched Ir-alkyl species, which upon a C–C reductive elimination gives the branched α-alkylated product.

Scheme 12. Ir-Catalyzed Enantioselective C(sp^3)–H Functionalization of *N*-Heterocycles

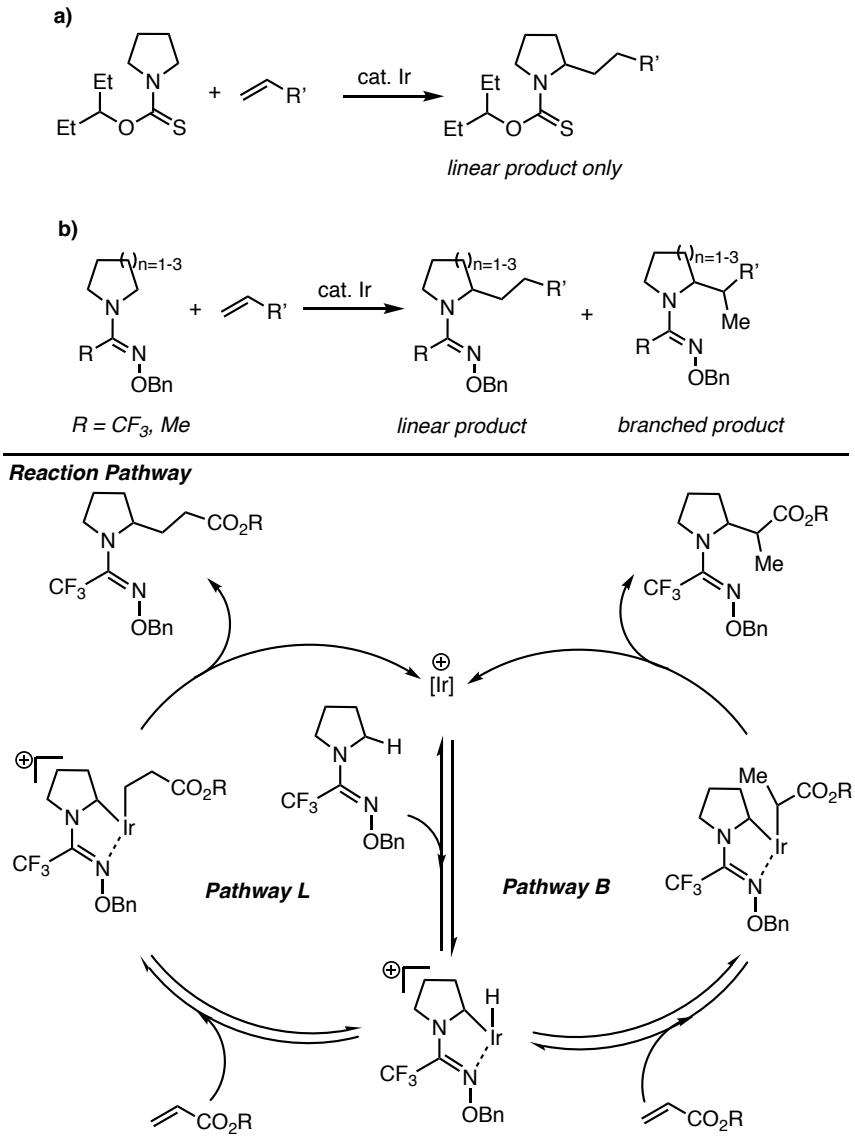

In 2015, Shibata and co-workers have developed an enantioselective Ir-catalyzed sp^3 C–H bond activation of γ-butyrolactam with various alkenes, such as styrene derivatives and electron-deficient olefins.[15] The present reaction provides a new simple protocol for the synthesis of chiral 5-alkylated γ-lactams and 4-alkylated γ-amino acids. Mechanistically, the oxidative addition of the *N*-adjacent methylene C–H bond to the Ir(I) catalyst coordinated to the chiral binaphthyl-based ligand is followed by insertion into olefins or alkynes to give the alkylated or alkenylated products. This strategy was further utilized for the C(sp^3)–H alkylation of butyrolactam to generate enantioenriched γ-lactams that are inherently important in natural products (Scheme 13). As an example,

the alkylated product from acrylate was transformed into the key intermediate in the synthesis of pyrrolam A.

Scheme 13. Ir-Catalyzed Enantioselective Alkylation of *N*-Adjacent C–H Bonds of Heterocycles and Applications

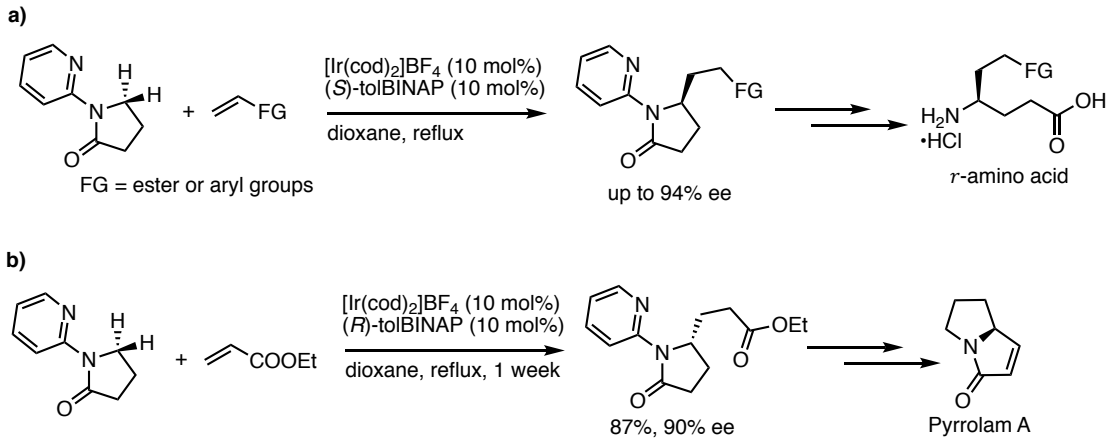

In addition, Yu and co-workers reported a Pd(II)/Pd(0)-catalyzed enantioselective functionalization of thioamines with boronic acids via the activation of C–H bonds in the substrate adjacent to the *N*-atom. This functionalization allowed the synthesis of essential motifs containing ethyl amines, azetidines, pyrrolidines, piperidines, azepanes, indolines and tetrahydroisoquinolines. The use of chiral phosphoric acid ligand demonstrated efficient coupling of activated methylene C–H bonds leading to their differentiation in a chiral environment (Scheme 14).[16]

Scheme 14. Enantioselective α-C(sp^3)–H Functionalization of Thioamines

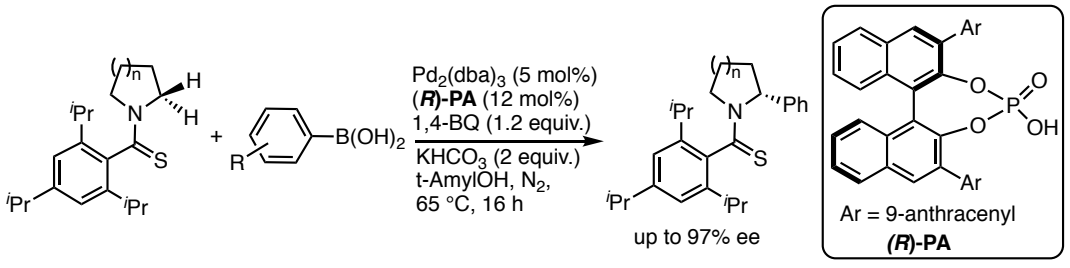

2.4 Metal-Catalyzed C(sp^3)–H Functionalization of Heterocycles via Carbene Insertion

By far the most excellent example of metal-catalyzed sp^3 C–H bond activation adjacent to nitrogen in heterocycles was the intermolecular, asymmetric C–H insertion of aryldiazoacetates into cyclic *N*-Boc-protected amines, which was catalyzed by dirhodium tetraprolinate complexes cat.1–cat.4 (Scheme 15).[17] This powerful method was originally reported by Davies and co-workers for the highly regio-, diastero-, and enantioselective C–H insertion of a range of arydiazoacetetes into *N*-Boc-pyrrolidine catalyzed by chiral dirhodium complex cat.1–4. Application of this method to cyclic amines of various ring sizes showed that the 5, 7, and 8-membered substrates worked very well, delivering C–H insertion products with a high degree of regio-, diastero-, and enantioselectivity.

Scheme 15. C(sp^3)–H Functionalization of Heterocycles via C–H Insertion

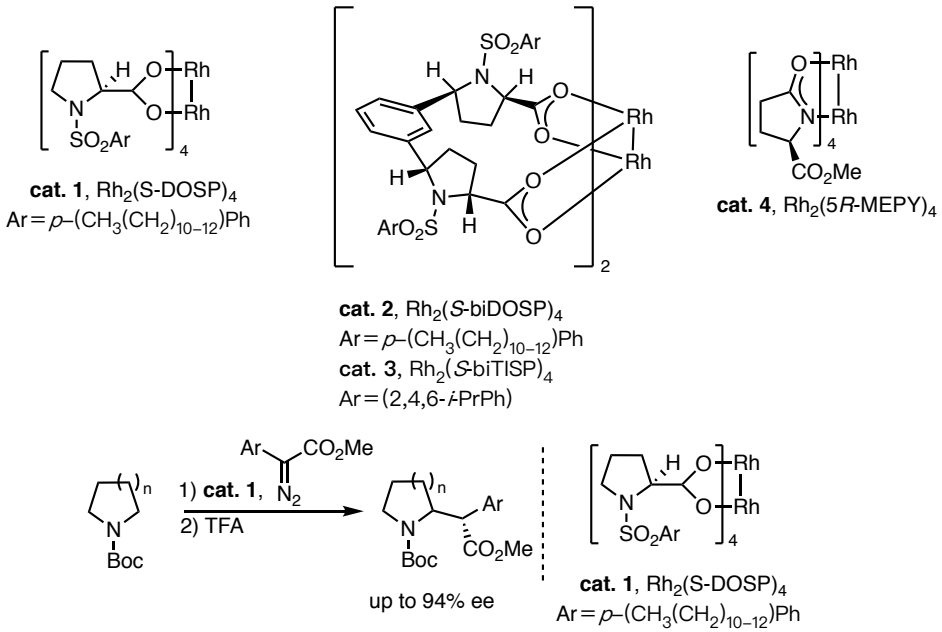

3. Metal (Di)Hydride Species in Organic Reactions

3.1 Introduction

Metal (di)hydride species has a long history, which can be traced to 1930s. Many efforts have been devoted to develop efficient catalysts to produce active and relatively stable metal (di)hydride. A) One strategy is that the metal (di)hydride intermediate could be *in situ* generated via catalyst abstraction from hydrogen donors and then apply it for hydrogenation/dehydrogenation reactions. B) Another strategy is that the prepared

precatalysts containing metal-(di)hydride bonds could be used for the reactions involving hydrogen transfer process.

3.2 Metal (Di)hydride as Intermediate for the Reactions

A typical example is the hydrogenation reaction. Hydrogenation is one of the most fundamental transformations in organic synthesis, and its industrial applications span from fine chemicals to pharmaceuticals synthesis. Direct hydrogenation with a pressure of H_2 gas and transfer hydrogenation (TH) are the two employed strategies for hydrogenation.[18] Simple bischelated ligands such as bisphophines produce ligand-metal-dihydride as the key intermediate, while ligand-metal cooperative catalysts produce hydride-ligand-metal-hydride as the key intermediate. These active intermediates could be used for hydrogenation of unsaturated bonds (Scheme 16).

Scheme 16. Metal (Di)hydride as Intermediate for the Hydrogenation

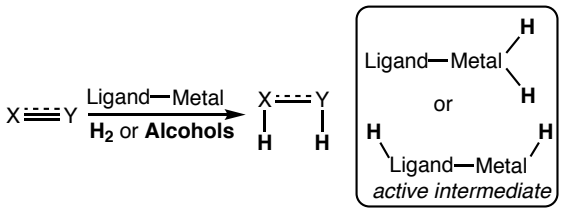

Ligand-modified copper hydride complexes have been well-known for 1,4-reduction reactions. Buchwald group found that these hydride complexes could undergo migratory insertion (hydrocupration) with relatively unactivated and electronically unpolarized olefins, producing alkylcopper intermediates that can be applied for a variety of useful bonds formations such as asymmetric hydroamination (Scheme 17).[19]

Scheme 17. Cu–H Complexes for Hydrofunctionalization Reaction

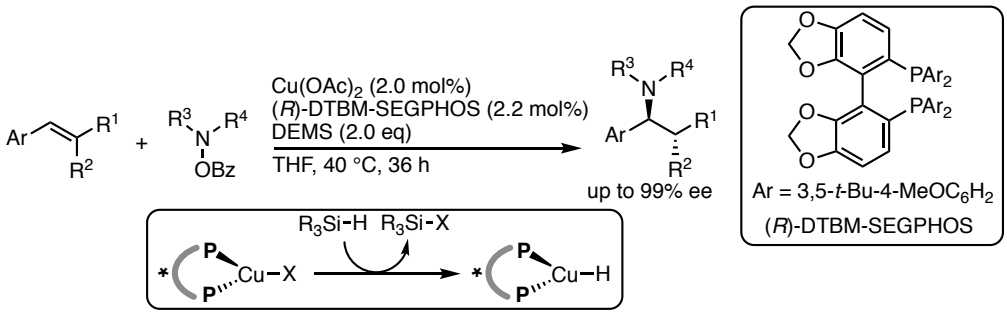

Sawamura group developed a 4-fold polystyrene-cross-linking bisphosphine ligand PS-DPPBz based on 1,2-bis(diphenylphosphino)benzene (DPPBz) exhibited high ligand performance in Cu/Co catalyzed hydroboration reactions (Scheme 18).[20] The location of the DPPBz bisphosphine moiety at the branching points of the cross-linked network organic polymer allowed controlled bisphosphine monochelation to transition metals.

Scheme 18. PS-DPPBz for Cu/Co-Catalyzed Hydroboration involving Cu–H/Co–H Complexes

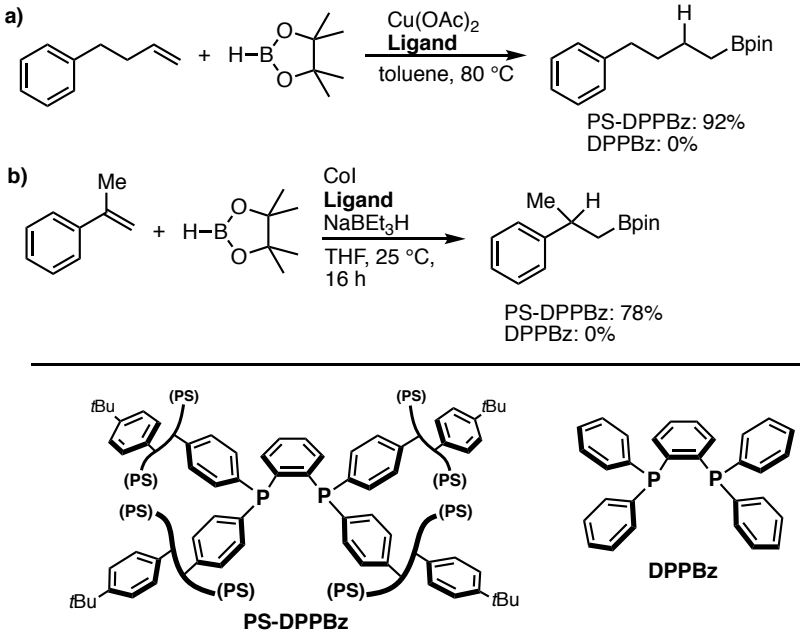

Dong group developed a series of Rh hydride catalysis and then applied them for efficient reactions. Recently, the group developed Rh hydride catalysis to solve a synthetic challenge by affording the enantioselective reduction of allenes, thereby yielding access to motifs commonly used in medicinal chemistry (Scheme 19).[21] A designed Josiphos ligand promotes the generation of chiral benzylic isomers in the presence of a Hantzsch ester as the reductant. This semi-reduction proceeds chemoselectively in the presence of other functional groups, which are typically reduced using conventional hydrogenations.

Scheme 19. Rh–H Complexes for Enantioselective Reduction of Allenes

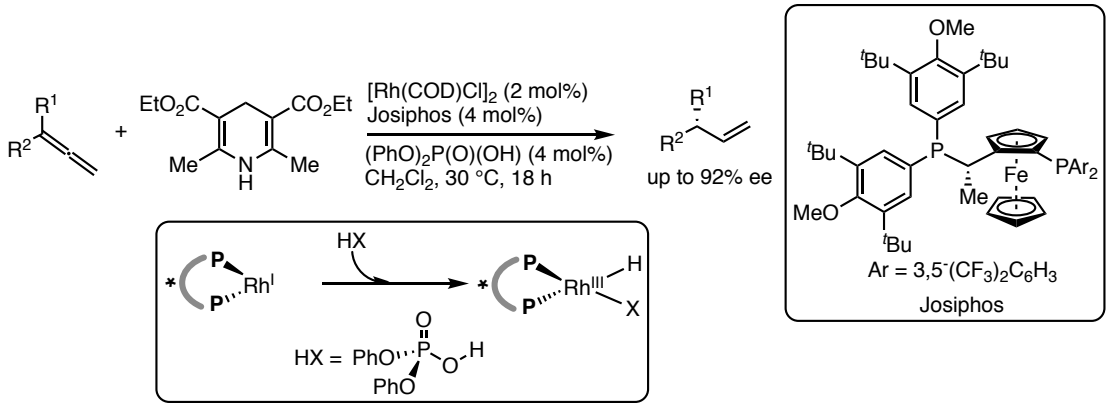

Moreover, several groups developed different ligand-metal cooperative catalysts for the acceptorless dehydrogenation reactions, the metal dihydride species generated from dehydrogenation of various heterocycles was proposed as a key intermediate to produce hydrogen gas (Scheme 20).[22] The pioneering work by Fujita and co-workers shows promising efficiency of metal−ligand bifunctional Ir(III) catalysts with 2-hydroxypyridine-type ancillary ligands. Importantly, the same catalyst systems were able to promote hydrogenation as a backward reaction, demonstrating the reversibility of the process. Later, Jones and co-workers reported iron catalyst system for similar reversible processes, while Xiao and co-workers developed a cyclometalated imino-Ir(III) catalyst. This method is not only used for the functionalization of partially saturated heterocycles to form heteroarenes but also potentially used for hydrogen storage carriers.

Scheme 20. Ligand-Metal Cooperative Catalysts for Acceptorless Dehydrogenation

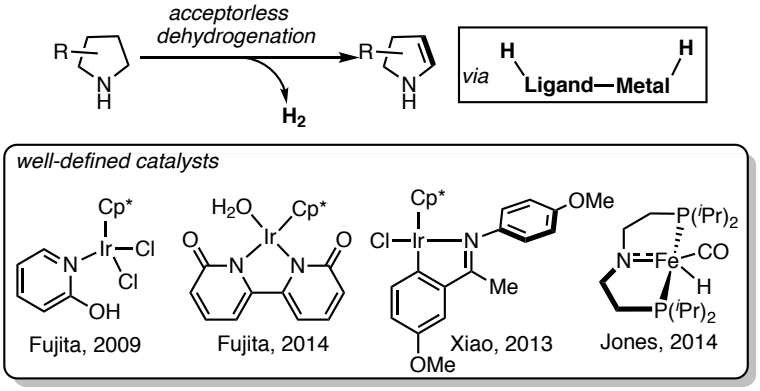

3.3 Precatalysts Containing Metal-(Di)hydride Bonds for the Reactions

Apart from above works, Milstein and co-workers developed ligand-metal cooperative catalyst. The pincer ligand in combination with additional strong field ligands (hydride, CO) stabilize d^6 low spin state of ruthenium, which enables binding of substrates such as H_2 or alcohols. Then applied the catalyst for hydrogenation/dehydrogenation of ketones/alcohols (Scheme 21).[23]

Scheme 21. Metal-Ligand Cooperative Catalysts for Hydrogenation/Dehydrogenation Reactions

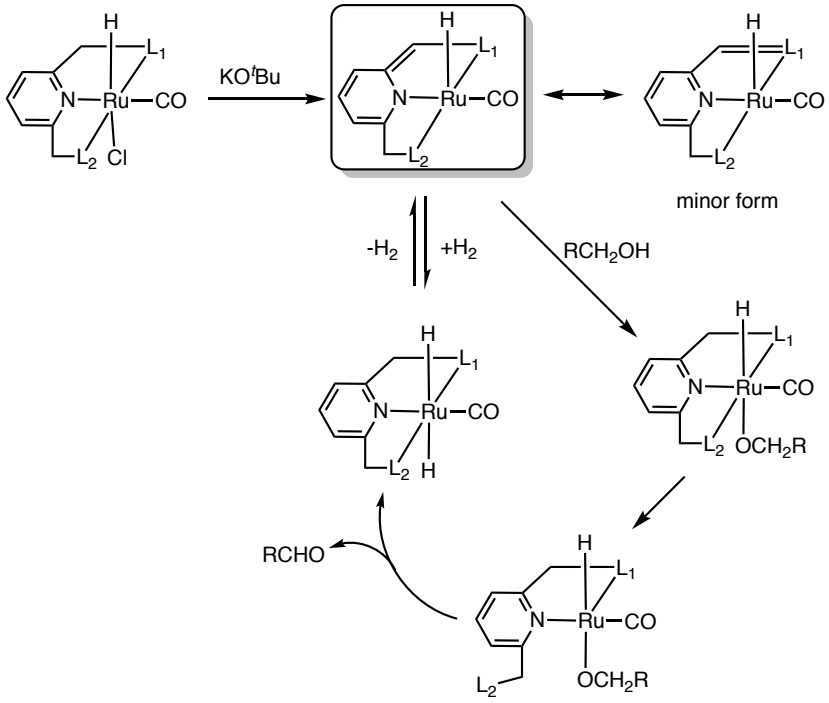

Chirik and co-workers developed α-diimine nickel(I) hydride complex for H/D exchange reaction (Scheme 22).[24] The dimeric inactive complex can be readily prepared. The platform derives from Brookhart catalyst, in which, the aryl groups were replaced by bulky aliphatic moieties. Owing to the repulsion between the bulky groups, dimeric inactive complex facilitates the generation of active monomeric Ni-H complex, then applied it for H/D exchange reactions in pharmaceuticals.

Scheme 22. α-Diimine Nickel(I) Hydride Complex for H/D Exchange

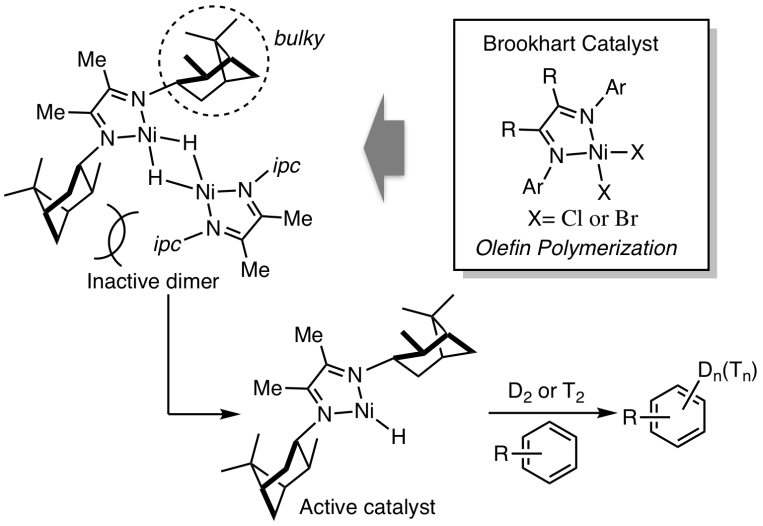

Based on these literatures and Sawamura group previous studies on the property of PS-DPPBz, the author considered to develop/discover simple bisphosphines for stabilization the iridium dihydride complex generated from C(sp^3)–H activation of heterocycles (Scheme 23) and then to utilize this complex for hydrogen transfer processes. To improve the efficiency of catalyst, inactive species such as hydride-bridged polynuclear complexes should be avoided. After examination of bisphosphine ligands, I found that the bulky and electron-rich ligand DCyPE ligated iridium catalyst shows high catalytic performance for transfer hydrogenation reaction with 1,4-dioxane as H source (Chapter 1). Another promising ligand is the heterogeneous PS-DPPBz, which can provide spatial isolation of catalytic center. The ligand was successfully used for both transfer hydrogenation reaction (Chapter 1) and acceptorless dehydrogenation/hydrogenation reactions (Chapter 2).

Scheme 23. Designed Strategy in this Thesis (My Work)

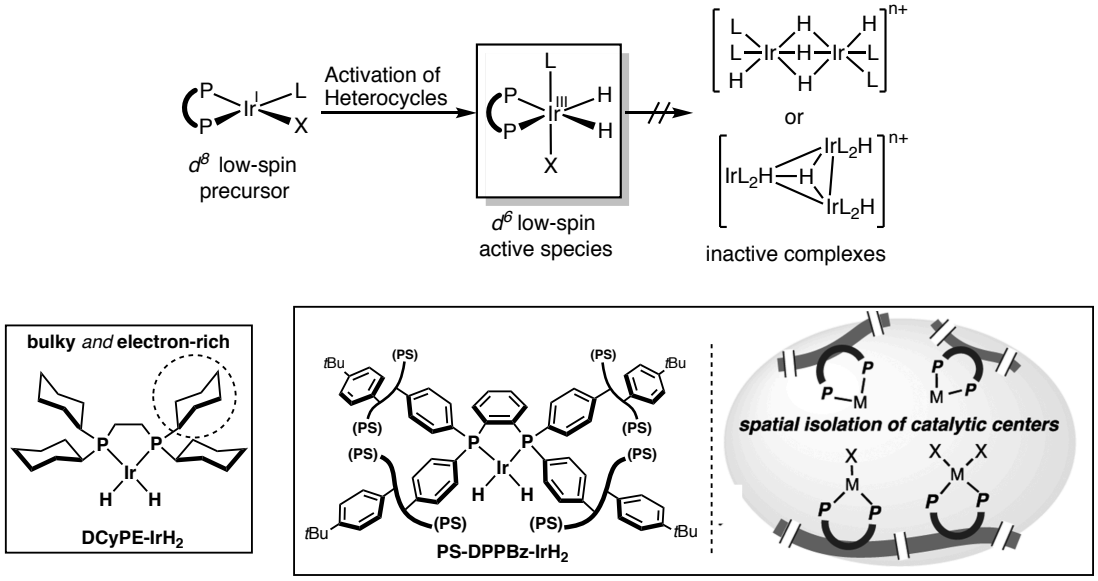

4. Overview of This Thesis

The author developed catalytic hydrogenation and dehydrogenation through C(sp^3)–H activation of heterocyclic compounds. In Chapter 1, iridium-catalyzed alkene-selective transfer hydrogenation with 1,4-dioxane as hydrogen donor is outlined: the commercially available bulky and electron-rich ligand DCyPE was identified to be a particularly high-performing ligand. A polystyrene-cross-linking bisphosphine PS-DPPBz produced a reusable heterogeneous catalyst. In Chapter 2, Ir-catalyzed reversible acceptorless dehydrogenation/hydrogenation of *N*-substituted and unsubstituted heterocycles enabled by a polymer-cross-linking bisphosphine is described. The reaction triggered by α-C(sp^3)–H activation of *N*-heterocycles.

4.1. Iridium-Catalyzed Alkene-Selective Transfer Hydrogenation with 1,4-Dioxane as Hydrogen Donor. (Chapter 1)

Chapter 1 describes iridium-catalyzed alkene-selective transfer hydrogenation with 1,4-dioxane as hydrogen donor. This hydrogenation protocol is alkene selective in the presence of polar unsaturated bonds such as C=O, C=N and C≡N bonds. Mechanistically, this reaction is triggered by oxidative addition of a 1,4-dioxane C(sp^3)–H bond.

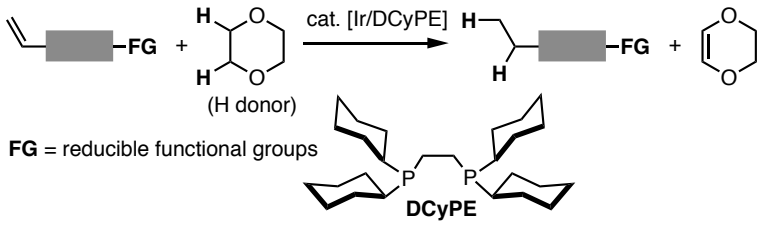

4.2. Ir-Catalyzed Reversible Acceptorless Dehydrogenation/Hydrogenation of N-Substituted and Unsubstituted Heterocycles Enabled by a Polymer-Cross-Linking Bisphosphine (Chapter 2)

This chapter describes a polystyrene-cross-linking bisphosphine-Ir complex (PS-DPPBz)-Ir for the acceptorless dehydrogenation of *N*-heterocycles. The protocol is applicable to the dehydrogenation of *N*-substituted indoline-type substrates, applicability to which has not been well explored with the reported catalytic systems. A catalytic reaction pathway involving oxidative addition of the *N*-adjacent C(sp^3)–H bond to the bisphosphine-Ir(I) species is proposed.

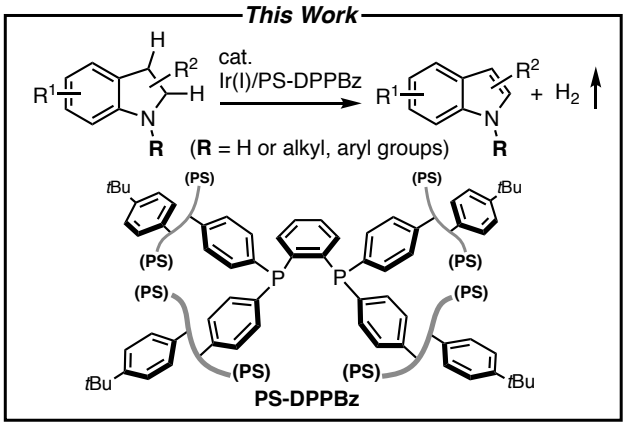
This Work
cat.
Ir(I)/PS-DPPBz
+ H2
(R = H or alkyl, aryl groups)
PS-DPPBz

Reference

(1) Campos, K. R. Direct sp^3 C–H Bond Activation Adjacent to Nitrogen in Heterocycles. *Chem. Soc. Rev.* **2007**, *36*, 1069–1084.

(2) Freeman, D. B.; Furst, L.; Stephenson, C. R. J. Functionally Diverse Nucleophilic Trapping of Iminium Intermediates Generated Utilizing Visible Light. *Org. Lett*. **2012**, *14*, 94–97.

(3) (a) Burk, M. J.; Crabtree, R. H.; Parnell, C. P.; Uriarte, R. J. Selective Stoichiometric and Catalytic Carbon-Hydrogen Bond Cleavage Reactions in Hydrocarbons by Iridium Complexes. *Organometallics* **1984**, *3*, 816–817. (b) Felkin, H.; Fillebeen-Khan, T.; Holmes-Smith, R.; Yingrui, L. Activation of C–H Bonds In Saturated Hydrocarbons. The Selective, Catalytic Functionalizations of Metal Groups by Means of A Soluble Iridium Polyhydride System. *Tetrahedron Lett.* **1985**, *26*, 1999–2000. (c) Burk, M. J.; Crabtree, R. H. Selective Catalytic Dehydrogenation of Alkanes to Alkenes. *J. Am. Chem. Soc*. **1987**, *109*, 8025–8032.

(4) (a) Choi, J.; MacArthur, A. H. R.; Brookhart, M.; Goldman, A. S. Chem.Rev. 2011, 111, 1761–1779. (b) Choi, J.; Goldman, A. Ir-Catalyzed Functionalization of C–H Bonds. In *Iridium Catalysis;* Andersson, P. G.; Springer: Berlin Heidelberg, 2011; Vol. *34*, pp 139–167. (c) Findlater, M.; Choi, J.; Goldman, A.; Brookhart, M. Alkane Dehydrogenation. In Alkane C–H Activation by Single-Site Metal Catalysis; Pérez, P. J., Ed.; Springer: The Netherlands, 2012; Vol. *38*, pp 113–141.

(5) Yao, W.; Zhang, Y.; Jia, X.; Huang, Z. Selective Catalytic Transfer Dehydrogenation of Alkanes and Heterocycles by an Iridium Pincer Complex. *Angew. Chem. Int. Ed*. **2014**, *53*, 1390–1394.

(6) Lyons, T. W.; Bézier, D.; Brookhart, M. Iridium Pincer-Catalyzed Dehydrogenation of Ethers Featuring Ethylene as the Hydrogen Acceptor. *Organometallics* **2015**, *34*, 4058–4062.

(7) Ishii, Y.; Chatani, N.; Kakiuchi, F.; Murai, S. Rhodium-Catalyzed Reaction of N-(2-Pyridinyl)piperazines with CO and Ethylene. A Novel Carbonylation at a C–H Bond in the Piperazine Ring. *Organometallics* **1997**, *16*, 3615–3622.

(8) Chatani, N.; Asaumi, T.; Yorimitsu, S.; Ikeda, T.; Kakiuchi, F.; Murai, S. $Ru_3(CO)_{12}$-Catalyzed Coupling Reaction of sp^3 C–H Bonds Adjacent to a Nitrogen Atom in Alkylamines with Alkenes. *J. Am. Chem. Soc.* **2001**, *123*, 10935–10941.

(9) Deboef. B.; Pastine, S. J.; Sames, D. Cross-Coupling of sp^3 C–H Bonds and Alkenes: Catalytic Cylization of Alkenes-Amide Substrates. *J. Am. Chem. Soc.* **2004**, *126*, 6556–6557.

(10) Bergman, S. D.; Storr, T. E.; Prokopcová, H.; Aelvoet, K.; Diels, G.; Meerpoel, L.; Maes, B. U. W. The Role of the Alcohol and Carboxylic Acid in Directed Ruthenium-Catalyzed C(sp^3)–H α-Alkylation of Cyclic Amines. *Chem. Eur. J.* **2012**, *18*, 10393.

(11) Kawamorita, S.; Miyazaki, T.; Iwai, T.; Ohmiya, H.; Sawamura, M. Rh-Catalyzed Borylation of N–Adjacent C(sp^3)–H Bonds with a Silica-Supported Triaryphosphine Ligand. *J. Am. Chem. Soc.* **2012**, *134*, 12924–12927.

(12) Reyes, R. L.; Sato, M.; Iwai, T.; Sawamura, M. Asymmetric Synthesis of α-Aminoboronates via Rhodium-Catalyzed Enantioselective C(sp3)–H Borylation. *J. Am. Chem. Soc.* **2020**, *142*, 589–597.

(13) Tran, A. T.; Yu, J.-Q. Practical Alkoxythiocarbonyl Auxiliaries for Iridium(I)-Catalyzed C–H Alkylation of Azacycles. *Angew. Chem. Int. Ed*. **2017**, *56*, 10530.

(14) Verma, P.; Richter, J. M.; Chekshin, N.; Qiao, J. X.; Yu, J.-Q. Iridium(I)-Catalyzed α-Alkylation of Saturated Azacycles. *J. Am. Chem. Soc.* **2020**, *142*, 5117–5125.

(15) Tahara, Y.; Michino, M.; Ito, M.; Kanyiva, K. S.; Shibata, T. Enantioselective sp^3 C–H alkylation of γ-butyrolactam by a Chiral Ir(I) Catalyst for the Synthesis of 4-Substituted γ-Amino Acids. *Chem. Commun*. **2015**, *51*, 16660–16663.

(16) Jain, P.; Verma, P.' Xia, G.; Yu, J.-Q. Enantioselective Amine a-Functionalization via Palladium-Catalyzed C–H Arylation of Thioamides. *Nat. Chem*. **2017**, *9*, 140–144.

(17) Davies, H. M. L.; Venkataramani, C.; Hansen, T.; Hopper, D. New Strategic Reactions for Organic Synthesis: Catalytic Asymmetric C–H Activation α to Nitrogen as a Surrogate for the Mannich Reaction. *J. Am. Chem. Soc.* **2003**, *125*, 6464–6468.

(18) Wang, D.; Astruc. The Golden Age of Transfer Hydrogenation. *Chem. Rev*. **2015,** *115*, 6621–6686.

(19) Liu, R. Y.; Buchwald, S. L. CuH-Catalyzed Olefin Functionalization: From Hydroamination to Carbonyl Addition. *Acc. Chem. Res.* **2020**, *53*, 1229–1243.

(20) Iwai, T.; Harada, T.; Shimada, H. Asano, K. Sawamura, M. A Polystyrene-Cross-Linking Bisphosphine: Controlled Metal Monochelation and Ligand-Enabled First-Row Transition Metal Catalysis. *ACS Catal.* **2017**, *7*, 1681.

(21) Chen, Z.; Dong, V. M. Enantioselective Semireduction of Allenes. *Nat. Commun*. **2017**, *8*, 784.

(22) (a) Yamaguchi, R.; Ikeda, C.; Takahashi, Y.; Fujita, K. Homogeneous Catalytic System for Reversible Dehydrogenation-Hydrogenation Reactions of Nitrogen Heterocycles with Reversible Interconversion of Catalytic Species. *J. Am. Chem. Soc.* **2009**, *131*, 8410–8412. (b) Muthaiah, S.; Hong, S. H. Acceptorless and Base-Free Dehydrogenation of Alcohols and Amines using Ruthenium-Hydride Complexes. *Adv. Synth. Catal*. **2012**, *354*, 3045–3053. (c) Wu, J.; Talwar, D.; Johnston, S.; Yan, M.; Xiao, J. Acceptorless Dehydrogenation of Nitrogen Heterocycles with a Versatile Iridium Catalyst. *Angew. Chem., Int. Ed.* **2013**, *52*, 6983–6987. (d) Fujita, K.; Tanaka, Y.; Kobayashi, M.; Yamaguchi, R. Homogeneous Perdehydrogenation and Perhydrogenation of Fused Bicyclic N-Heterocycles Catalyzed by Iridium Complexes Bearing a Functional

Bipyridonate Ligand. *J. Am. Chem. Soc.* **2014**, *136*, 4829–4832. (e) Chakraborty, S.; Brennessel, W. W.; Jones, W. D. A Molecular Iron Catalyst for the Acceptorless Dehydrogenation and Hydrogenation of *N*-Heterocycles. *J. Am. Chem. Soc.* **2014**, *136*, 8564–8567.

(23) Zhang, J.; Leitus, G.; Ben-David, Y.; Milstein, D. Facile Conversion of Alcohols into Esters and Dihydrogen Catalyzed by New Ruthenium Complexes. *J. Am. Chem. Soc.* **2005**, *127*, 10840–10841.

(24) Zarate, C.; Yang, H.; Bezdek. M.; Hesk, D.; Chirik, P. J. Ni(I)–X Complexes Bearing a Bulky α-Diimine Ligand: Synthesis, Structure, and Superior Catalytic Performance in the Hydrogen Isotope Exchange in Pharmaceuticals. *J. Am. Chem. Soc.* **2019**, *141*, 5034–5044.

Chapter 1

Iridium-Catalyzed Alkene-Selective Transfer Hydrogenation with 1,4-Dioxane as Hydrogen Donor

The iridium-catalyzed transfer hydrogenation of alkenes using 1,4-dioxane as a hydrogen donor is described. The use of 1,2-bis(dicyclohexylphosphino)ethane (DCyPE), featuring bulky and highly electron-donating properties, led to high catalytic activity. A polystyrene-cross-linking bisphosphine PS-DPPBz produced a reusale heterogeneous catalyst. These homogeneous and heterogeneous protocols achieved chemoselective transfer hydrogenation of alkenes over other potentially reducible functional groups such as carbonyl, nitro, cyano, and imino groups in the same molecule.

Introduction

Transition metal catalyzed transfer hydrogenations are useful methods for reducing polar unsaturated bonds in organic molecules due to their high chemoselectivity without the need to use flammable hydrogen gas or complex equipment.[1] Furthermore, they have potential for enantioselective catalysis. In fact, transfer hydrogenations of ketones[2] and imines[3] with protic H donor molecules such as 2-propanol and formic acid have been well established (Scheme 1). Noyori–Ikariya-type transfer hydrogenation is a typical highly enantioselective reaction (Scheme 2).[4] In contrast, the chemoselective transfer hydrogenation of C=C bonds in the presence of C=O bonds and other potentially reducible functional groups such as benzylic ethers, nitriles and imines is a long-standing challenge. Although transfer hydrogenation protocols achieving appreciable but incomplete chemoselectivities in favor of C=C bonds over ketoic C=O bonds have been reported,[5–7] the substrates were restricted to conjugated enone derivatives or the selectivities relied on careful control of the reaction conditions.

Scheme 1. Catalytic Transfer Hydrogenation of C=X Bonds (X=O, NR) with 2-Propanol

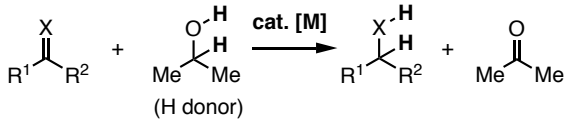

Scheme 2. Noyori-Ikariya-type Asymmetric Transfer Hydrogenation

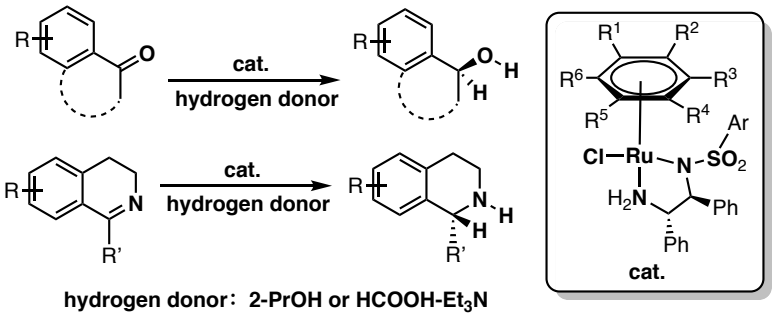

In my investigation of metal-catalyzed C(sp^3)–H functionalizations,[8,9] I encountered a significant reduction of C=C bonds of alkenes with 1,4-dioxane as a two-H donor in the presence of $[IrCl(cod)]_2$ and some bisphosphine ligands under reasonably mild reaction conditions (bath temperature 120–145 °C, 1–4 mol% Ir, Scheme 3). Importantly, this transfer hydrogenation was exclusively selective toward C=C bonds over C=O bonds of ketones, which are the preferred reduction sites under most transfer hydrogenation conditions.[2,3] Although a similar transfer hydrogenation of alkenes with 1,4-dioxane catalyzed by the Wilkinson complex $[RhCl(PPh_3)_3]$ had been

reported in 1972, the reaction conditions were harsh (170 °C) and the substrate scope was limited to a few simple cycloalkenes.[10] Therefore, I decided to investigate the interesting Ir catalysis for ligand effects, substrate scope, and chemoselectivity, having applications in organic synthesis in mind. As a result, 1,2-bis(dicyclohexylphosphino)ethane (DCyPE) was identified as an optimal ligand, which produced, in combination with $[IrCl(cod)]_2$, a catalyst that promoted the highly chemoselective transfer hydrogenation of conjugated polar alkenes and isolated non-polar alkenes in the presence of ketones or other potentially reducible functional groups (Scheme 3). To date, a broadly useful and versatile metal-catalyzed protocol that enables selective transfer hydrogenation of isolated non-polar alkenes in the presence of ketones has not been reported. Although Huang and co-workers recently realized a similar transformation through the utilization of ethanol as a hydrogen donor catalyzed by an Ir-NCP catalyst, only two isolated non-polar alkenes were used and chemoselectivity was not totally controlled.[11]

Scheme 3. C=C Reduction with 1,4-Dioxane

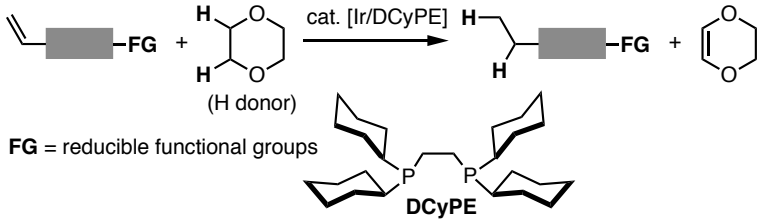

Results and Discussion

Specifically, stirring and heating of a solution of cyclic ketone **1a** (1.1 g, 8.0 mmol) bearing a *tert*-alkyl-substituted terminal alkene moiety, $[IrCl(cod)]_2$ (26.8 mg, 0.04 mmol, 1 mol% Ir), and DCyPE (33.8 mg, 0.08 mmol, 1 mol%) in refluxing 1,4-dioxane (10 mL) (bath temperature 120 °C) under argon atmosphere over 4 h led to complete conversion of the starting material and afforded the corresponding saturated ketone (**2a**) in 97% isolated yield (eq 1). Notably, no other reduction products **3a** and **4a** were produced. The protocol is operationally simple, and 1,4-dioxane serves as a good solvent for a range of organic compounds, suggesting a practical merit of this hydrogenation method.[12]

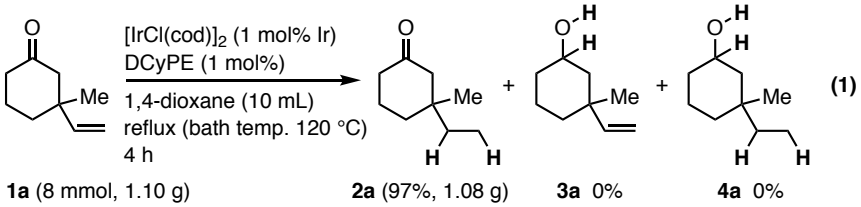

Monitoring reaction time courses by ^1H NMR spectroscopy clearly showed the difference between 1,4-dioxane and 2-propanol as hydrogen donors (Figure 1). Thus,

consistent with the above-mentioned results from the gram-scale reaction, the Ir-catalyzed transfer hydrogenation (1 mol% Ir) of **1a** (0.2 mmol) in 1,4-dioxane heated at 120 °C in a sealed screw vial was exclusively chemoselective throughout the reaction (Figure 1a). On the other hand, the reaction in 2-propanol at 60 °C (4 mol% Ir) was only alkene-selective from the initiation of the reaction up to the half-conversion of the substrate (Figure 1b). After the brief appearance of enol **3a** (40 min, 57% conv. of **1a**), overreduction product **4a** started to form and became the major component at 90 min. A similar trend was observed in the transfer hydrogenation of a conjugated polar alkene

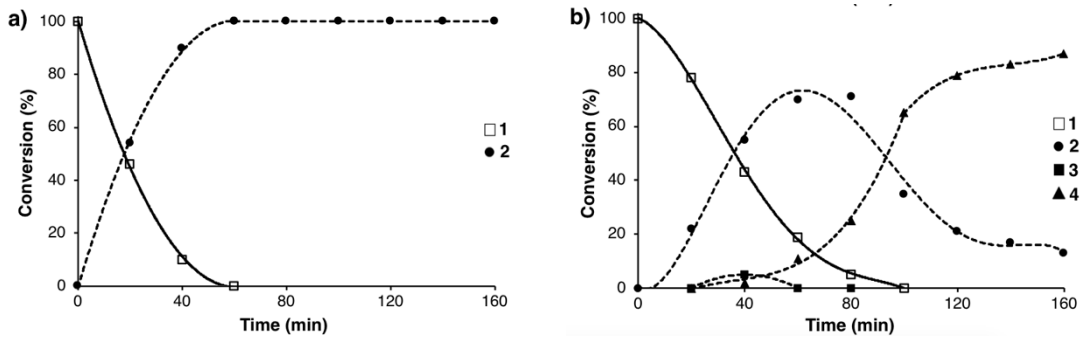

Figure 1. Time Courses of Transfer Hydrogenation of **1a**.

Reaction conditions: a) **1a** (0.2 mmol), $[IrCl(cod)]_2$ (1 mol% Ir), DCyPE (1 mol%), 1,4-dioxane (1 mL), 120 °C (Teflon®-sealed screw vial). b) **1a** (0.2 mmol), $[IrCl(cod)]_2$ (4 mol% Ir), DCyPE (4 mol%), 2-propanol (1 mL), 60 °C (Teflon®-sealed screw vial).

The author also conducted time course of transfer hydrogenation of an enone **1q** with 1,4-dioxane as hydrogen donor. Stirring and heating of a solution of (*E*)-4-phenylbut-3-en-2-one (**1q**, 29.2 mg, 0.2 mmol, 1 equiv), $[IrCl(cod)]_2$ (2.7 mg, 0.04 mmol, 4 mol% Ir), and DCyPE (3.4 mg, 0.08 mmol, 4 mol%) in refluxing 1,4-dioxane (1 mL) (bath temperature 120 °C) under argon atmosphere (eq 2). As depicted in Figure 2, the Ir-catalyzed transfer hydrogenation of **1q** in 1,4-dioxane was exclusively chemoselective throughout the reaction. The alkene-selective reduction product **2q** was obtained in quantitative yield, while other reduction products such as reduction of carbonyl moiety product **3q** was not detected any all. The trend is consistent with transfer hydrogenation of non-conjugate ketone **1a** just as described above, which shows the merit of using 1,4-dioxane as hydrogen donor.

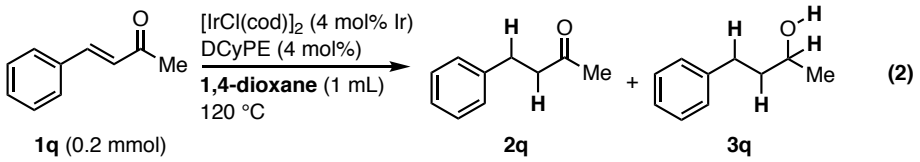

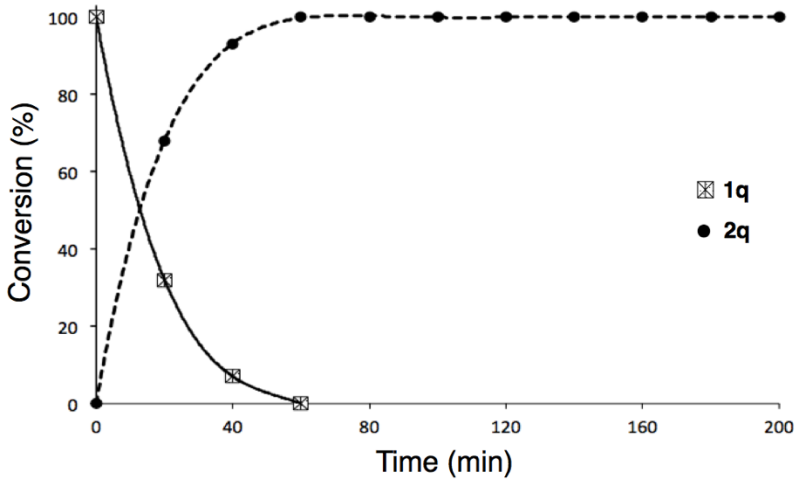

Figure 2. Time-Conversion Curve of Transfer Hydrogenation of **1q** using 1,4-Dioxane as H Donor

Reaction conditions: **1q** (0.2 mmol), $[IrCl(cod)]_2$ (4 mol% Ir), DCyPE (4 mol%), 1,4-dioxane (1 mL), 120 °C (Teflon®-sealed screw vial).

To further demonstrate different reduction trends using 1,4-dioxane and 2-propanol as hydrogen donors for transfer hydrogenation reaction, time course of transfer hydrogenation of **1q** with 2-propanol was also conducted. Stirring and heating of a solution of (*E*)-4-phenylbut-3-en-2-one (**1q**, 29.2 mg, 0.2 mmol, 1 equiv), $[IrCl(cod)]_2$ (2.7 mg, 0.04 mmol, 4 mol% Ir), and DCyPE (3.4 mg, 0.08 mmol, 4 mol%) in 2-propanol (1 mL) (bath temperature 70 °C) under argon atmosphere (eq 3). The result was shown in Figure 3, which appeared different trend comparing with 1,4-dioxane as hydrogen donor (Figure 2). The reaction in 2-propanol was only alkene-selective since the initiation of the reaction till the half-conversion of the substrate (~20 min). Overreduction product **3q** started to form and became a major component at 120 min. In summary, chemoselective reduction of C=C bonds over C=O bonds was achieved using 1,4-dioxane as hydrogen donor, while no chemoselectivity was detected when 1,4-dioxane was replaced by 2-propanol.

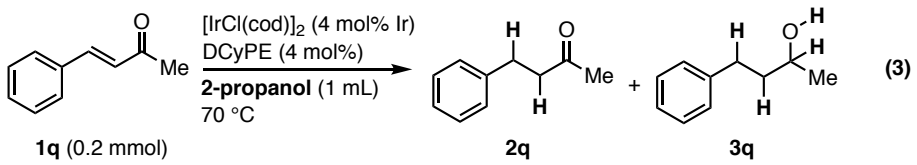

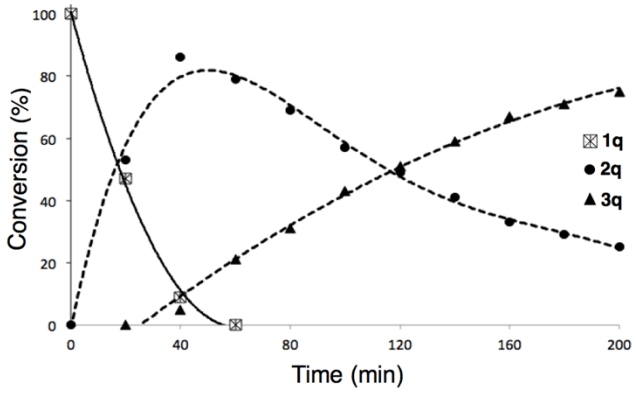

Figure 3. Time-Conversion Curve of Transfer Hydrogenation of **1q** Using 2-propanol as H Donor

Reaction conditions: **1q** (0.2 mmol), $[IrCl(cod)]_2$ (4 mol% Ir), DCyPE (4 mol%), 2-propanol (1 mL), 70 °C (Teflon®-sealed screw vial).

The author also examined other promising ethers as hydrogen donors such as tetrahydrofuran and 1,2-diethoxyethane. Initially, the reaction was performed at 90 °C in the presence of 2 mol% catalyst using (*E*)-4-phenylbut-3-en-2-one as model substrate. The desired alkene-selective reduction product **2q** was obtained in 63% NMR yield. In contrast, only 12% NMR yield of product was detected when tetrahydrofuran (THF) was used as hydrogen donor. In addition, the reaction was conducted at 120 °C to compare different reactivity between 1,4-dioxane and 1,2-diethoxyethane (eq 5). Obviously, 1,4-dioxane as hydrogen donor shows high reactivity, while 1,2-diethoxyethane as hydrogen donor induced no reactivity.

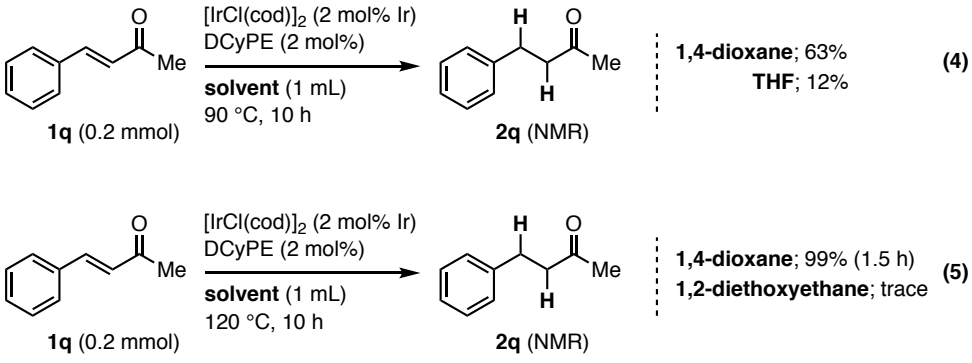

Other phosphines were also examined for ligand performance in the transfer hydrogenation of 4-*tert*-butylstyrene (**1b**) with 1,4-dioxane on a smaller reaction scale (**1b**, 0.2 mmol, 0.5 mol% Ir, Ir/L 1:1, 1,4-dioxane 1 mL, 120 °C in a sealed vial, 1 h). The results are summarized in Table 1. 1,2-bis(diphenylphosphino)benzene (DPPBz) induced slight activity, giving **2b** in 9% yield (entry 9). The yield of **2b** was improved to 44% with a bulkier variant (SciOPP) of DPPBz having *P*-3,5-di-*tert*-butylphenyl groups instead of the *P*-Ph groups (entry 10). Similarly, another bulkier variant (DCyPBz) with *P*-Cy groups also gave an increased product yield of 26% (entry 2).

Changing the 1,2-phenylene backbone of DCyPBz to the 3,4-thiophene-diyl backbone (DCyPT, entry 3)) caused a significant increase of the yield (45%). This may be attributed to the higher electron-donating ability of the 3,4-thiophen-diyl than the phenylene group. While PS-DPPBz gave **2b** in a yield (11%, entry 11) comparable to that with the corresponding homogeneous ligand DPPBz under the otherwise same conditions, the polymer effect was significant at a longer reaction time (9 h, 1 mol% Ir): 97% yield with PS-DPPBz, 48% yield with DPPBz.

Similar trends were observed in the examination of bisphosphine ligands with saturated carbon backbones. Namely, while a small-bite-angle ligand (DPPM, entry 12) with *P*-Ph groups did not induce the reaction, changing the *P*-Ph groups to *P*-Cy groups (DCyPM, entry 4) gave a highly active catalyst, leading to 89% yield. Analogously, the replacement of the *P*-Ph groups of 1,2-bis(diphenylphosphino)ethane (DPPE, entry 13) with *P*-Cy groups led to a dramatic increase in the product yield (from 5% to 99%, entry 1), while the effect of the change to *P*-Et groups was only marginal (12% yield, entry 8). Overall, the reactivity of the transfer hydrogenation was enhanced by steric bulk and more electron-donating ligands. Monodentate phosphine ligands (entries 18–21) and large-bite-angle bisphosphine ligands such as DPPF (entry 16) or Xantphos (entry 17) were totally ineffective.

Table 1. Ligand Effects in the Ir-Catalyzed Transfer Hydrogenation of **1b**[a]

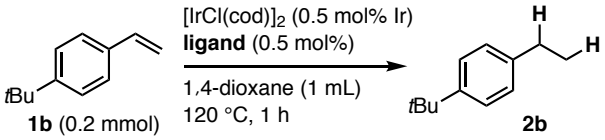

Entry	Ligand		**2b** [%, ^{1}H NMR]
1	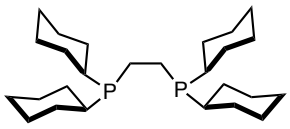	**DCyPE**	**99**
2	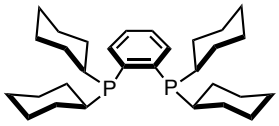	DCyPBz	26
3	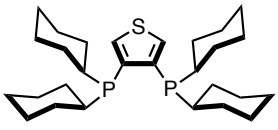	DCyPT	45
4	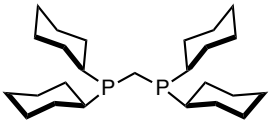	DCyPM	89

5	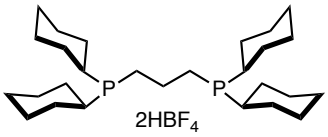	DCyPP·2HBF$_4$ + NaO*t*Bu (1 mol%)	0
6	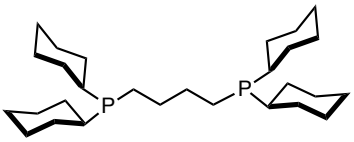	DCyPB	0
7	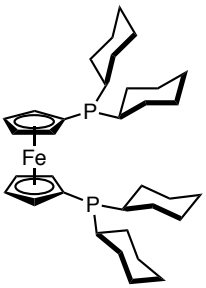	DCyPF	0
8	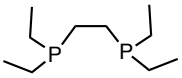	DEtPE	12
9	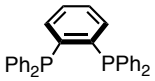	DPPBz	9
10	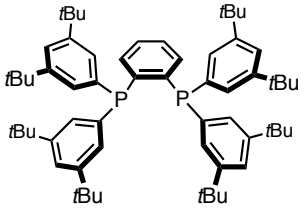	SciOPP	44
11	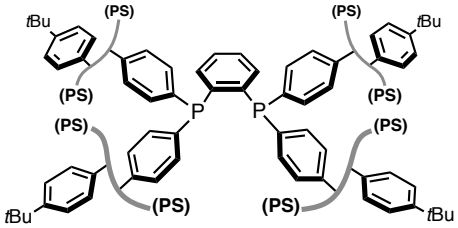	PS-DPPBz	11
12	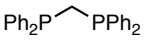	DPPM	0
13	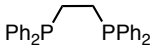	DPPE	5
14	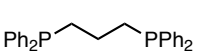	DPPP	0
15	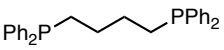	DPPB	0
16	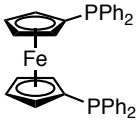	DPPF	0

17	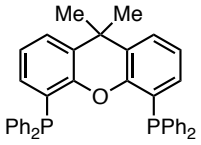	Xantphos	0
18		PPh_3 (1 mol%)	0
19		P*n*Bu_3 (1 mol%)	0
20		PCy_3 (1 mol%)	0
21		P*t*Bu_3 (1 mol%)	0

[a]Reaction condition : **1b** (0.2 mmol), $[IrCl(cod)]_2$ (0.5 mol% Ir), Ligand (0.5 mol%), 1,4-dioxane (1 mL), 120 °C (Teflon®-sealed screw vial).

The effects of transition metal species in the transfer hydrogenation of **1b** were also investigated (Table 2). $[IrCl(cod)]_2$ shows higher reactivity (entry 1), while the yield of product was decreased to 56% when $[IrCl(cod)]_2$ was changed to $[IrCl(coe)_2]_2$ (entry 2). In the replacement of anionic chloride in $[IrCl(cod)]_2$ with methoxyl led to little reactivity. Cationic $[Ir(cod)_2]BF_4$ and $[IrCl_2Cp^*]$ induced no reactivity. Other transition metal species such as Rh, Ru or Co are inactive for this reaction.

Table 2. Metal Effects in the Transfer Hydrogenation of **1b**[a]

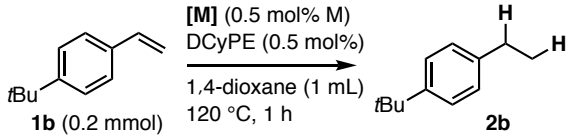

Entry	Metal	**2b** [%, ^{1}H NMR]
1	**$[IrCl(cod)]_2$**	**99**
2	$[IrCl(coe)_2]_2$	56
3	$[Ir(OMe)(cod)]_2$	4
4	$[Ir(cod)_2]BF_4$	0
5	$[IrCl_2Cp^*]$ + NaO*t*Bu (1 mol%) (w/o DCyPE)	0
6	$[RhCl(cod)]_2$	0
7	$[RuCl_2(p\text{-cymene})]_2$	0
8	CoI_2 + $NaBEt_3H$ (1 mol%)	0

[a]Reaction condition **A**: **1b** (0.2 mmol), [M] (0.5 mol%), DCyPE (0.5 mol%), 1,4-dioxane (1 mL), 120 °C (Teflon®-sealed screw vial).

With the optimized reaction conditions in hand, I then explored the transfer hydrogenation of various simple alkenes (Scheme 4). Styrene derivatives (**1b–j**) underwent transfer hydrogenation smoothly. In general, substrates with an electron-

donating substituent at the *para* position of the aromatic ring were more reactive and required lower reaction temperature (120 °C) and catalyst loading (1 mol% Ir). Remarkably, the benzyloxy group in **1c** and the nitro group in **1f** remained untouched. Substrates bearing either exocyclic C=C bonds (**1h**) or cyclic olefinic bonds (**1j**) were hydrogenated in high yields. The protocol was also applicable to various aliphatic alkenes (**1k–p**). Notably, the allyl and benzyl ether moieties of **1o** were innocent of hydrogenolysis reactivity.

Alkynes also underwent the transfer hydrogenation using 1,4-dioxane as H donor with the same catalyst. Diphenylacetylene (5) was converted to 1,2-diphenylethane (6) through double transfer hydrogenation with 4 mol % Ir loading at 140 °C over 20 h (eq 6), while the reaction of a terminal alkyne phenylacetylene suffered from significant oligomerization under the same reaction condition

Scheme 4. Scope of Simple Alkenes[a]

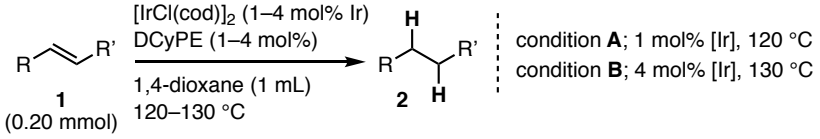

aryl alkenes

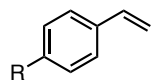

1b R = *t*Bu, 99% (**A**, 1 h)
1c R = OBn, 95% (**A**, 3 h)
1d R = OMe, 94% (**A**, 3 h)
1e R = CO_2Me, 95% (**B**, 10 h)
1f R = NO_2, 98% (**B**, 2 h)

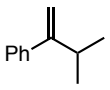

1g, 96% (**A**, 3 h)

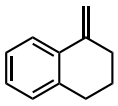

1h, 95% (**B**, 10 h)

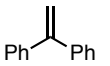

1i, 94% (**B**, 3h)

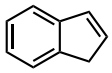

1j, 92% (**B**, 10 h)

aliphatic alkenes

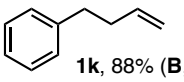

1k, 88% (**B**, 10 h)

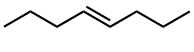

1l, 99% (**B**, 10 h)[a]

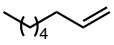

1m, 96% (**A**, 3 h)[a]

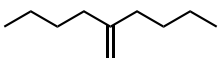

1n, 96% (**A**, 3 h)[a]

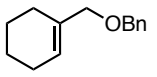

1o, 93% (**B**, 20 h)

1p, 65% (**B**, 40 h)[a]

[a]Reaction condition **A**: **1** (0.2 mmol), $[IrCl(cod)]_2$ (1 mol% Ir), DCyPE (1 mol%), 1,4-dioxane (1 mL), 120 °C (Teflon®-sealed screw vial). Reaction condition **B**: **1** (0.2 mmol), $[IrCl(cod)]_2$ (4 mol% Ir), DCyPE (4 mol%), 1,4-dioxane (1 mL), 130 °C (Teflon®-sealed screw vial). Yields of isolated product are shown. [a]Yield was determined by ^1H NMR analysis of the crude product.

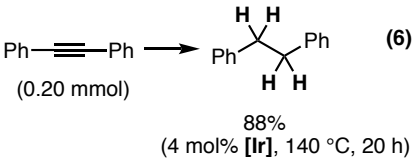

(6)

The chemoselectivity of this protocol toward C=C hydrogenation was further examined with various functionalized alkenes as showcased in Scheme 5. Benzylideneacetone derivatives (**1q**–**w**) bearing electron-donating or withdrawing groups on the aromatic ring were suitable substrates, providing the desired products with excellent yields and exclusive chemoselectivity. The protocol was applicable to the sulfide-functionalized enone (**1v**), although a higher reaction temperature and longer reaction time were required. The aromatic ring could be polycyclic (**1x**, **1y**) or *S*-heterocyclic (**1ab**). An aliphatic conjugated enone (**1z**) and chalcone (**1aa**) also underwent clean C=C reduction. The protocol was also applicable to more sterically hindered enones such as 4,4-dimethyl-2-cyclohexene-1-one (**1ac**) and (*E*)-4-phenylpent-3-en-2-one (**1ad**). Conjugated enoates (**1ae, 1af**) and an enamide (**1ag**) were also reduced at the C=C bond.

Scheme 5 also shows the scope of functionalized non-polar alkenes. Terminal alkenes bearing an acetophenone or cyclohexanone (**1ah–al**) underwent site-selective reduction at the alkene moiety. Tolerance toward nitro and cyano groups was confirmed in the reaction of the biphenyl derivatives **1am** and **1an**. The C=N bond in *N*-sulfonyl ketimine **1ao** also remained untouched. The chemoselective transfer hydrogenation of an estrone derivative (**1ap**) highlights the synthetic utility of this hydrogenation method.

Scheme 5. Alkene-Selective Transfer Hydrogenations

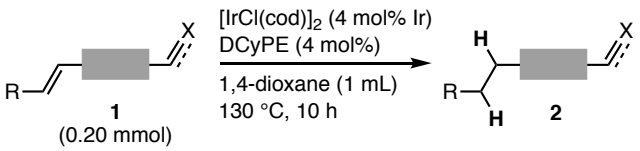

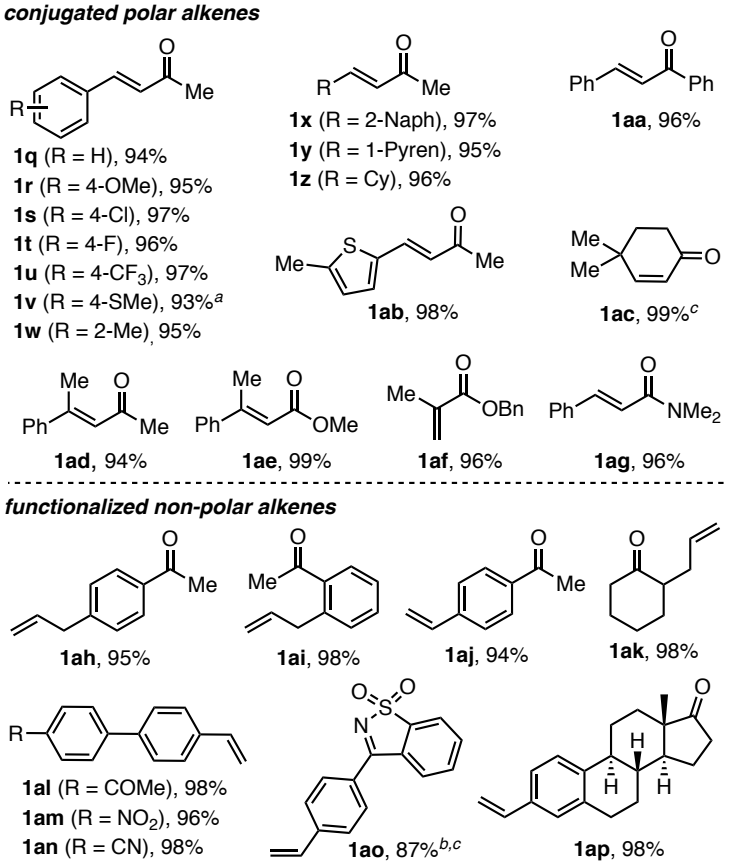

Reaction conditions: **1** (0.2 mmol), $[IrCl(cod)]_2$ (4 mol% Ir), DCyPE (4 mol%), 1,4-dioxane (1 mL), 130 °C (Teflon®-sealed screw vial), 10 h. Yields shown are of isolated product. [a]Run at 145 °C (glass pressure tube) over 48 h. [b]Run in 1,4-dioxane (1.5 mL) at 145 °C (glass pressure tube) over 48 h. [c]Yield was determined by 1H NMR analysis of the crude product.

To gain insight into the mechanism, the effects of deuterated 1,4-dioxane were investigated. Thus, the Ir-catalyzed transfer hydrogenation of **1c** (0.1 mmol, 4 mol% Ir) in a mixed solvent system composed of 1,4-dioxane (0.3 mL) and 1,4-dioxane-d_8 (0.3 mL) conducted at 130 °C proceeded at a much reduced rate than in the single component non-deuterated 1,4-dioxane, resulting in the formation of **2c** in only 48% yield after 24 h with no *D*-incorporation in the product (eq 7). When the reaction was performed in the single component deuterated solvent 1,4-dioxane-d_8 (0.3 mL) under

the same reaction conditions, the deuterated product was obtained in 13% yield with 82% *D*-incorporation in the methylene group and 118% *D*-incorporation in the methyl group (eq 8). The ^{1}H NMR was depicted in Figure 4. These results prove that 1,4-dioxane is the hydrogen donor. The unusually high kinetic isotope effect suggests that dissociations of two different C(sp^3)–H bonds in 1,4-dioxane, one at C(2) and the other at C(3), doubly affect the rate of the catalysis. Namely, it is suggested that both C(2)–H oxidative addition to an Ir center forming an Ir-monohydride species and the subsequent *β*-hydride elimination giving an Ir(III) dihydride species may contribute to the total kinetics of the catalysis. Furthermore, the unequal *D*-incorporation at C(α) and C(β) of **2c** is suggestive of the occurrence of *β*-hydride elimination of a benzylic alkyliridium intermediate.

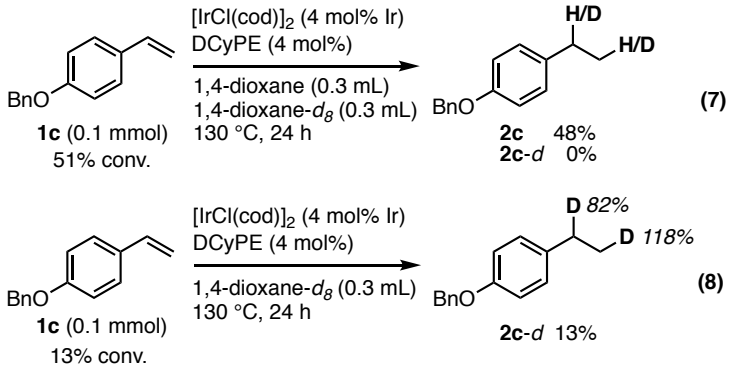

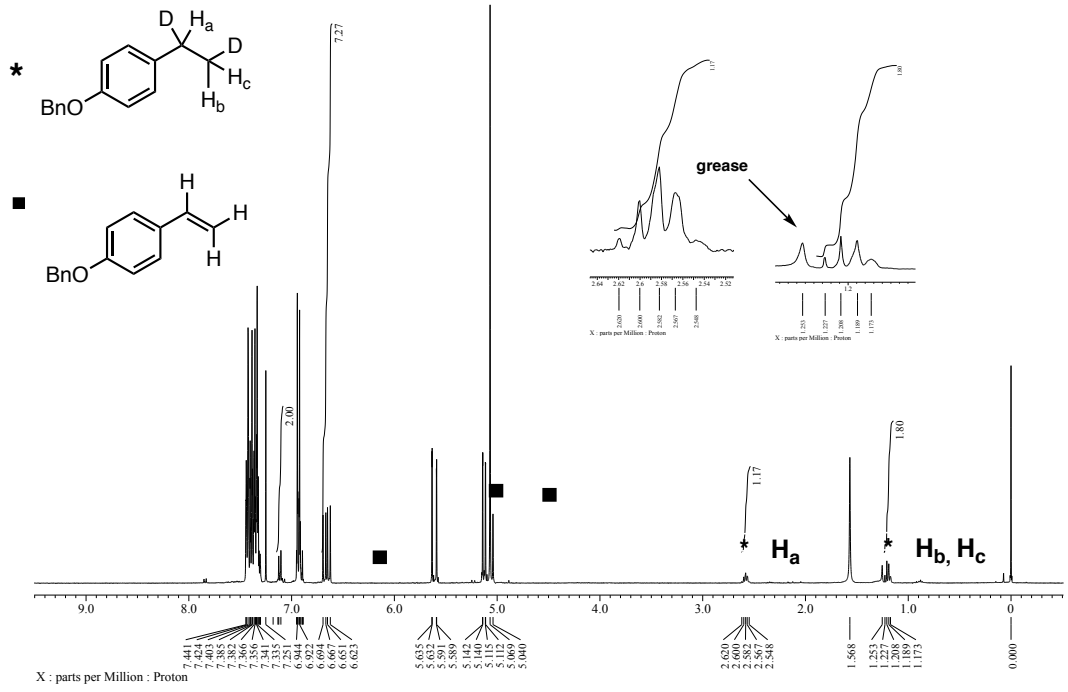

Figure 4. ^{1}H NMR Spectrum of the Material obtained from the Reaction of **1c** in 1,4-Dioxane-d_8 (400 MHz, $CDCl_3$)

On the basis of the above experimental results, a catalytic reaction pathway for the transfer hydrogenation of an alkene with 1,4-dioxane can be proposed as outlined in Scheme 6. Oxidative addition of a C(sp^3)–H bond in 1,4-dioxane to the Ir(I) center in **A** yields Ir(III) monohydride **B**. Subsequent *β*-hydride elimination generates Ir(III) dihydride species **C**, which, depending on the nature of the phosphine ligand bound to the Ir atom, should be in equilibrium with hydride-bridged dimeric iridium complex **C**-dimer as an off cycle species.[13] The alkene coordinates to **C** to form **D**. This is followed by insertion of the alkene to the Ir–H bond of **D** to form Ir-alkyl complex **E**, which undergoes reductive elimination to produce the 1,2-hydrogenation product **2** with regeneration of **A**. [14] In contrast, a reaction pathway for the transfer hydrogenation with 2-propanol would involve the generation of alcohol-bound Ir-hydride species (**F**), which may offer a route for outer-sphere concerted transfer of proton and hydride. This would be responsible for the reactivity of the C=O bonds.

Scheme 6. Proposed Reaction Pathway

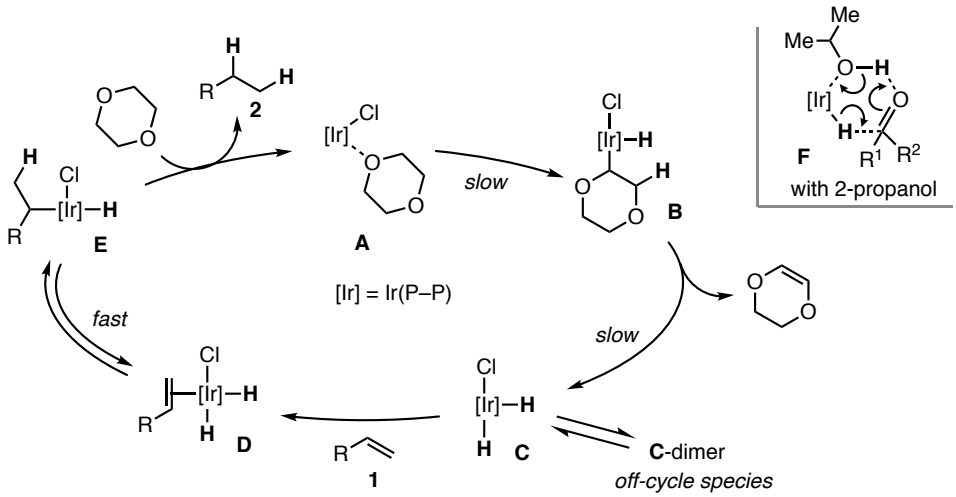

According to this C(sp^3)–H activation triggered reaction pathway, the ligand electronic effect favoring the electron-rich nature may be due to the promotion of oxidative addition of the C(sp^3)–H bond of 1,4-dioxane in **A** to form **B**, while the favorable effect of the sterically hindered bisphosphine ligands can be ascribed to an inhibitory effect for the dimerization of **C**.

This mechanistic consideration prompted us to use a polystyrene-cross-linking bisphosphine PS-DPPBz[15] as an effective ligand for a reusable heterogeneous catalyst system (Scheme 7), as its excellent ligand performance has been demonstrated for some heterogeneous transition metal catalysis. The characteristic ligand property was due to spatial isolation of the bisphosphine unit in the polymer matrix, inhibiting the formation of a bischelated metal complex or a dimer of a monochelate complex (*c.f.* **C**-dimer in Scheme 6). Specifically, the hydrogenation of **1a** (1 mmol) with 1,4-dioxane (0.33 M) at 145 °C in the presence of $[IrCl(cod)]_2$ and PS-DPPBz (Ir/L 1:1, 1 mol% Ir) was

complete at 4 h (98% yield by ^{1}H NMR analysis) (Scheme 7, 1st run). The [Ir-(PS-DPPBz)] catalyst in a form of orange-colored beads could be reused until the third reaction cycle without a significant reduction of the product yield under the identical reaction conditions (4–5 h), while the catalytic efficiency was gradually reduced after the third cycle. The photographic images of the reaction mixtures are shown in Figure 5.

Scheme 7. Heterogeneous Transfer Hydrogenation of **1a** with 1,4-Dioxane and [Ir-(PS-DPPBz)] Catalyst System[a]

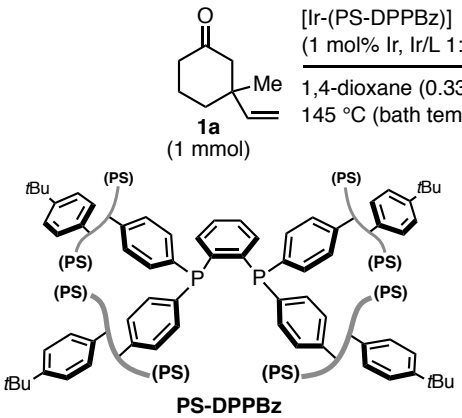

Cycle	Time [h]	Yield [%]
1st	4	98
2nd	4	92
3rd	5	96
4th	5	64
5th	9	45

[a]Reaction conditions: **1a** (1 mmol), $[IrCl(cod)]_2$ (0.005 mmol, 1 mol% Ir), PS-DPPBz (0.1 mmol/g, 0.01 mmol, 1 mol%), 1,4-dioxane (0.33 M), 145 °C (glass pressure tube). Yield was determined by ^{1}H NMR analysis of crude product.

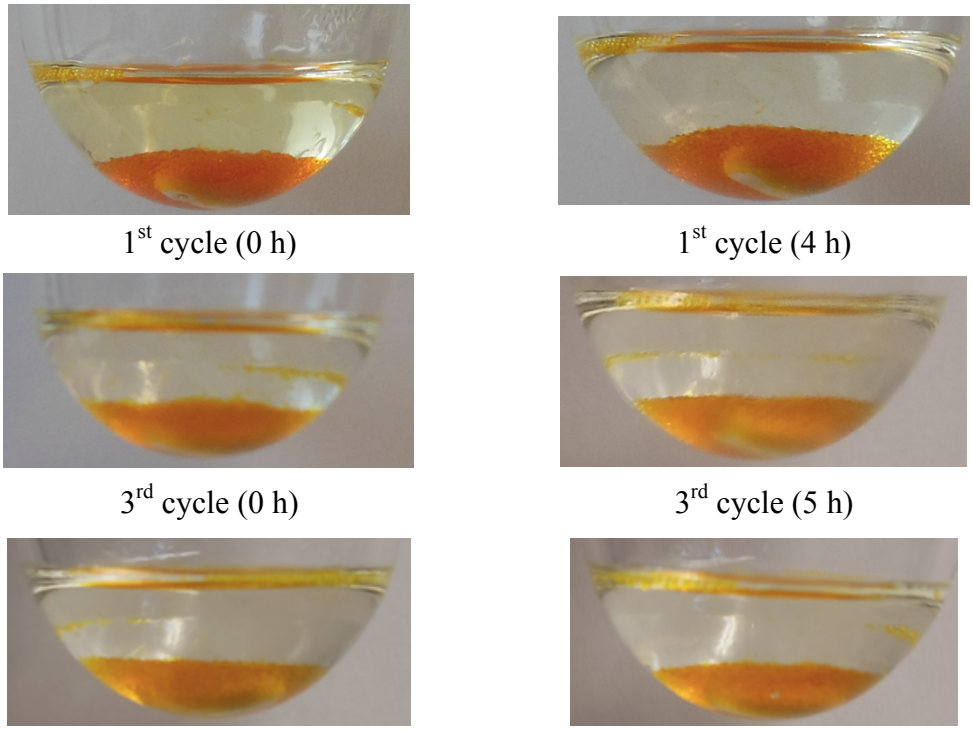

1st cycle (0 h) 1st cycle (4 h)

3rd cycle (0 h) 3rd cycle (5 h)

5th cycle (0 h) 5th cycle (9 h)

Figure 5. Photographic Images of the Reaction Mixture in 1st, 3rd and 5th cycles

Conclusion

In conclusion, I have developed a new operationally simple method for the transfer hydrogenation of alkenes with 1,4-dioxane as a hydrogen donor. The commercially available bulky and electron-rich ligand DCyPE was identified to be a particularly high-performing ligand. A polystyrene-cross-linking bisphosphine PS-DPPBz produced a reusable heterogeneous catalyst. In contrast to the transition metal catalyzed transfer hydrogenation with protic hydrogen donor reagents or solvents, the present hydrogenation protocol is alkene selective in the presence of polar unsaturated bonds such as C=O, C=N and C≡N bonds. Mechanistically, this hydrogenation is triggered by oxidative addition of a 1,4-dioxane C(sp^3)–H bond. I anticipate this method to find widespread application in organic synthesis.

Experimental Section
Instrumentation and Chemicals

NMR spectra were recorded on a JEOL ECXII, operating at 400 MHz for ^{1}H NMR, 100.5 MHz for ^{13}C NMR, 376 MHz for ^{19}F NMR. Chemical shift values for ^{1}H NMR and ^{13}C NMR are referenced to Me_4Si (0 ppm) and the solvent resonance ($CDCl_3$, 77 ppm), respectively. ^{19}F NMR is reference to CF_3COOH (–76.55 ppm). High-resolution mass spectra were recorded at the Instrumental Analysis Division, Global Facility Center, Creative Research Institution, Hokkaido University (JEOL JMS-T100GCv for EI-MS) and the GC–MS & NMR Laboratory, Research Faculty of Agriculture, Hokkaido University (JEOL JMS-T100GCv for FD-MS). Melting points were determined on a micro melting point apparatus using micro cover glass (Yanaco MP-500D). Optical rotations were measured on a JASCO P-2200. TLC analyses were performed on commercial glass plates bearing 0.25-mm layer of Merck Silica gel $60F_{254}$. Silica gel (Kanto Chemical Co., Silica gel 60 N, spherical, neutral) was used for column chromatography. IR spectra were measured with a PerkinElmer Frontier instrument.

All reactions were carried out under nitrogen or argon atmosphere. Materials were obtained from commercial suppliers or prepared according to standard procedures unless otherwise noted. 1,4-Dioxane (dehydrated-Super-) was purchased from Kanto Chemical Co., Inc., and degassed by freeze-pump-thaw cycle. 1,4-Dioxane-d_8 was purchased from Cambridge Isotope Laboratories, Inc., and used as received. $[IrCl(cod)]_2$ was prepared according to the reported procedure.[16]

Synthesis of the Substrates

Alkenes **1b**, **1d**–**1f**, **1j**–**1m**, **1p**, **1q**, **1aa**, **1ac**, **1af**, **1ak** are commercial available. Other substrates listed in Figure 6 are reported in the literature.

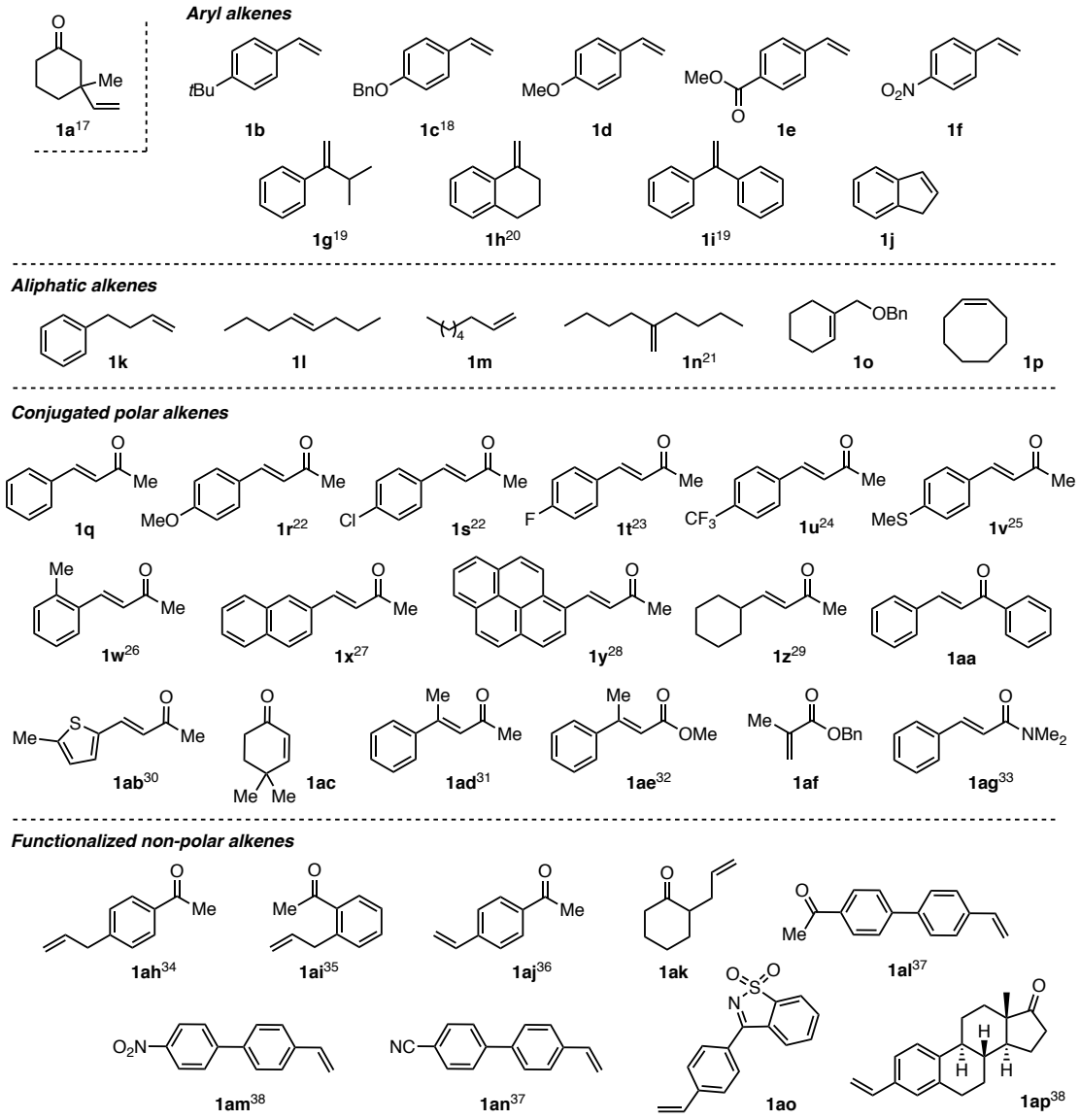

Figure 6. Alkene Substrates used in this Work.

((Cyclohex-1-en-1-ylmethoxy)methyl)benzene (1o)

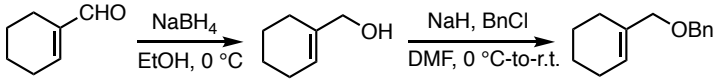

$NaBH_4$ (318 mg, 8.4 mmol, 1.2 equiv) was added in several portions to a stirring solution of 1-cyclohexene-1-carboxaldehyde (775 mg, 7.0 mmol, 1.0 equiv) in ethanol (15 mL) at 0 °C. After the reaction mixture was stirred at this temperature for 2 h, saturated NH_4Cl solution (10 mL) and H_2O (5 mL) were added to the mixture. The resulting mixture was stirred for 5 min, and then extracted with CH_2Cl_2 (3 × 10 mL). The organic layer was dried over Na_2SO_4, filtered and evaporated to afford the

corresponding cyclohexenylmethanol, which was used without further purification. To a solution of cyclohexenylmethanol in DMF (15 mL) at 0 °C was added 55% NaH in mineral oil (367 mg, 8.4 mmol, 1.2 equiv) and benzyl chloride (1.06 g, 8.4 mmol, 1.2 equiv). After the reaction mixture was stirred at room temperature overnight, the reaction was quenched with saturated NH_4Cl solution (20 mL). The resulting mixture was extracted with CH_2Cl_2 (3 × 10 mL). The organic layer was reduced under vacuum. The residue was purified by silica gel column chromatography (hexane/EtOAc (95:5)) to provide **1o** (1.16 g, 63% yield) as colorless liquid. **^{1}H NMR** (400 MHz, $CDCl_3$): δ 1.69–1.58 (m, 4H), 2.05–2.02 (m, 4H), 3.88 (s, 2H), 4.46 (s, 2H), 5.71 (br-s, 1H), 7.39–7.25 (m, 5H). **^{13}C NMR** (100.5 MHz, $CDCl_3$): δ 22.38, 22.50, 25.00, 25.93, 71.57, 75.01, 125.21, 127.41, 127.69 (2C), 128.29 (2C), 134.85, 138.62. **IR** (ATR): 732, 1029, 1073, 1096, 1117, 1361, 1450, 2850, 2921 cm^{-1}. **EI-HRMS** (*m/z*): $[M]^+$ Calcd for $C_{14}H_{18}O$, 202.13576. found. 202.13529.

3-(4-Vinylphenyl)benzo[*d*]isothiazole 1,1-dioxide (1ao)

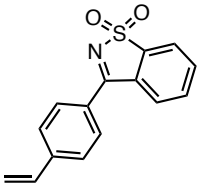

Saccharine (1 equiv, 2.00 g, 10.92 mmol) was dissolved in THF (20 mL) and cooled to 0 °C. (4-Vinylphenyl)magnesium bromide (2.2 equiv, 24.02 mmol, in situ prepared from 4-bromostyrene and magnesium) was added dropwise. The cooling bath was removed and the mixture was stirred at room temperature for 16 h. After NH_4Cl (0.6 g) was added at 0 °C, the mixture was stirred at room temperature for 30 min. Filtration over alumina with ethyl acetate as eluent, removal of the solvent under reduced pressure and recrystallization from hot ethanol gave **1ao** as a white solid (1.71 g, 6.35 mmol, 58%). **M.P.** 177.1–179.6 °C. **^{1}H NMR** (400 MHz, $CDCl_3$) δ 5.48 (d, J = 11.0 Hz, 1H), 5.95 (d, J = 17.4 Hz, 1H), 6.81 (dd, J = 17.9, 11.0 Hz, 1H), 7.63 (d, J = 8.2 Hz, 2H), 7.81–7.73 (m, 2H), 8.02–7.92 (m, 4H). **^{13}C NMR** (100.5 MHz, $CDCl_3$): δ 117.56, 123.06, 126.51, 126.88 (2C), 129.49, 129.98 (2C), 130.57, 133.34, 133.62, 135.57, 141.06, 142.64, 170.46. **IR** (ATR): 756, 803, 853, 967, 1170, 1331, 1526, 1604 cm^{-1}. **EI-HRMS** (*m/z*): $[M]^+$ Calcd for $C_{15}H_{11}NO_2S$, 269.05105. found. 269.05157.

Experimental Procedures

General Procedure for Scheme 4, Condition A: In a nitrogen-filled glove box, $[IrCl(cod)]_2$ (0.67 mg, 0.001 mmol, 1 mol% Ir; prepared c = 0.005 mol/L 1,4-dioxane solution, 0.2 mL), DCyPE (0.85 mg, 0.002 mmol, 1 mol%; prepared c = 0.01 mol/L 1,4-dioxane solution, 0.2 mL) and 1,4-dioxane (0.6 mL; total 1 mL) were placed successively in a 10-mL glass tube containing a magnetic stirring bar. After stirring at room temperature for 5 min, alkene substrate **1** (0.2 mmol) was added. The tube was sealed with a screw caps with a Teflon®-coated sealing disk, and was removed from the

glove box. The mixture was stirred at 120 °C for 1–3 h. After being cooled to room temperature, the solvent was removed *in vacuo*. An internal standard (1,1,2,2-tetrachloroethane) was added to the residue. The yield of the hydrogenated product **2** was determined by ^{1}H NMR. The crude material was purified by silica gel column chromatography to give the hydrogenated product **2**.

General Procedure for Scheme 4, Condition B: In a nitrogen-filled glove box, $[IrCl(cod)]_2$ (2.7 mg, 0.004 mmol, 4 mol% Ir), DCyPE (3.4 mg, 0.008 mmol, 4 mol%) in 1,4-dioxane (1 mL) were placed successively in a 10-mL glass tube containing a magnetic stirring bar. After stirring at room temperature for 5 min, alkene substrate **1** (0.2 mmol) was added. The tube was sealed with a screw caps with a Teflon®-coated sealing disk, and was removed from the glove box. The mixture was stirred at 130 °C for 2–40 h. After being cooled to room temperature, the solvent was removed *in vacuo*. An internal standard (1,1,2,2-tetrachloroethane) was added to the residue. The yield of the hydrogenated product **2** was determined by ^{1}H NMR. The crude material was purified by silica gel column chromatography to give the hydrogenated product **2**.

General Procedure for Scheme 5: In a nitrogen-filled glove box, $[IrCl(cod)]_2$ (2.7 mg, 0.004 mmol, 4 mol% Ir), DCyPE (3.4 mg, 0.008 mmol, 4 mol%) in 1,4-dioxane (1 mL) were placed successively in a 10-mL glass tube containing a magnetic stirring bar. After stirring at room temperature for 5 min, alkene substrate **1** (0.2 mmol) was added. The tube was sealed with a screw caps with a Teflon®-coated sealing disk, and was removed from the glove box. The mixture was stirred at 130 °C for 10 h. After being cooled to room temperature, the solvent was removed *in vacuo*. An internal standard (1,1,2,2-tetrachloroethane) was added to the residue. The yield of the hydrogenated product **2** was determined by ^{1}H NMR. The crude material was purified by silica gel column chromatography to give the hydrogenated product **2**.

Gram-Scale Reaction of 1a (Eq 1): An oven-dried 50 mL two-necked, round-bottomed flask equipped with a magnetic stirring bar and refulx condenser was charged with $[IrCl(cod)]_2$ (26.8 mg, 0.04 mmol, 1 mol% Ir) and DCyPE (33.8 mg, 0.08 mmol, 1 mol%). After the flask was evacuated and backfilled with argon three times, 1,4-dioxane (10 mL) was added. The resulting solution was stirred for 5 min at room temperature. Then, the substrate 3-methyl-3-vinylcyclohexan-1-one **1a** (1.10 g, 8 mmol, 1.0 equiv) was added. The mixture was stirred at 120 °C for 4 h. After the reaction flask was cooled to room temperature, the solvent was removed under reduced pressure. The residue was purified by silica gel column chromatography (hexane/EtOAc, 95:5) to give the corresponding hydrogenated product **2a** in 97% (1.08 g) isolated yield as colorless oil.

Gram-Scale Reaction of 1q: An oven-dried 50 mL two-necked, round-bottomed flask equipped with a magnetic stirring bar and refulx condenser was charged with

$[IrCl(cod)]_2$ (94 mg, 0.14 mmol, 4 mol% Ir) and DCyPE (118 mg, 0.28 mmol, 4 mol%). After the flask was evacuated and backfilled with argon three times, 1,4-dioxane (10 mL) was added. The resulting solution was stirred for 5 min at room temperature. Then, the substrate (*E*)-4-phenylbut-3-en-2-one **1q** (1.02 g, 7 mmol, 1.0 equiv) was added. The mixture was stirred at 130 °C for 36 h. After the reaction flask was cooled to room temperature, the solvent was removed under reduced pressure. The residue was purified by silica gel column chromatography (hexane/EtOAc, 95:5) to give the corresponding hydrogenated product **2q** in 95% (0.98 g) isolated yield as colorless oil.

Catalyst Reuse (Scheme 7): In a nitrogen-filled glove box, PS-DPPBz (0.1 mmol/g, 100 mg, 0.01 mmol, 1 mol%), $[IrCl(cod)]_2$ (3.4 mg, 0.01 mmol, 1 mol% Ir) and 1,4-dioxane (2 mL) were successively placed in a 100-mL glass pressure tube containing a magnetic stirring bar. The tube was sealed with a screw cap and removed from the glove box. After stirring at 100 °C for 10 min, the tube was placed inside the glove box. A solution of 3-methyl-3-vinylcyclohexan-1-one (**1a**, 138.2 mg, 1 mmol, 1 equiv) in 1,4-dioxane (1 mol/L, 1 mL) was added, and the tube was sealed with a screw cap and was removed from the glove box. The mixture was stirred at 145 °C for 4 h. After the reaction was completed, the tube was placed inside the glove box. The solution phase was taken out with a glass pipette, and PS resin was washed with hot 1,4-dioxane (1 mL). Then, a hot solution of **1a** (1 mmol, 1 equiv) in 1,4-dioxane (0.33 M) was added to the pressure tube quickly. The tube was sealed with a screw cap and removed from the glove box. The mixture was stirred at 145 °C for 4 h. After the crude reaction mixture was evaporated under vacuum, an internal standard (1,1,2,2-tetrachloroethane) was added to the residue. The yield of **2a** was determined by ^{1}H NMR analysis. This reuse procedure was repeated for additional 3 times (1st run, 98% (4 h); 2nd run, 92% (4 h); 3rd run, 96% (5 h); 4th run, 64% (5 h); 5th run, 45% (9 h)).

Characterization of Products

3-Ethyl-3-methylcyclohexan-1-one (2a)

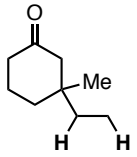

[4 mol% Ir, 130 °C (**condition B**), 10 h] The product **2a** (26.0 mg, 93% yield) was isolated by silica gel column chromatography with hexane/EtOAc (95:5). Colorless oil. **^{1}H NMR** (400 MHz, $CDCl_3$): δ 0.84 (t, J = 7.6 Hz, 3H), 0.90 (s, 3H), 1.34–1.29 (m, 2H), 1.56–1.49 (m, 1H), 1.66–1.59 (m, 1H), 1.90–1.82 (m, 2H), 2.20–2.08 (m, 2H), 2.28 (t, J = 6.8 Hz, 2H). **^{13}C NMR** (100.5 MHz, $CDCl_3$): δ 7.73, 22.10, 24.39, 33.90, 35.33, 38.65, 41.05, 53.37, 212.60. **IR** (ATR): 729, 917, 1079, 1228, 1313, 1381, 1462, 1709, 2879, 2939, 2963 cm^{-1}.

1-(*tert*-Butyl)-4-ethylbenzene (2b)

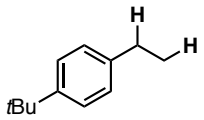

[1 mol% Ir, 120 °C (**condition A**), 1 h] The product **2b** (32.1 mg, 99% yield) was isolated by silica gel column chromatography with hexane/EtOAc (99:1). Colorless oil. **^{1}H NMR** (400 MHz, $CDCl_3$): δ 1.24 (t, J = 7.6 Hz, 3H), 1.31 (s, 9H), 2.63 (q, J = 7.8 Hz, 2H), 7.14 (d, J = 8.0 Hz, 2H), 7.32 (d, J = 8.0 Hz, 2H). **^{13}C NMR** (100.5 MHz, $CDCl_3$): δ 15.51, 28.25, 31.42 (3C), 34.31, 125.17 (2C), 127.49 (2C), 141.14, 148.32. **IR** (ATR): 732, 829, 909, 1268, 1518, 2871, 2964 cm^{-1}.

1-(Benzyloxy)-4-ethylbenzene (2c)

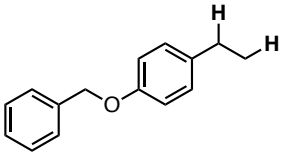

[1 mol% Ir, 120 °C (**condition A**), 3 h] The product **2c** (40.2 mg, 95% yield) was isolated by silica gel column chromatography with hexane/EtOAc (95:5). Colorless oil. **^{1}H NMR** (400 MHz, $CDCl_3$): δ 1.21 (t, J = 7.6 Hz, 3H), 2.59 (q, J = 7.6 Hz, 2H), 5.03 (s, 2H), 6.92–6.89 (m, 2H), 7.12–7.10 (m, 2H), 7.29–7.44 (m, 5H). **^{13}C NMR** (100.5 MHz, $CDCl_3$): δ 15.86, 27.96, 70.00, 114.64 (2C), 127.45 (2C), 127.85, 128.52 (2C), 128.71 (2C), 136.65, 137.22, 156.80. **IR** (ATR): 731, 827, 1025, 1175, 1234, 1380, 1510, 2963, 3032 cm^{-1}.

1-Ethyl-4-methoxybenzene (2d)

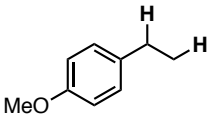

[1 mol% Ir, 120 °C (**condition A**), 3 h] The product **2d** (25.5 mg, 94% yield) was isolated by silica gel column chromatography with hexane/EtOAc (95:5). Colorless oil. **^{1}H NMR** (400 MHz, $CDCl_3$): δ 1.21 (t, J = 7.6 Hz, 3H), 2.59 (q, J = 7.6 Hz, 2H), 3.79 (s, 3H), 6.85–6.80 (m, 2H), 7.14–7.10 (m, 2H). **^{13}C NMR** (100.5 MHz, $CDCl_3$): δ 15.91, 27.94, 55.23, 113.67 (2C), 128.68 (2C), 136.36, 157.55. **IR** (ATR): 811, 827, 1035, 1176, 1238, 1300, 1511, 1611, 2963 cm^{-1}.

Methyl 4-ethylbenzoate (2e)

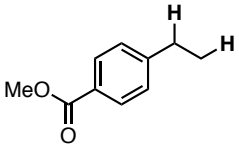

[4 mol% Ir, 130 °C (**condition B**), 10 h] The product **2e** (31.0 mg, 95% yield) was isolated by silica gel column chromatography with hexane/EtOAc (95:5). Colorless oil.

^{1}H NMR (400 MHz, $CDCl_3$): δ 1.26 (t, J = 7.6 Hz, 3H), 2.71 (q, J = 7.8 Hz, 2H), 3.90 (s, 3H), 7.26 (d, J = 8.8 Hz, 2H), 7.95 (d, J = 8.4 Hz, 2H). **^{13}C NMR** (100.5 MHz, $CDCl_3$): δ 15.23, 28.94, 51.96, 127.57, 127.88 (2C), 129.68 (2C), 149.74, 167.21. **IR** (ATR): 730, 853, 908, 1020, 1179, 1276, 1435, 1611, 1717, 2969 cm^{-1}.

1-Ethyl-4-nitrobenzene (2f)

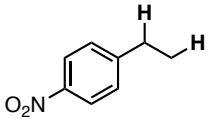

[4 mol% Ir, 130 °C (**condition B**), 2 h] The product **2f** (29.6 mg, 98% yield) was isolated by silica gel column chromatography with hexane/EtOAc (95:5). Colorless oil. **^{1}H NMR** (400 MHz, $CDCl_3$): δ 1.28 (t, J = 7.6 Hz, 3H), 2.76 (q, J = 7.6 Hz, 2H), 7.36–7.34 (m, 2H), 8.16–8.13 (m, 2H). **^{13}C NMR** (100.5 MHz, $CDCl_3$): δ 15.05, 28.83, 123.61 (2C), 128.62 (2C), 146.16, 152.01. **IR** (ATR): 731, 849, 1053, 1110, 1341, 1512, 1599, 2971 cm^{-1}.

(3-Methylbutan-2-yl)benzene (2g)

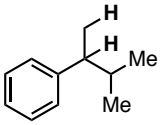

[1 mol% Ir, 120 °C (**condition A**), 3 h] The product **2g** (28.4 mg, 96% yield) was isolated by silica gel column chromatography with hexane/EtOAc (99:1). Colorless oil. **^{1}H NMR** (400 MHz, $CDCl_3$): δ 0.74 (d, J = 6.9 Hz, 3H), 0.93 (d, J = 6.9 Hz, 3H), 1.23 (d, J = 7.3 Hz, 3H), 1.79–1.72 (m, 1H), 2.45–2.36 (m, 1H), 7.19–7.14 (m, 3H), 7.29–7.25 (m, 2H). **^{13}C NMR** (100.5 MHz, $CDCl_3$): δ 18.75, 20.17, 21.18, 34.42, 46.84, 125.65, 127.64 (2C), 128.00 (2C), 147.09. **IR** (ATR): 750, 770, 1015, 1056, 1385, 1452, 2872, 2959 cm^{-1}.

1-Methyl-1,2,3,4-tetrahydronaphthalene (2h)

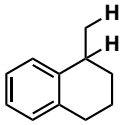

[4 mol% Ir, 130 °C (**condition B**), 10 h] The product **2h** (27.7 mg, 95% yield) was isolated by silica gel column chromatography with hexane/EtOAc (99:1). Colorless oil. **^{1}H NMR** (400 MHz, $CDCl_3$): δ 1.29 (d, J = 6.9 Hz, 3H), 1.57–1.53 (m, 1H), 1.80–1.68 (m, 1H), 1.91–1.88 (m, 2H), 2.82–2.71 (m, 2H), 2.93–2.87 (m, 1H), 7.24–7.04 (m, 4H). **^{13}C NMR** (100.5 MHz, $CDCl_3$): δ 20.36, 22.85, 29.94, 31.42, 32.40, 125.35, 125.55, 128.07, 128.97, 136.83, 142.13. **IR** (ATR): 728, 753, 796, 1043, 1374, 1445, 1489, 2867, 2929 cm^{-1}.

Ethane-1,1-diyldibenzene (2i)

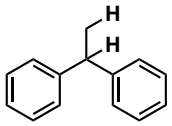

[4 mol% Ir, 130 °C (**condition B**), 3 h] The product **2i** (34.2 mg, 94% yield) was isolated by silica gel column chromatography with hexane/EtOAc (99:1). Colorless oil. **^{1}H NMR** (400 MHz, $CDCl_3$): δ 1.63 (d, J = 7.3 Hz, 3H), 4.15 (q, J = 7.2 Hz, 1H), 7.29–7.15 (m, 10H). **^{13}C NMR** (100.5 MHz, $CDCl_3$): δ 21.83, 44.73, 125.99 (2C), 127.59 (4C), 128.32 (4C), 146.33 (2C). **IR** (ATR): 729, 754, 782, 909, 1025, 1374, 1449, 1493, 1599, 2931, 2967, 3026 cm^{-1}.

2,3-Dihydro-1*H*-indene (2j)

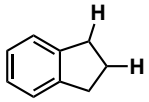

[4 mol% Ir, 130 °C (**condition B**), 10 h] The product **2j** (21.7 mg, 92% yield) was isolated by silica gel column chromatography with hexane/EtOAc (99:1). Colorless oil. **^{1}H NMR** (400 MHz, $CDCl_3$): δ 2.06 (quin, J = 7.6 Hz, 2H), 2.91 (t, J = 7.6 Hz, 4H), 7.15–7.11 (m, 2H), 7.25–7.21 (m, 2H). **^{13}C NMR** (100.5 MHz, $CDCl_3$): δ 25.32, 32.85 (2C), 124.35 (2C), 125.94 (2C), 144.14 (2C). **IR** (ATR): 736, 748, 1459, 1482, 2867, 2845, 2944 cm^{-1}.

Butylbenzene (2k)

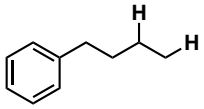

[4 mol% Ir, 130 °C (**condition B**), 10 h] The product **2k** (23.9 mg, 88% yield) was isolated by silica gel column chromatography with hexane/EtOAc (99:1). Colorless oil. **^{1}H NMR** (400 MHz, $CDCl_3$): δ 0.92 (t, J = 7.3 Hz, 3H), 1.38–1.33 (m, 2H), 1.64–1.54 (m, 2H), 2.61 (t, J = 7.8 Hz, 2H), 7.19–7.15 (m, 3H), 7.29–7.25 (m, 2H). **^{13}C NMR** (400 MHz, $CDCl_3$): δ 13.96, 22.37, 33.68, 35.66, 125.52, 128.19 (2C), 128.39 (2C), 142.88. **IR** (ATR): 743, 910, 1030, 1104, 1378, 1454, 1496, 1604, 2859, 2929, 2958, 3027 cm^{-1}.

Octane (2l)

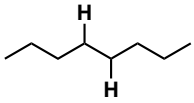

[4 mol% Ir, 130 °C (**condition B**), 10 h (for **1l**)] 99% yield (based on ^{1}H NMR analysis of the crude product). **^{1}H NMR** (400 MHz, $CDCl_3$): δ 0.88 (t, J = 6.4 Hz, 6H), 1.32–1.27 (m, 12H).

Octane (2l)

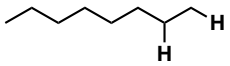

[1 mol% Ir, 120 °C (**condition A**), 3 h (for **1m**)] 96% yield (based on ^{1}H NMR analysis of the crude product). **^{1}H NMR** (400 MHz, $CDCl_3$): δ 0.88 (t, J = 6.4 Hz, 6H), 1.32–1.27 (m, 12H).

5-Methylnonane (2n)

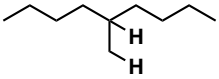

[1 mol% Ir, 120 °C (**condition A**), 3 h] 96% yield (based on ^{1}H NMR analysis of the crude product). **^{1}H NMR** (400 MHz, $CDCl_3$): δ 0.91–0.84 (m, 9H), 1.30–1.08 (m, 13H).

((Cyclohexylmethoxy)methyl)benzene (2o)

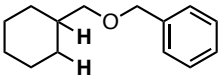

[4 mol% Ir, 130 °C (**condition B**), 20 h] The product **2o** (38.0 mg, 93% yield) was isolated by silica gel column chromatography with hexane/EtOAc (95:5). Colorless oil. **^{1}H NMR** (400 MHz, $CDCl_3$): δ 0.99–0.87 (m, 2H), 1.30–1.10 (m, 3H), 1.81–1.58 (m, 6H), 3.27 (d, J = 6.4 Hz, 2H), 4.49 (s, 2H), 7.34–7.25 (m, 5H). **^{13}C NMR** (400 MHz, $CDCl_3$): δ 25.87 (2C), 26.61, 30.12 (2C), 38.09, 72.91, 76.28, 127.37, 127.50 (2C), 128.29 (2C), 138.79. **IR** (ATR): 732, 1028, 1096, 1117, 1361, 1450, 2850, 2921 cm^{-1}. **FD-HRMS** (m/z): $[M]^+$ Calcd for $C_{14}H_{20}O$, 204.15142. found. 204.15158.

Cyclooctane (2p)

[4 mol% Ir, 130 °C (**condition B**), 40 h] 65% yield (based on ^{1}H NMR analysis of the crude product). **^{1}H NMR** (400 MHz, $CDCl_3$): δ 1.54 (s, 16H).

4-Phenylbutan-2-one (2q)

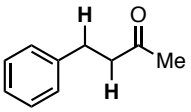

[4 mol% Ir, 130 °C (**condition B**), 10 h] The product **2q** (27.8 mg, 94% yield) was isolated by silica gel column chromatography with hexane/EtOAc (95:5). Colorless oil. **^{1}H NMR** (400 MHz, $CDCl_3$): δ 2.14 (s, 3H), 2.76 (t, J = 7.8 Hz, 2H), 2.90 (t, J = 7.6 Hz, 2H), 7.21–7.17 (m, 3H), 7.30–7.25 (m, 2H). **^{13}C NMR** (100.5 MHz, $CDCl_3$): δ 29.66, 30.05, 45.14, 126.06, 128.25 (2C), 128.45 (2C), 140.93, 207.97. **IR** (ATR): 749, 915, 1031, 1081, 1161, 1228, 1283, 1356, 1454, 1497, 1603, 1714, 2927, 3028 cm^{-1}.

4-(4-Methoxyphenyl)butan-2-one (2r)

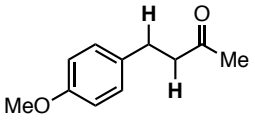

[4 mol% Ir, 130 °C (**condition B**), 10 h] The product **2r** (33.8 mg, 95% yield) was isolated by silica gel column chromatography with hexane/EtOAc (95:5). Colorless oil. **^{1}H NMR** (400 MHz, $CDCl_3$): δ 2.12 (s, 3H), 2.72 (t, J = 7.3 Hz, 2H), 2.83 (t, J = 7.3 Hz, 2H), 3.77 (s, 3H), 6.84–6.79 (m, 2H), 7.26–7.08 (m, 2H). **^{13}C NMR** (100.5 MHz, $CDCl_3$): δ 28.76, 30.02, 45.35, 55.14, 113.77 (2C), 129.13 (2C), 132.89, 157.82, 208.12. **IR** (ATR): 743, 820, 1033, 1159, 1178, 1243, 1512, 1612, 1712, 2936 cm^{-1}.

4-(4-Chlorophenyl)butan-2-one (2s)

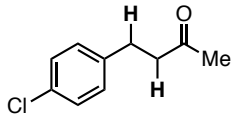

[4 mol% Ir, 130 °C (**condition B**), 10 h] The product **2s** (35.4 mg, 97% yield) was isolated by silica gel column chromatography with hexane/EtOAc (95:5). Colorless oil. **^{1}H NMR** (400 MHz, $CDCl_3$): δ 2.14 (s, 3H), 2.74 (t, J = 7.3 Hz, 2H), 2.86 (t, J = 7.3 Hz, 2H), 7.13–7.10 (m, 2H), 7.26–7.22 (m, 2H). **^{13}C NMR** (100.5 MHz, $CDCl_3$): δ 28.93, 30.10, 44.89, 128.53 (2C), 129.68 (2C), 131.80, 139.43, 207.54. **IR** (ATR): 811, 1015, 1093, 1161, 1359, 1408, 1493, 1714, 2923 cm^{-1}.

4-(4-Fluorophenyl)butan-2-one (2t)

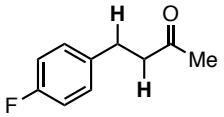

[4 mol% Ir, 130 °C (**condition B**), 10 h] The product **2t** (31.9 mg, 96% yield) was isolated by silica gel column chromatography with hexane/EtOAc (95:5). Colorless oil. **^{1}H NMR** (400 MHz, $CDCl_3$): δ 2.14 (s, 3H), 2.74 (t, J = 7.6 Hz, 2H), 2.87 (t, J = 7.6 Hz, 2H), 6.99–6.94 (m, 2H), 7.16–7.11 (m, 2H). **^{13}C NMR** (100.5 MHz, $CDCl_3$): δ 28.80, 30.11, 45.16, 115.19 (d, $J_{C–F}$ = 21.1 Hz, 2C), 129.67 (d, $J_{C–F}$ = 7.6 Hz, 2C), 136.57 (d, $J_{C–F}$ = 3.8 Hz), 161.3 (d, $J_{C–F}$ = 243.4 Hz), 207.75. **^{19}F NMR** (376 MHz, $CDCl_3$): δ –117.87. **IR** (ATR): 749, 822, 913, 1158, 1220, 1366, 1509, 1716, 2902 cm^{-1}.

4-(4-(Trifluoromethyl)phenyl)butan-2-one (2u)

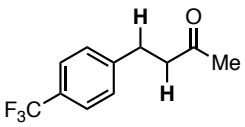

[4 mol% Ir, 130 °C (**condition B**), 10 h] The product **2u** (42.1 mg, 97% yield) was isolated by silica gel column chromatography with hexane/EtOAc (95:5). Colorless oil. **^{1}H NMR** (400 MHz, $CDCl_3$): δ 2.15 (s, 3H), 2.78 (t, J = 7.6 Hz, 2H), 2.95 (t, J = 7.4 Hz, 2H), 7.30 (d, J = 8.2 Hz, 2H), 7.52 (d, J = 8.2 Hz, 2H). **^{13}C NMR** (100.5 MHz,

$CDCl_3$): δ 29.23, 29.89, 44.41, 124.07 (q, J_{C-F} = 272.1 Hz), 125.42 (q, J_{C-F} = 3.8 Hz, 2C), 128.30 (q, J_{C-F} = 32.6 Hz), 128.62 (2C), 145.17, 207.14. **^{19}F NMR** (376 MHz, $CDCl_3$): δ –63.26. **IR** (ATR): 731, 823, 1019, 1066, 1108, 1160, 1323, 1716, 2936 cm^{-1}.

4-(4-(Methylthio)phenyl)butan-2-one (2v)

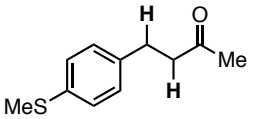

[4 mol% Ir, 145 °C, 48 h in 10 ml a glass pressure tube] The product **2v** (36.2 mg, 93% yield) was isolated by silica gel column chromatography with hexane/EtOAc (95:5). Pale yellow oil. **^{1}H NMR** (400 MHz, $CDCl_3$): δ 2.14 (s, 3H), 2.46 (s, 3H), 2.74 (t, J = 7.4 Hz, 2H), 2.85 (t, J = 7.4 Hz, 2H), 7.10 (d, J = 8.4 Hz, 2H), 7.19 (d, J = 8.0, Hz, 2H). **^{13}C NMR** (100.5 MHz, $CDCl_3$): δ 16.16, 29.10, 30.09, 45.05, 127.07 (2C), 128.81 (2C), 135.69, 137.99, 207.84. **IR** (ATR): 806, 1016, 1095, 1160, 1358, 1405, 1495, 1711, 2920 cm^{-1}.

4-(*o*-Tolyl)butan-2-one (2w)

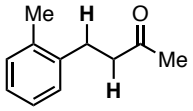

[4 mol% Ir, 130 °C (**condition B**), 10 h] The product **2w** (30.7 mg, 95% yield) was isolated by silica gel column chromatography with hexane/EtOAc (95:5). Colorless oil. **^{1}H NMR** (400 MHz, $CDCl_3$): δ 2.16 (s, 3H), 2.31 (s, 3H), 2.72–2.69 (m, 2H), 2.90–2.86 (m, 2H), 7.16–7.09 (m, 4H). **^{13}C NMR** (100.5 MHz, $CDCl_3$): δ 19.25, 26.96, 30.00, 43.82, 126.07, 126.22, 128.48, 130.24, 135.85, 139.00, 208.06. **IR** (ATR): 755, 1027, 1161, 1261, 1359, 1493, 1716, 2922 cm^{-1}.

4-(Naphthalen-2-yl)butan-2-one (2x)

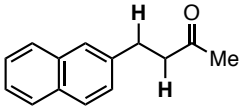

[4 mol% Ir, 130 °C (**condition B**), 10 h] The product **2x** (38.2 mg, 97% yield) was isolated by silica gel column chromatography with hexane/EtOAc (95:5). Colorless oil. **^{1}H NMR** (400 MHz, $CDCl_3$): δ 2.15 (s, 3H), 2.84 (t, J = 7.6 Hz, 2H), 3.06 (t, J = 7.8 Hz, 2H), 7.32 (dd, J = 8.5, 1.6 Hz, 1H), 7.46–7.42 (m, 2H), 7.62 (s, 1H), 7.80–7.76 (m,, 3H). **^{13}C NMR** (100.5 MHz, $CDCl_3$): δ 29.81, 30.13, 45.04, 125.29, 125.99, 126.35, 127.00, 127.40, 127.56, 128.06, 132.00, 133.51, 138.44, 207.95. **IR** (ATR): 748, 814, 859, 1161, 1360, 1408, 1508, 1601, 1714, 2922, 3053 cm^{-1}.

4-(Pyren-1-yl)butan-2-one (2y)

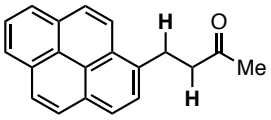

[4 mol% Ir, 130 °C (**condition B**), 10 h] The product **2y** (52.0 mg, 95% yield) was isolated by silica gel column chromatography with hexane/EtOAc (95:5). Pale yellow solid. **M.P.** 89.1–91.7 °C. **^{1}H NMR** (400 MHz, $CDCl_3$): δ 2.15 (s, 3H), 2.97 (t, J = 7.8 Hz, 2H), 3.61 (t, J = 7.8 Hz, 2H), 7.86 (d, J = 7.8 Hz, 1H), 8.01–7.96 (m, 3H), 8.11–8.08 (m, 2H), 8.17–8.15 (m, 2H), 8.21 (d, J = 9.2 Hz, 1H). **^{13}C NMR** (100.5 MHz $CDCl_3$): δ 27.25, 30.15, 45.29, 122.89, 124.83, 124.88, 125.01, 125.87, 126.76, 127.09, 127.43, 127.54, 128.43, 129.99, 130.78, 131.34, 135.08, 207.94 (two carbons are missing due to overlapping). **IR** (ATR): 720, 759, 842, 1160, 1183, 1360, 1416, 1711, 2948, 3040 cm^{-1}. **EI-HRMS** (*m/z*): $[M]^+$ Calcd for $C_{20}H_{16}O$, 272.12011. found. 272.11987.

4-Cyclohexylbutan-2-one (2z)

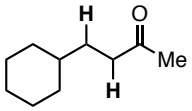

[4 mol% Ir, 130 °C (**condition B**), 10 h] The product **2z** (29.6 mg, 96% yield) was isolated by silica gel column chromatography with hexane/EtOAc (95:5). Colorless oil. **^{1}H NMR** (400 MHz, $CDCl_3$): δ 0.92–0.83 (m, 2H), 1.26–1.07 (m, 4H), 1.49–1.44 (m, 2H), 1.70–1.62 (m, 5H), 2.14 (s, 3H), 2.43 (t, J = 7.8 Hz, 2H). **^{13}C NMR** (100.5 MHz, $CDCl_3$): δ 26.21 (2C), 26.49, 29.83, 31.18, 33.06 (2C), 37.18, 41.35, 209.73. **IR** (ATR): 891, 1162, 1356, 1449, 1716, 2851, 2921 cm^{-1}.

1,3-Diphenylpropan-1-one (2aa)

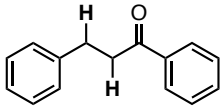

[4 mol% Ir, 130 °C (**condition B**), 10 h] The product **2aa** (40.3 mg, 96% yield) was isolated by silica gel column chromatography with hexane/EtOAc (95:5). White solid. **^{1}H NMR** (400 MHz, $CDCl_3$): δ 3.07 (t, J = 7.8 Hz, 2H), 3.31 (t, J = 7.8 Hz, 2H), 7.32–7.19 (m, 5H), 7.47–7.43 (m, 2H), 7.58–7.51 (m, 1H), 7.98–7.95 (m, 2H). **^{13}C NMR** (100.5 MHz, $CDCl_3$): δ 30.07, 40.43, 126.10, 128.00 (2C), 128.40 (2C), 128.50 (2C), 128.57 (2C), 133.05, 136.77, 141.25, 199.20. **IR** (ATR): 743, 974, 1028, 1205, 1290, 1448, 1598, 1683, 3027, 3062 cm^{-1}.

4-(5-Methylthiophen-2-yl)butan-2-one (2ab)

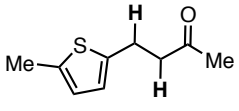

[4 mol% Ir, 130 °C (**condition B**), 10 h] The product **2ab** (33.0 mg, 98% yield) was isolated by silica gel column chromatography with hexane/EtOAc (95:5). Colorless oil. **^{1}H NMR** (400 MHz, $CDCl_3$): δ 2.16 (s, 3H), 2.42 (s, 3H), 2.78 (t, J = 7.6 Hz, 2H), 3.02 (t, J = 7.6 Hz, 2H), 6.56–6.52 (m, 2H). **^{13}C NMR** (100.5 MHz, $CDCl_3$): δ 15.23, 24.04, 30.06, 45.21, 124.22, 124.66, 137.73, 141.26, 207.46. **IR** (ATR): 735, 794, 1162,1230, 1357, 1714, 2920 cm^{-1}.

4,4-Dimethylcyclohexan-1-one (2ac)

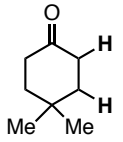

[4 mol% Ir, 130 °C (**condition B**), 10 h] 99% yield (based on ^{1}H NMR analysis of the crude product). **^{1}H NMR** (400 MHz, $CDCl_3$): δ 1.09 (s, 6H), 1.65 (t, J = 7.0 Hz, 4H), 2.30 (t, J = 6.8, Hz, 4H).

4-Phenylpentan-2-one (2ad)

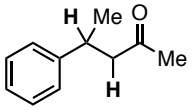

[4 mol% Ir, 130 °C (**condition B**), 10 h] The product **2ad** (30.6 mg, 94% yield) was isolated by silica gel column chromatography with hexane/EtOAc (95:5). Colorless oil. **^{1}H NMR** (400 MHz, $CDCl_3$): δ 1.26 (d, J = 7.2 Hz, 3H), 2.06 (s, 3H), 2.66 (dd, J = 16.0, 8.0 Hz, 1H), 2.76 (dd, J = 16.8, 6.4 Hz, 1H), 3.35–3.26 (m, 1H), 7.22–7.16 (m, 3H), 7.32–7.28 (m, 2H). **^{13}C NMR** (100.5 MHz, $CDCl_3$): δ 21.97, 30.55, 35.38, 51.92, 126.27, 126.71 (2C), 128.50 (2C), 146.11, 207.87. **IR** (ATR): 758, 910, 1025, 1162, 1357, 1453, 1494, 1603, 1714, 2963, 3029 cm^{-1}.

4-Phenylpentan-2-one (2ae)

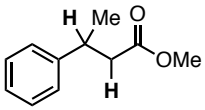

[4 mol% Ir, 130 °C (**condition B**), 10 h] The product **2ae** (35.2 mg, 99% yield) was isolated by silica gel column chromatography with hexane/EtOAc (95:5). Colorless oil. **^{1}H NMR** (400 MHz, $CDCl_3$): δ 1.30 (d, J = 6.8 Hz, 3H), 2.54 (dd, J = 15.2, 8.0 Hz, 1H), 2.62 (dd, J = 14.8, 6.8 Hz, 1H), 3.33–3.24 (m, 1H), 3.62 (s, 3H), 7.23–7.18 (m, 3H), 7.32–7.28 (m, 2H). **^{13}C NMR** (100.5 MHz, $CDCl_3$): δ 21.74, 36.37, 42.69, 51.49, 126.37, 126.67 (2C), 128.47 (2C), 145.64, 172.83. **IR** (ATR): 763, 841, 881, 1022, 1085, 1166, 1268, 1436, 1736, 2963, 3029 cm^{-1}.

Benzyl isobutyrate (2af)

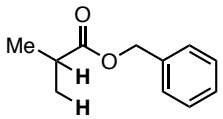

[4 mol% Ir, 130 °C (**condition B**), 10 h] The product **2af** (34.3 mg, 96% yield) was isolated by silica gel column chromatography with hexane/EtOAc (95:5). Colorless oil. **^{1}H NMR** (400 MHz, $CDCl_3$): δ 1.19 (d, J = 6.9 Hz, 6H), 2.60 (sept, J = 6.8 Hz, 1H), 5.11 (s, 2H), 7.39–7.28 (m, 5H). **^{13}C NMR** (100.5 MHz, $CDCl_3$): δ 18.93 (2C), 33.96, 65.98, 127.92 (2C), 128.04, 128.48 (2C), 136.20, 176.91. **IR** (ATR): 733, 909, 966, 1070, 1147, 1188, 1258, 1343, 1456, 1733, 2975 cm^{-1}.

***N*,*N*-Dimethyl-3-phenylpropanamide (2ag)**

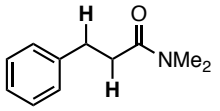

[4 mol% Ir, 130 °C (**condition B**), 10 h] The product **2ag** (34.3 mg, 96% yield) was isolated by silica gel column chromatography with hexane/EtOAc (80:20). Colorless oil. **^{1}H NMR** (400 MHz, $CDCl_3$): δ 2.62 (t, J = 7.8 Hz, 2H), 2.91 (s, 3H), 2.95 (s, 3H), 2.97 (t, J = 7.6 Hz, 2H), 7.23–7.18 (m, 3H), 7.31–7.26 (m, 2H). **^{13}C NMR** (100.5 MHz, $CDCl_3$): δ 31.30, 35.28, 35.37, 37.10, 126.03, 128.36 (2C), 128.40 (2C), 141.43, 172.13. **IR** (ATR): 753, 851, 1076, 1140, 1266, 1346, 1397, 1454, 1495, 1640, 2931, 3027 cm^{-1}.

1-(4-Propylphenyl)ethan-1-one (2ah)

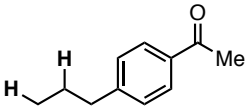

[4 mol% Ir, 130 °C (**condition B**), 10 h] The product **2ah** (30.8 mg, 95% yield) was isolated by silica gel column chromatography with hexane/EtOAc (95:5). Colorless oil. **^{1}H NMR** (400 MHz, $CDCl_3$): δ 0.95 (t, J = 7.3 Hz, 3H), 1.66 (sext, J = 7.2 Hz, 2H), 2.58 (s, 3H), 2.64 (t, J = 7.6 Hz, 2H), 7.26 (d, J = 8.2 Hz, 2H), 7.88 (d, J = 8.7 Hz, 2H). **^{13}C NMR** (100.5 MHz, $CDCl_3$): δ 13.70, 24.18, 26.50, 37.95, 128.38 (2C), 128.60 (2C), 134.83, 148.50, 197.88. **IR** (ATR): 740, 759, 955, 1046, 1250, 1355, 1600, 1685, 1738, 2872, 2962 cm^{-1}.

1-(2-Propylphenyl)ethan-1-one (2ai)

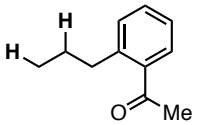

[4 mol% Ir, 130 °C (**condition B**), 10 h] The product **2ai** (31.7 mg, 98% yield) was isolated by silica gel column chromatography with hexane/EtOAc (95:5). Colorless oil. **^{1}H NMR** (400 MHz, $CDCl_3$): δ 0.96 (t, J = 7.6 Hz, 3H), 1.59 (sext, J = 7.2 Hz, 2H),

2.57 (s, 3H), 2.82 (t, J = 7.8 Hz, 2H), 7.27–7.23 (m, 2H), 7.38 (td, J = 7.2, 1.2 Hz, 1H), 7.63–7.61 (m, 1H). **^{13}C NMR** (100.5 MHz, $CDCl_3$): δ 14.15, 24.90, 29.98, 35.93, 125.61, 128.90, 131.15, 131.19, 138.06, 142.55, 202.38. **IR** (ATR): 757, 954, 1046, 1072, 1249, 1355, 1684, 2932, 2962 cm^{-1}. **EI-HRMS** (*m/z*): $[M]^+$ Calcd for $C_{11}H_{14}O$, 162.10446. found. 162.10483.

1-(4-Ethylphenyl)ethan-1-one (2aj)

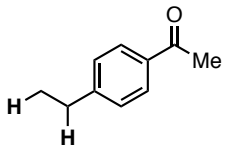

[4 mol% Ir, 130 °C (**condition B**), 10 h] The product **2aj** (27.5 mg, 94% yield) was isolated by silica gel column chromatography with hexane/EtOAc (95:5). Colorless oil. **^{1}H NMR** (400 MHz, $CDCl_3$): δ 1.26 (t, J = 7.6 Hz, 3H), 2.58 (s, 3H), 2.71 (q, J = 7.6 Hz, 2H), 7.28 (d, J = 8.7 Hz, 2H), 7.89 (d, J = 8.2 Hz, 2H). **^{13}C NMR** (100.5 MHz, $CDCl_3$): δ 15.18, 26.52, 28.88, 128.01 (2C), 128.50 (2C), 134.83, 150.02, 197.86. **IR** (ATR): 731, 830, 956, 1182, 1267, 1357, 1607, 1681, 2968 cm^{-1}.

2-Propylcyclohexan-1-one (2ak)

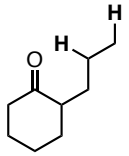

[4 mol% Ir, 130 °C (**condition B**), 10 h] The product **2ak** (27.7 mg, 98% yield) was isolated by silica gel column chromatography with hexane/EtOAc (95:5). Colorless oil. **^{1}H NMR** (400 MHz, $CDCl_3$): δ 0.90 (t, J = 7.4 Hz, 3H), 1.43–1.11 (m, 4H), 1.91–1.60 (m, 4H), 2.15–1.95 (m, 2H), 2.38–2.30 (m, 3H). **^{13}C NMR** (100.5 MHz, $CDCl_3$): δ 14.17, 20.25, 24.76, 28.00, 31.52, 33.77, 41.92, 50.44, 213.68. **IR** (ATR): 734, 815, 1064, 1119, 1449, 1709, 2862, 2932 cm^{-1}.

1-(4'-Ethyl-[1,1'-biphenyl]-4-yl)ethan-1-one (2al)

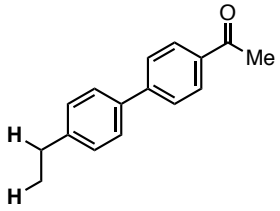

[4 mol% Ir, 130 °C (**condition B**), 10 h] The product **2al** (44.0 mg, 98% yield) was isolated by silica gel column chromatography with hexane/EtOAc (95:5). White solid. **^{1}H NMR** (400 MHz, $CDCl_3$): δ 1.28 (t, J = 7.6 Hz, 3H), 2.64 (s, 3H), 2.71 (q, J = 7.6 Hz, 2H), 7.31 (d, J = 8.2 Hz, 2H), 7.56 (d, J = 8.4 Hz, 2H), 7.68 (d, J = 8.4 Hz, 2H),

8.02 (d, J = 8.7 Hz, 2H). **^{13}C NMR** (100.5 MHz, $CDCl_3$): δ 15.54, 26.66, 28.54, 126.96 (2C), 127.17 (2C), 128.48 (2C), 128.88 (2C), 135.53, 137.15, 144.56, 145.72, 197.78. **IR** (ATR): 745, 819, 913, 1078, 1267, 1359, 1398, 1679, 2967 cm^{-1}

4-Ethyl-4'-nitro-1,1'-biphenyl (2am)

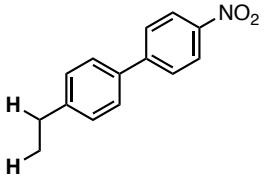

[4 mol% Ir, 130 °C (**condition B**), 10 h] The product **2am** (43.7 mg, 96% yield) was isolated by silica gel column chromatography with hexane/EtOAc (95:5). Pale yellow solid. **^{1}H NMR** (400 MHz, $CDCl_3$): δ 1.28 (t, J = 7.6 Hz, 3H), 2.72 (q, J = 7.6 Hz, 2H), 7.32 (d, J = 8.4 Hz, 2H), 7.55 (d, J = 8.0 Hz, 2H), 7.71 (d, J = 8.8 Hz, 2H), 8.26 (d, J = 8.4 Hz, 2H). **^{13}C NMR** (100.5 MHz, $CDCl_3$): δ 15.45, 28.54, 124.04 (2C), 127.27 (2C), 127.44 (2C), 128.66 (2C), 135.99, 145.35, 146.75, 147.53. **IR** (ATR): 754, 828, 856, 1344, 1486, 1515, 1597, 2849, 2917 cm^{-1}.

4'-Ethyl-[1,1'-biphenyl]-4-carbonitrile (2an)

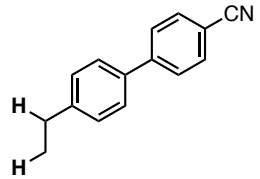

[4 mol% Ir, 130 °C (**condition B**), 10 h] The product **2an** (40.6 mg, 98% yield) was isolated by silica gel column chromatography with hexane/EtOAc (95:5). White solid. **^{1}H NMR** (400 MHz, $CDCl_3$): δ 1.28 (t, J = 7.8 Hz, 3H), 2.71 (q, J = 7.5 Hz, 2H), 7.31 (d, J = 7.8 Hz, 2H), 7.51 (d, J = 7.8 Hz, 2H), 7.71–7.68 (m, 4H). **^{13}C NMR** (100.5 MHz, $CDCl_3$): δ 15.48, 28.53, 110.46, 119.03, 127.11 (2C), 127.44 (2C), 128.62 (2C), 132.52 (2C), 136.44, 145.03, 145.56. **IR** (ATR): 730, 818, 957. 1004, 1186, 1266, 1358, 1398, 1601, 1679, 2967 cm^{-1}.

3-(4-Ethylphenyl)benzo[*d*]isothiazole 1,1-dioxide (2ao)

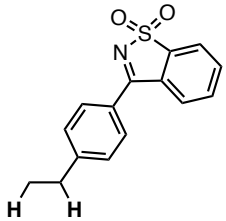

[4 mol% Ir, 145°C, 48 h in 10 ml glass pressure tube] 87% yield (based on ^{1}H NMR analysis of the crude product, using 1,1,2,2-tetrabromoethane as an internal standard).

Analytically pure **2ao** was isolated by silica gel column chromatography with hexane/EtOAc (95:5), albeit with significant loss of **2ao** (11.4 mg, 21% isolated yield). White solid. **M.P.** 121.2–122.8 °C. **^{1}H NMR** (400 MHz, $CDCl_3$): δ 1.32 (t, J = 7.8 Hz, 3H), 2.79 (q, J = 7.6 Hz, 2H), 7.44 (d, J = 8.2 Hz, 2H), 7.80–7.71 (m, 2H), 7.95–7.91 (m, 3H), 8.01 (d, J = 6.9 Hz, 1H). **^{13}C NMR** (100.5 MHz, $CDCl_3$): δ 15.17, 29.05, 123.00, 126.62, 127.85, 128.77 (2C), 129.75 (2C), 130.73, 133.23, 133.53, 141.12, 150.72, 170.85. **IR** (ATR): 731, 801, 969, 1172, 1265, 1334, 1507, 1532, 1609, 2970, 3057 cm^{-1}. **EI-HRMS** (*m/z*): $[M]^+$ Calcd for $C_{15}H_{13}NO_2S$, 271.06670. found. 271.06657.

(8*R*,9*S*,13*S*,14*S*)-3-Ethyl-13-methyl-6,7,8,9,11,12,13,14,15,16-decahydro-17*H*-cyclopenta[*a*]phenanthren-17-one (2ap)

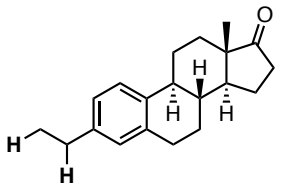

[4 mol% Ir, 130 °C (**condition B**), 10 h] The product **2ap** (55.4 mg, 98% yield) was isolated by silica gel column chromatography with hexane/EtOAc (95:5). White solid. **M.P.** 141.3–142.5 °C. **^{1}H NMR** (400 MHz, $CDCl_3$): δ 0.91 (s, 3H), 1.23 (t, J = 7.6 Hz, 3H), 1.63–1.37 (m, 6H), 2.19–1.91 (m, 4H), 2.35–2.26 (m, 1H), 2.54–2.40 (m, 2H), 2.59 (t, J = 7.6 Hz, 2H), 2.91–2.89 (m, 2H), 6.96 (s, 1H), 7.00 (d, J = 8.0 Hz, 1H), 7.22 (d, J = 8.4 Hz, 1H). **^{13}C NMR** (100.5 MHz, $CDCl_3$): δ 13.82, 15.60, 21.57, 25.72, 26.56, 28.27, 29.40, 31.57, 35.86, 38.21, 44.27, 48.01, 50.46, 125.32 (1C+1C, overlapping), 128.50, 136.31, 136.94, 141.71, 221.07. **IR** (ATR): 823, 890, 1007, 1084, 1258, 1456, 1500, 1737, 2868, 2928, 2961 cm^{-1}. **EI-HRMS** (*m/z*): $[M]^+$ Calcd for $C_{20}H_{26}O$, 282.19836. found. 282.19795. **$[\alpha]_D^{25}$** +171.957 (*c* 0.42, $CHCl_3$).

References

(1) For selected reviews on transfer hydrogenation reactions, see: (a) Brieger, G.; Nestrick, T. J. Catalytic Transfer Hydrogenation. *Chem. Rev*. **1974**, *74*, 567–580. (b) Johnstone, R. A. W.; Wilby, A. H.; Entwistle, I. D. Heterogeneous Catalytic Transfer Hydrogenation and its Relation to Other Methods for Reduction of Organic Compounds. *Chem. Rev*. **1985**, *85*, 129–170. (c) Zassinovich, G.; Mestroni, G.; Gladiali, S. Asymmetric Hydrogen Transfer Reactions Promoted by Homogeneous Transition Metal Catalysts. *Chem. Rev*. **1992**, *92*, 1051–1069. (d) Fujita, K.; Yamaguchi, R. Cp*Ir Complex-Catalyzed Hydrogen Transfer Reactions Directed towards Environmentally Benign Organic Synthesis. *Synlett* **2005**, 560–571. (e) Dobereiner, G. E.; Crabtree, R. H. Dehydrogenation as a Substrate-Activating Strategy in Homogeneous Transition-Metal Catalysis. *Chem. Rev*. **2010**, *110*, 681–703. (f) Wang, D.; Astruc, D. The Golden Age of Transfer Hydrogenation. *Chem. Rev*. **2015**, *115*, 6621–6686. (g) Werkmeister, S.; Neumann, J.; Junge, K.; Beller, M. Pincer-Type Complexes for Catalytic (De)Hydrogenation and Transfer (De)Hydrogenation Reactions: Recent Progress. *Chem. Eur. J.* **2015**, *21*, 12226–12250.

(2) For selected references on transfer hydrogenation of ketones, see: (a) Reetz, M. T.; Li, X. An Efficient Catalyst System for the Asymmetric Transfer Hydrogenation of Ketones: Remarkably Broad Substrate Scope. *J. Am. Chem. Soc*. **2006**, *128*, 1044–1045. (b) Clarke, Z. E.; Maragh, P. T.; Dasgupta, T. P.; Gusev, D. G.; Lough, A. J.; Abdur-Rashid, K. A Family of Active Iridium Catalysts for Transfer Hydrogenation of Ketones. *Organometallics* **2006**, *25*, 4113–4117. (c) Sonnenberg, J. F.; Coombs, N.; Dube, P. A.; Morris, R. H. Iron Nanoparticles Catalyzing the Asymmetric Transfer Hydrogenation of Ketones. *J. Am. Chem. Soc*. **2012**, *134*, 5893–5899. (d) Johnson, T. C.; Totty, W. G.; Wills, M. Application of Ruthenium Complexes of Trizole-Containing Tridentate Ligands to Asymmetric Transfer Hydrogenation of Ketones. *Org. Lett.* **2012**, *14*, 5230–5233. (e) Zuo, W.; Lough, A. J.; Li, Y. F.; Morris, R. H. Amine(imine)diphosphine Iron Catalyst for Asymmetric Transfer Hydrogenation of Ketones and Imines. *Science* **2013**, *342*, 1080–1083. (f) Touge, T.; Nara, H.; Fujiwhara, M.; Kayaki, Y.; Ikariya, T. Efficient Access to Chiral Benzhydrols via Asymmetric Transfer Hydrogenation of Unsymmetrical Benzophenones with Bifunctional Oxo-Tether Ruthenium Catalysts. *J. Am. Chem. Soc*. **2016**, *138*, 10084–10087**.**

(3) For selected references on transfer hydrogenation of imines, see: (a) Uematsu, N.; Fujii, A.; Hashiguchi, S.; Ikariya, T.; Noyori, R. Asymmetric Transfer Hydrogenation of Imines. *J. Am. Chem. Soc.* **1996**, *118*, 4916–4917. (b) Gnanamgari, D.; Moores, A.; Rajaseelan, E.; Grabtree, R. H. Transfer Hydrogenation of Imines and Alkenes and Direct Reduction Amination of Aldehydes Catalyzed by Triazole-Derived Iridium(I) Carbene Complexes. *Organometallics* **2007**, *26*, 1226–1230. (c) Wang, C.; Pettman, A.; Bacsa, J.; Xiao,

J. A Versatile Catalyst for Reductive Amination by Transfer Hydrogenation. *Angew. Chem., Int. Ed*. **2010**, *49*, 7548–7552. (d) Li, S.; Li, G.; Meng, W.; Du, H. A Frustrated Lewis Pair Catalyzed Asymmetric Transfer Hydrogenation of Imines Using Ammonia Borane. *J. Am. Chem. Soc*. **2016**, *138*, 12956–12962.

(4) (a) Hashiguchi, S.; Fujii, A.; Takehara, J.; Ikariya, T.; Noyori, R. Asymmetric Transfer Hydrogenation of Aromatic Ketones Catalyzed by Chiral Ruthenium(II) Complexes. *J. Am. Chem. Soc*. **1995**, *117*, 7562–7563. (b) Noyori, R.; Hashiguchi, S. Asymmetric Transfer Hydrogenation Catalyzed by Chiral Ruthenium Complexes. *Acc. Chem. Res*. **1997**, *30*, 97–102. (c) Noyori, R. Asymmetric Catalysis: Science and Opportunities. *Angew. Chem., Int. Ed*. **2002**, *41*, 2008–2022. (d) Ikariya, T.; Murata, K.; Noyori, R. Bifunctional Transition Metal-Based Molecular Catalysts for Asymmetric Syntheses. *Org. Biomol. Chem*. **2006**, *4*, 393–406.

(5) For alcohol as a hydrogen donor, see: (a) Sasson, Y.; Blum, J. Dichlorotris(triphenylphosphine)ruthenium-Catalyzed Hydrogen Transfer from Alcohols to Saturated and α,β-Unsaturated Ketones. *J. Org. Chem.* **1975**, *40*, 1887–1896. (b) Sakaguchi, S.; Yamaga, T.; Ishii, Y. Iridium-Catalyzed Transfer Hydrogenation of α,β-Unsaturated and Saturated Carbonyl Compounds with 2-Propanol. *J. Org. Chem*. **2001**, *66*, 4710–4712. (c) Ding, B.; Zhang, Z.; Liu, Y.; Sugiya, M.; Imamoto, T.; Zhang, W. Chemoselective Transfer Hydrogenation of α,β-Unsaturated Ketones Catalyzed by Pincer-Pd Complexes Using Alcohol as a Hydrogen Source. *Org. Lett*. **2013**, *15*, 3690–3693. (d) Chen, S.-J.; Lu, G.-P.; Cai, C. A Base-Controlled Chemoselective Transfer Hydrogenation of α,β-Unsaturated Ketones Catalyzed by $[IrCp^*Cl_2]_2$ with 2-Propanol. *RSC Adv*. **2015**, *5*, 13208–13211.

(6) For hydrosilane as a hydrogen donor, see: (a) Keinan, E.; Greenspoon, N. Highly Chemoselective Palladium-Catalyzed Conjugate Reduction of α,β-Unsaturated Carbonyl Compounds with Silicon Hydrides and Zinc Chloride Cocatalyst. *J. Am. Chem. Soc*. **1986**, *108*, 7314–7325. (b) Appella, D. H.; Moritani, Y.; Shintani, R.; Ferreira, E. M.; Buchwald, S. L. Asymmetric Conjugate Reduction of α,β-Unsaturated Esters Using a Chiral Phosphine-Copper Catalyst. *J. Am. Chem. Soc*. **1999**, *121*, 9473–9474. (c) Moritani, Y.; Appella, D. H.; Jurkauskas, V.; Buchwald, S. L. Synthesis of α–Alkyl Cyclopentanones in High Enantiomeric Excess via Copper-Catalyzed Asymmetric Conjugate Reduction. *J. Am. Chem. Soc*. **2000**, *122*, 6797–6798. (d) Lipshutz, B. H.; Servesko, J. M. CuH-Catalyzed Asymmetric Conjugate Reduction of Acyclic Enones. *Angew. Chem., Int. Ed*. **2003**, *42*, 4789–4792.

(7) For formate as a hydrogen donor, see: (a) Himeda, Y.; Onozawa-Komatsuzaki, N.; Miyazawa, S.; Sugihara, H.; Hirose, T.; Kasuga, K. pH-Dependent Catalytic Activity and Chemoselectivity in Transfer Hydrogenation Catalyzed by Iridium Complex with 4,4'-Dihyroxys-2,2'-bipyridine. *Chem. Eur. J*. **2008**, *14*, 11076–11081. (b) Li, X.; Li, L.; Tang, Y.; Zhong, L.; Cun, L.; Zhu, J.; Liao, J.; Deng, J.

Chemoselective Conjugate Reduction of α,β-Unsaturated Ketones Catalyzed by Rhodium Amido Complexes in Aqueous Media. *J. Org. Chem*. **2010**, *75*, 2981–2988.

(8) For selected reviews on metal-catalyzed C(sp^3)–H functionalization reactions, see: (a) Labinger, J. A.; Bercaw, J. E. Understanding and Exploiting C–H Bond Activation. *Nature* **2002**, *417*, 507–514. (b) Hartwig, J. F. Carbon-Heteroatom Bond Formation Catalysed by Organometallic Complexes. *Nature* **2008**, *455*, 314–322. (c) Lyons, T. W.; Sanford, M. S. Palladium-Catalyzed Ligand-Directed C–H Functionalization Reactions. *Chem. Rev*. **2010**, *110*, 1147–1169. (d) Shang, R.; Ilies, L.; Nakamura, E. Iron-Catalyzed C–H Bond Activation. *Chem. Rev*. **2017**, *117*, 9086–9139. (e) He, J.; Wasa, M.; Chan, K. S. L.; Shao, Q.; Yu, J.-Q. Palladium-Catalyzed Transformation of Alkyl C–H Bonds. *Chem. Rev.* **2017**, *117*, 8754–8786. (f) Chu, C. K.; Rovis, T. Complementary Strategies for Directed C(sp^3)–H Functionalization: A Comparison of Transition-Metal-Catalyzed Activation, Hydrogen Atom Transfer, and Carbene/Nitrene Transfer. *Angew. Chem., Int. Ed.* **2018**, *57*, 62–101.

(9) For our work on C(sp^3)–H functionalization, see: (a) Kawamorita, S.; Miyazaki, T.; Iwai, T.; Ohmiya, H.; Sawamura, M. Rh-Catalyzed Borylation of N-Adjacent C(sp^3)–H Bonds with a Silica-Supported Triaryphosphine Ligand. *J. Am. Chem. Soc*. **2012**, *134*, 12924–12927. (b) Kawamorita, S.; Murakami, R.; Iwai, T.; Sawamura, M. Synthesis of Primary and Secondary Alkylboronates through Site-Selective C(sp^3)–H Activation with Silica-Supported Monophosphine–Ir Catalysts. *J. Am. Chem. Soc*. **2013**, *135*, 2947–2950. (c) Reyes, R. L.; Harada, T.; Taniguchi, T.; Monde, K.; Iwai, T.; Sawamura, M. Enantioselective Rh- or Ir-Catalyzed Directed C(sp^3)–H Borylation with Phosphoramidite Chiral Ligands. *Chem. Lett*. **2017**, *46*, 1747–1750. (d) Murakami, R.; Sano, K.; Iwai, T.; Taniguchi, T.; Monde, K.; Sawamura, M. Palladium-Catalyzed Asymmetric C(sp^3)–H Allylation of 2-Alkylpyridines. *Angew. Chem., Int. Ed.* **2018**, *57*, 9465–9469. (e) Reyes, R. L.; Iwai, T.; Maeda, S.; Sawamura, M. Iridium-Catalyzed Asymmetric Borylation of Unactivated Methylene C(sp^3)–H Bonds. *J. Am. Chem. Soc.* **2019**, *141*, 6817–6821.

(10) (a) Nishiguchi, T.; Tachi, K.; Fukuzumi, K. Hydrogen Transfer from Dioxane to an Olefin Catalyzed by Chlorotris(triphenylphosphine)rhodium(I). *J. Am. Chem. Soc*. **1972**, *94*, 8916–8917. (b) Nishiguchi, T.; Fukuzumi, K. Transfer-Hydrogenation and Transfer-Hydrogenolysis. III. Hydrogen Transfer from Dioxane to Olefins Catalyzed by Chlorotris(triphenylphosphine)rhodium(I). *J. Am. Chem. Soc*. **1974**, *96*, 1893–1897.

(11) Wang, Y.; Huang, Z.; Leng, X.; Zhu, H.; Liu, G.; Huang, Z. Transfer Hydrogenation of Alkenes Using Ethanol Catalyzed by a NCP Pincer Iridium Complex: Scope and Mechanism. *J. Am. Chem. Soc*. **2018**, *140*, 4417–4429.

(12) THF also served as a hydrogen donor albeit with much lower reaction efficacy. A linear ether 1,2-diethoxyethane induced no transfer hydrogenation (See SI).

Ohmura and Suginome described the occurrence of transfer hydrogenation of alkenes and alkynes from THF or octane solvents as side reactions of Ir-catalyzed reactions. (a) Torigoe, T.; Ohmura, T.; Suginome, M. Iridium-Catalyzed Intramolecular Methoxy C–H Addition to Carbon–Carbon Triple Bonds: Direct Synthesis of 3-Substituted Benzofurans from *o*-Methoxyphenylalkynes. *Chem. Eur. J.* **2016**, *22*, 10415–10419. (b) Torigoe, T.; Ohmura, T.; Suginome, M. Asymmetric Cycloisomerization of *o*-Alkenyl-*N*-Methylanilines to Indolines by Iridium-Catalyzed C(sp^3)–H Addition to Carbon–Carbon Double Bonds. *Angew. Chem., Int. Ed*. **2017**, *56*, 14272–14276.

(13) Tani, K.; Iseki, A.; Yamagata, T. Efficient Transfer Hydrogenation of Alkynes and Alkenes with Methanol Catalysed by Hydrido(methoxo)iridium(III) Complexes. *Chem. Commun.* **1999**, 1821–1822.

(14) Samec, J. S. M.; Bäckvall, J.-E.; Andersson, P. G.; Brandt, P. Mechanistic Aspects of Transition Metal-Catalyzed Hydrogen Transfer Reactions. *Chem. Soc. Rev*. **2006**, *35*, 237–248.

(15) (a) Iwai, T.; Harada, T.; Shimada, H.; Asano, K.; Sawamura, M. A Polystyrene-Cross-Linking Bisphosphine: Controlled Metal Monochelation and Ligand-Enabled First-Row Transition Metal Catalysis. *ACS Catal*. **2017**, *7*, 1681–1692. (b) Yamazaki, Y.; Arima, N.; Iwai, T.; Sawamura, M. Heterogeneous Nickel-Catalyzed Cross-Coupling between Aryl Chlorides and Alkyllithiums Using a Polystyrene-Cross-Linking Bisphosphine Ligand. *Adv. Synth. Catal.* **2019**, *361*, 2250–2254. (c) Nishizawa, A.; Takahira, T.; Yasui, K.; Fujimoto, H.; Iwai, T.; Sawamura, M.; Chatani, N.; Tobisu, M. Nickel-Catalyzed Decarboxylation of Aryl Carbamates for Converting Phenols into Aromatic Amines. *J. Am. Chem. Soc.* **2019**, *141*, 7261–7265.

(16) Walter, R.; Kirchner, S.; Franz, R. Method for Producing $[IrCl(cod)]_2$. U.S. Patent 6,399,804, **2002**.

(17) de Miguel, I.; Herradón, B.; Mann, E. Intramolecular Azide-Alkene 1,3-Dipolar Cycloaddition/Enamine Addition(s) Cascade Reaction: Synthesis of Nitrogen-Containing Heterocycles. *Adv. Synth. Catal*. **2012**, *354*, 1731–1736.

(18) Erdeljac, N.; Kehr, G.; Ahlqvist, M.; Knerr, L.; Gilmour, R. Exploring Physicochemical Space via Bioisostere of the Trifluormethyl and Ethyl Groups (BITE): Attenuating Lipophilicity in Fluorinated Analogues of Gilenya® for Multiple Sclerosis. *Chem. Commun.* **2018**, 54, 12002–12005.

(19) Gonzalez-de-Castro, A.; Xiao, J. Green and Efficient: Iron-Catalyzed Selective Oxidation of Olefins to Carbonyls with O_2. *J. Am. Chem. Soc*. **2015**, *137*, 8206–8218.

(20) Liwosz, T. W.; Chemler, S. R. Copper-Catalyzed Oxidative and Allylic Amination of Alkenes. *Chem. Eur. J.* **2013**, *19*, 12771–12777.

(21) Iwasaki, M.; Hayashi, S.; Hirano, K.; Yorimitsu, H.; Oshima, K. $Pd(OAc)_2/P(^cC_6H_{11})_3$-Catalyzed Allylation of Aryl Halides with Homoallyl Alcohols via Retro-Allylation. *J. Am. Chem. Soc*. **2007**, *129*, 4463–4469.

(22) Sammet, K.; Gastl, C.; Baro, A.; Laschat, S.; Fisher, P.; Fettig, I. Enders' SAMP-Hydrazone as Traceless Auxiliary in the Asymmetric 1,4-Addition of Cuprates to Enones. *Adv. Synth. Catal*. **2010**, *352*, 2281–2290.

(23) Chen, W.; Chen, H.; Xiao, F.; Deng, G.-J. Palladium-Catalyzed Conjugate Addition of Arysulfonyl Hydrazides to α, β-Unsaturated Ketones. *Org. Biomol. Chem*. **2013**, *11*, 4295–4298.

(24) Youn, S. W.; Kim, B. S.; Jagdale, A. R. Pd-Catalyzed Sequential C-C Bond Formation and Cleavage: Evidence for an Unexpected Generation of Arypalladium(II) Species. *J. Am. Chem. Soc.* **2012**, *134*, 11308–11311.

(25) Kim, M.; Jung, H.; Aragonès, A. C.; Díez-Pérez, I.; Ahn, K.-H.; Chung, W.-J.; Kim, D.; Koo, S. Role of Ring *Ortho* Substituents on the Configuration of Carotenoid Polyene Chains. *Org. Lett*. **2018**, *20*, 493‑496.

(26) Titu, D.; Chadha, A. Enantiomerically Pure Allylic Alcohols: Preparation by Candida Parapsilosis ATCC 7330 Mediated Deracemisation. *Tetrahedron: Asymmetry* **2008**, *19*, 1698–1701.

(27) Wang, M.; Lin, L.; Shi, J.; Liu, X.; Kuang, Y.; Feng, X. Asymmetric Crossed-Conjugate Addition of Nitroalkenes to Enones by a Chiral Bifunctional Diamine Organocatalyst. *Chem. Eur. J.* **2011**, *17*, 2365–2368.

(28) Magoulas, G. E.; Bariamis, S. E.; Athanassopoulos, C. M.; Haskopoulos, A.; Dedes, P. G.; Krokidis, M. G.; Karamanos, N. K.; Kletsas, D.; Papaioannou, D.; Maroulis, G. Syntheses, Antiproliferative Activity and Theoretical Characterization of Acitretin-Type Retinoids with Changes in the Lipophilic Part. *Eur. J. Med. Chem*. **2011**, *46*, 721–737.

(29) Canela, M.-D.; Pérez-Pérez, M.-J.; Noppen, S.; Sáez-Calvo, G.; Díaz, J. F.; Camarasa, M.-J.; Liekens, S.; Priego, E.-M. Novel Colchicine-Site inders with a Cyclohexanedione Scaffold Identified through a Ligand-Based Virtual Screening Approach. *J. Med. Chem.* **2014**, *57*, 3924–3938.

(30) Das, D.; Pratihar, S.; Roy, S. Heterobimetallic Pd-Sn Catalysis: Michael Addition Reaction with C-, N-, O-, and S-Nucleophiles and in Situ Diagnostics. *J. Org. Chem*. **2013**, *78*, 2430–2442.

(31) Brenna, E.; Crotti, M.; Pieri, M. De.; Gatti, F. G.; Manenti, G.; Monti, D. Chemo-Enzymatic Oxidative Rearrangement of Tertiary Allylic Alcohols: Synthetic Application and Integration into A Cascade Process. *Adv. Synth. Catal*. **2018**, *360*, 3677–3686.

(32) Michelet, B.; Bour, C.; Gandon, V. Gallium-Assisted Transfer Hydrogenation of Alkenes. *Chem. Eur. J.* **2014**, *20*, 14488–14492.

(33) Li, W.; Yin, C.; Yang, X.; Liu, H.; Zheng, X.; Yuan, M.; Li, R.; Fu, H.; Chen, H. Cu(II)-Mediated Keto C(sp^3)–H Bond α–Acyloxylation of *N,N*-dialkylamides with Aromatic Carboxylic Acids. *Org. Biomol. Chem*. **2017**, *15*, 7594–7599.

(34) Kotha, S.; Behera, M.; Shah, V. R. A Simple Synthetic Approach to Allylated Aromatics via the Suzuki-Miyaura Cross-Coupling. *Synlett* **2005**, 1877–1880.

(35) Tarantino, K. T.; Liu, P.; Knowles, R. R. Catalytic Ketyl-Olefin Cyclizations Enabled by Proton-Coupled Electron Transfer. *J. Am. Chem. Soc*. **2013**, *135*, 10022–10025.
(36) Molander, G. A.; Rivero, M. R. Suzuki Cross-Coupling Reactions of Potassium Alkenyltrifluoroborates. *Org. Lett*. **2002**, *4*, 107‑109.
(37) Ma, X.; Liu, Y.; Liu, P.; Xie, J.; Dai, B.; Liu, Z. A Rapid and Efficient Catalysis System for the Synthesis of 4-Vinylbiphenyl Derivatives. *App. Organometal. Chem*. **2013**, *27*, 707–710.
(38) Scheidt, F.; Neufeld, J.; Schafer, M.; Thiehoff, C.; Gilmour, R. Catalytic Geminal Diflurination of Styrenes for the Construction of Fluorine-rich Bioisosteres. *Org. Lett*. **2018**, *20*, 8073‑8076.

Chapter 2

Iridium-Catalyzed Reversible Acceptorless Dehydrogenation/Hydrogenation of *N*-Substituted and Unsubstituted Heterocycles Enabled by a Polymer-Cross-Linking Bisphosphine

The polystyrene-cross-linking bisphosphine ligand PS-DPPBz was effective for the Ir-catalyzed reversible acceptorless dehydrogenation/hydrogenation of *N*-heterocycles. Notably, this protocol is applicable to the dehydrogenation of *N*-substituted indoline derivatives with various *N*-substituents with different electronic and steric natures. A reaction pathway involving oxidative addition of an *N*-adjacent C(sp^3)−H bond to a bisphosphine-coordinated Ir(I) center is proposed for the dehydrogenation of *N*-substituted substrates.

Introduction

The dehydrogenation of *N*-heterocycles is a fundamentally important transformation for the construction of unsaturated heterocycles, such as indoles and quinolines, that are found in biological molecules.[1] Typically, these transformations can be achieved through the stoichiometric use of strong oxidants such as DDQ and $KMnO_4$ or through catalytic reactions employing olefinic hydrogen acceptors in stoichiometric amounts.[2] Compared to these reactions, catalytic acceptorless dehydrogenations can be cleaner and atom-economical processes, producing only molecular hydrogen as a side product.[3,4] In addition, catalytic acceptorless dehydrogenation has the potential to be a chemical hydrogen storage process.[5] The pioneering work by Fujita et al. shows promising efficiency of metal-ligand bifunctional Ir(III) catalysts with 2-hydroxypyridine-type ancillary ligands (Scheme 1, top).[3a,d,h] Importantly, the same catalyst systems were able to promote hydrogenation as a backward reaction, demonstrating the reversibility of the process. Later, Jones and co-workers reported iron and cobalt catalyst systems for similar reversible processes,[3e,g] while Xiao and co-workers developed a cyclometalated imino-Ir(III) catalyst.[3c] Regardless of these advances, the catalytic acceptorless dehydrogenation/hydrogenation of *N*-heterocycles is largely limited to reactions involving heterocyclic compounds with one or more free N–H bonds (Scheme 1, top). Although several novel protocols have emerged more recently for the dehydrogenation of *N*-substituted heterocycles using photoredox catalysts in combination with a cobalt or a palladium catalyst (Scheme 2a),[6] a frustrated Lewis pair catalyst (Scheme 2b),[7] or a quinone catalyst (Scheme 2c),[8] electron-withdrawing groups on the N atom such as acetyl or tosyl groups completely inhibited the reaction.

Here, I report the heterogeneous catalytic acceptorless dehydrogenation of *N*-heterocycles enabled by a combination of $[IrCl(cod)]_2$ and the polystyrene-cross-linking bisphosphine PS-DPPBz (Scheme 1, bottom).[9] Applicability toward indoline-type *N*-heterocycles with electron-donating or -withdrawing *N*-substituents is a notable feature of this catalysis. The same (PS-DPPBz)-Ir catalyst system also promoted backward hydrogenation of *N*-heteroarenes with molecular hydrogen.

Scheme 1. Acceptorless Dehydrogenation by Transition Metals

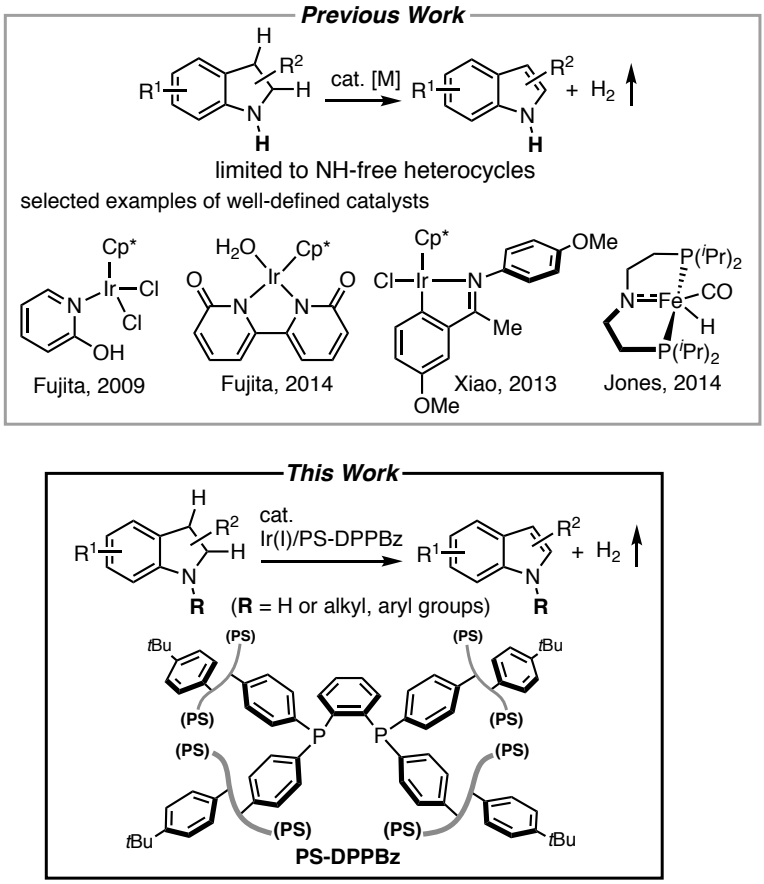

Scheme 2. Acceptorless Dehydrogenation of *N*-Substituted Heterocycles

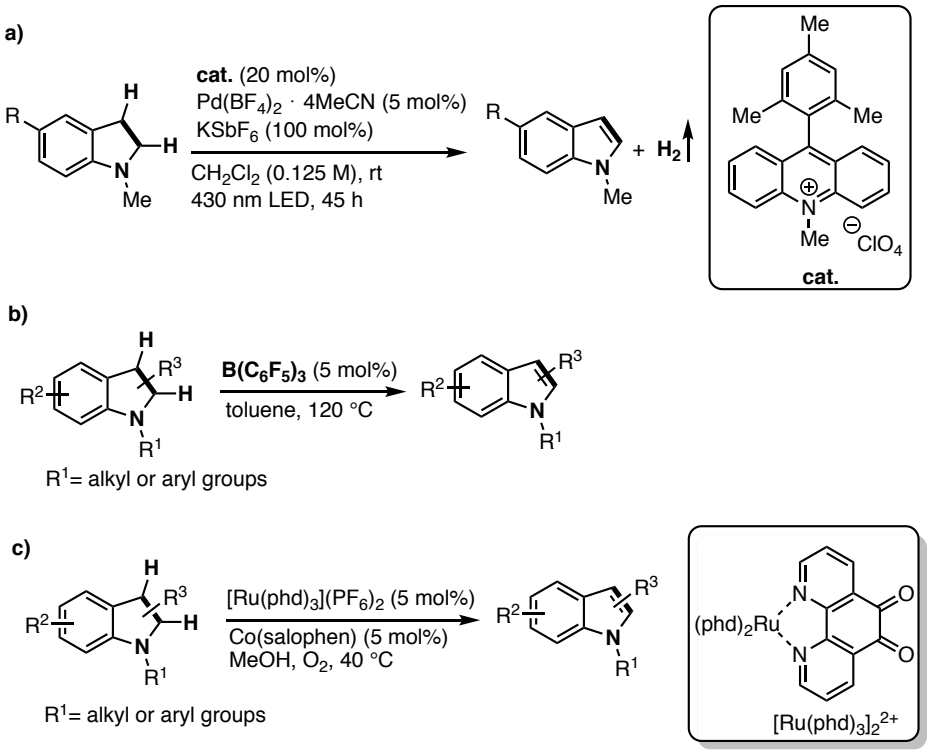

Results and Discussion

The acceptorless dehydrogenation of *N*-methylindoline (**1a**) in the presence of $[IrCl(cod)]_2$ (2 mol% Ir) and PS-DPPBz (2 mol%) proceeded in *p*-xylene at 130 °C over 3 h to give *N*-methylindole (**2a**) in 91% NMR yield (Scheme 3). I found that the same reaction also occurred with the commercially available Fujita's bipyridonate-Cp*Ir(III) catalyst (**cat.1**) under the same conditions but in a much lower yield (47%).

Scheme 3. Ir-Catalyzed Acceptorless Dehydrogenation of *N*-Substituted Heterocycles

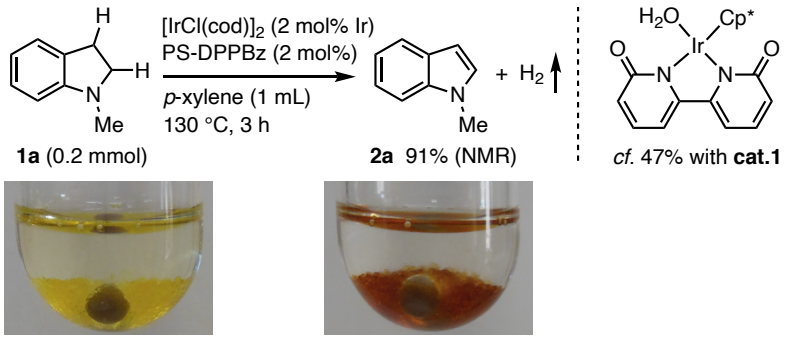

During the reaction with (PS-DPPBz)-Ir catalyst, the polymer-bound catalyst changed its color from yellow to dark red, while the solution phase remained colorless (Scheme 3). This observation indicates that virtually all Ir species was retained in the

polymer matrix. The recovered catalyst was reusable for the following dehydrogenation albeit with significant reduction in the product yield (1st run, 87%; 2nd run, 52%; 3rd run, 46%, Scheme 4). The decrease in the activity of the recovered catalysts should be deduced to partial structure change of the polymer-bound catalyst to an inactive form rather than to metal leaching as the solution remained colorless. The ^{31}P CP/MAS NMR signal of the recovered catalyst appeared with nearly the same chemical shift value to that of the (PS-DPPBz)-Ir catalyst precursor but with apparent broadening (Figures 1–3).[11] That can explain the reduced reactivity of catalyst in reuse experiments.

Scheme 4. Catalyst Reuse Experiments and its Photographic Images

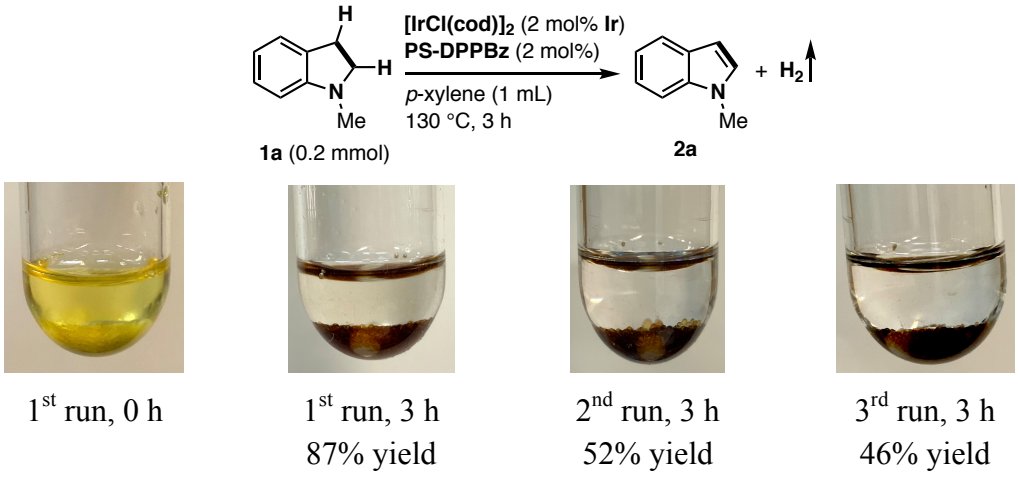

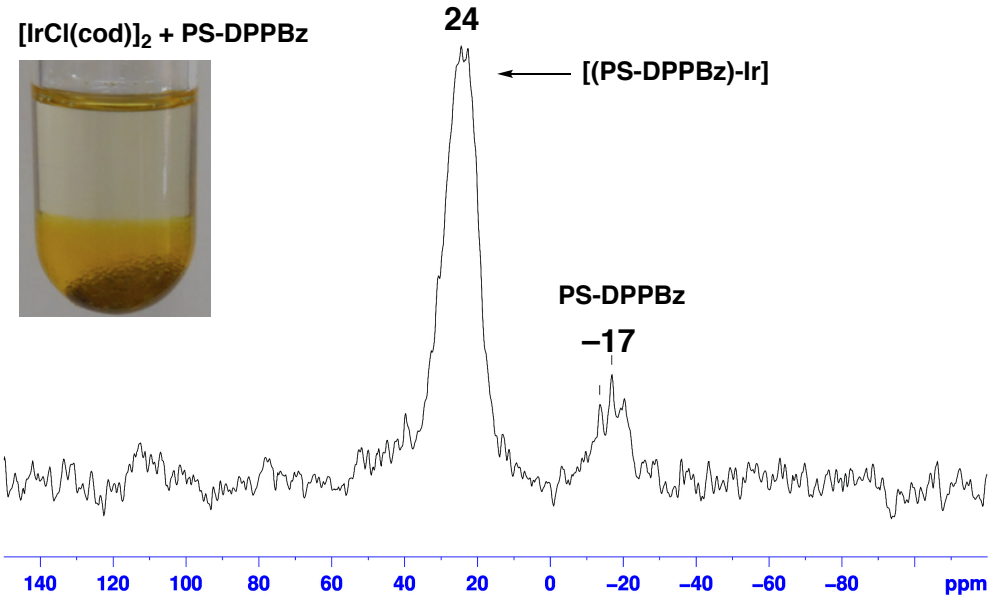

Figure 1. A Photographic Image of the Reaction Mixture of $[IrCl(cod)]_2$ and PS-DPPBz in *p*-xylene. The ^{31}P CP/MAS NMR spectrum of polymer beads obtained after fitration and drying under vacuum.

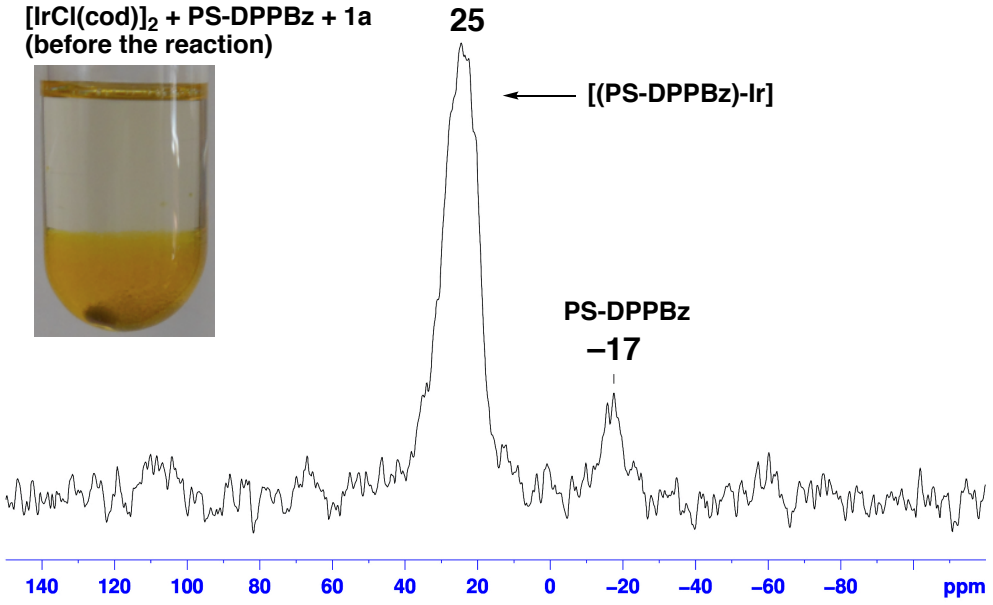

Figure 2. A Photographic Image before the Reaction of **1a** with $[IrCl(cod)]_2$ and PS-DPPBz in *p*-xylene. The ^{31}P CP/MAS NMR spectrum of polymer beads obtained after fitration and drying under vacuum.

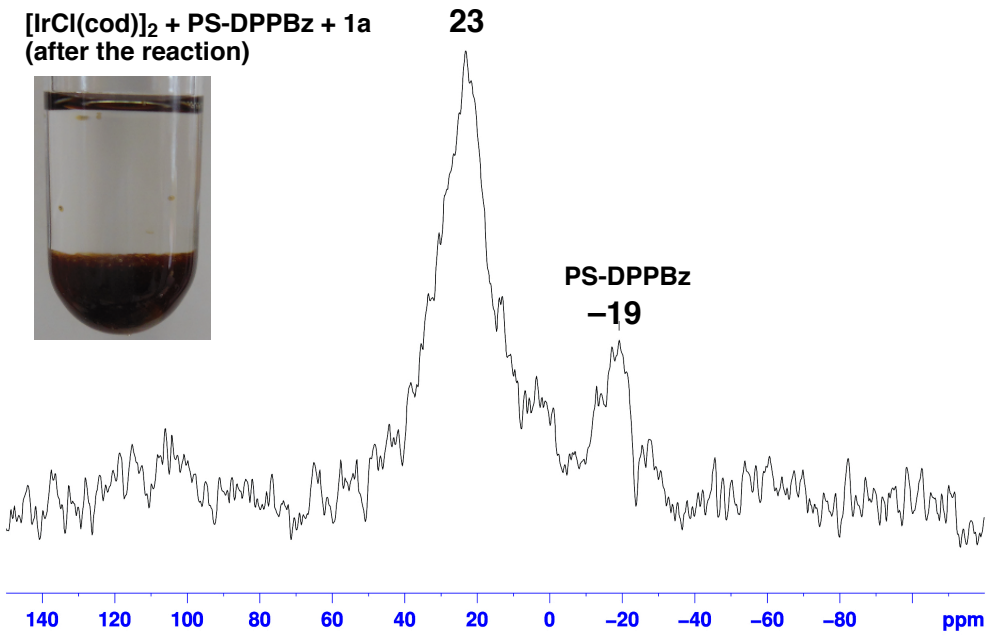

Figure 3. A Photographic Image after the Reaction of **1a** with $[IrCl(cod)]_2$ and PS-DPPBz in *p*-xylene. The ^{31}P CP/MAS NMR spectrum of polymer beads obtained after fitration and drying under vacuum.

To investigate the different characters between PS-DPPBz and its homogeneous form DPPBz, the author conducted parallel experiment using DPPBz instead of PS-DPPBz (eq 1). The reaction at 130 °C (closed system) was monitored by ^{31}P NMR spectroscopy. Several signals were detected during the reaction (~17 h), which indicate that catalyst deactivation pathways may occurred and some inactive catalyst species should be formed in this process. This observation can explain the low reactivity of DPPBz. While the signal at 23.2 ppm remained after 17 h, which is similar to the ^{31}P CP/MAS NMR signal of the recovered catalyst from the (PS-DPPBz)-Ir catalyst precursor (Figure 4).

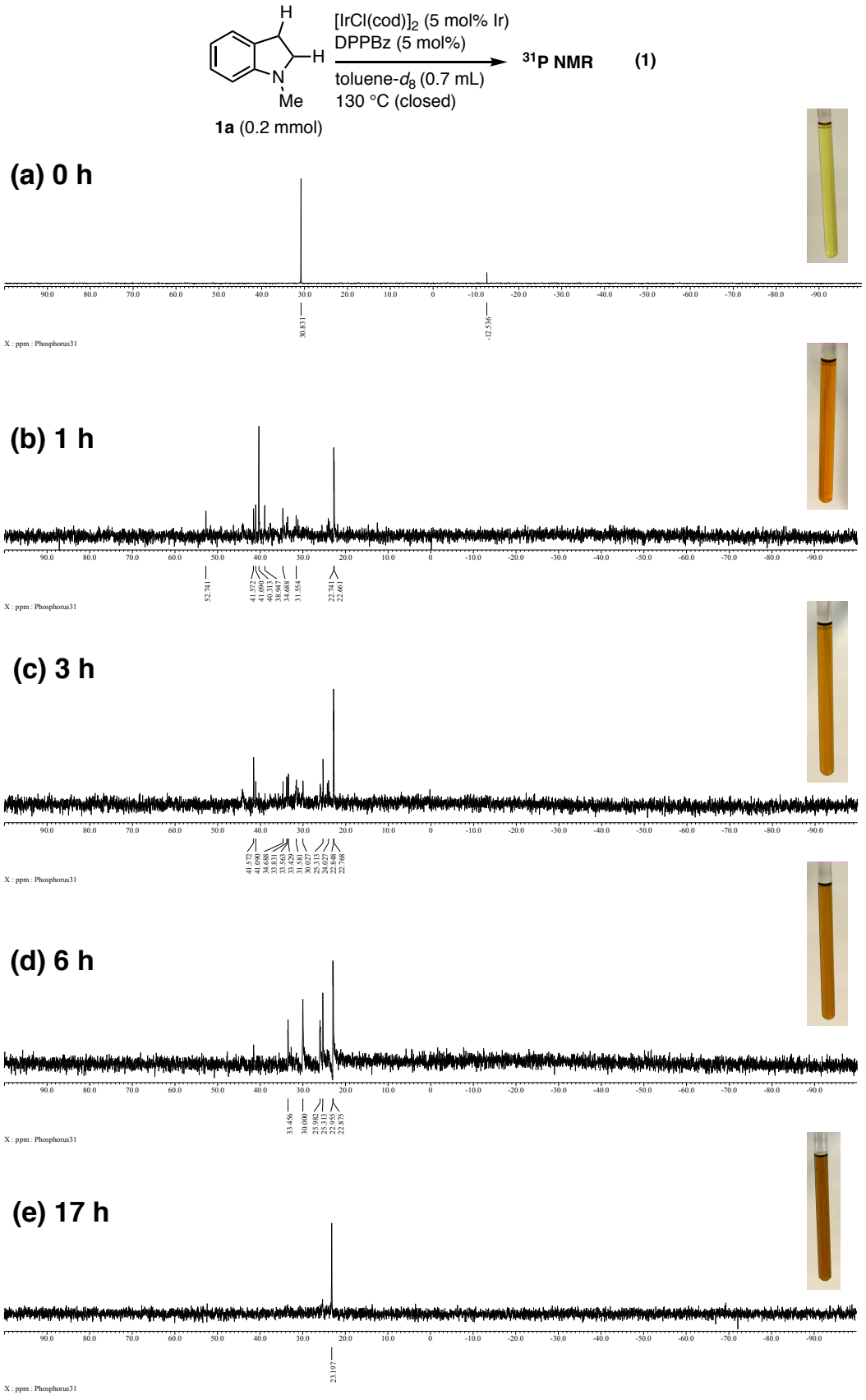

Figure 4. Photographic Images and ^{31}P NMR Spectra of the Reaction Mixture of $[IrCl(cod)]_2$, DPPBz and **1a** in toluene-d_8 [(a) 0 h; (b) 1 h; (c) 3 h; (d) 6 h; (e) 17 h]

To further study the inactive species, the author conducted the reaction with a shorter reaction time (3 h) and a slightly higher catalyst loading (10 mol%) at 130 °C (eq 2). The red precipitates formed immediately once the reaction mixture was stirred at 130 °C. After the reaction, the resulting mixture was analyzed with ^{31}P NMR spectroscopy (Figure 5). The signal at 56 ppm was assignable to [Ir(DPPBz)$_2$]X. The signals at 41 ppm and 33 ppm have remained elusive. This results indicates that DPPBz causes bischelation to an Ir(I) complex and other species, which serve as inactive species and thus decrease the efficiency of catalysis.

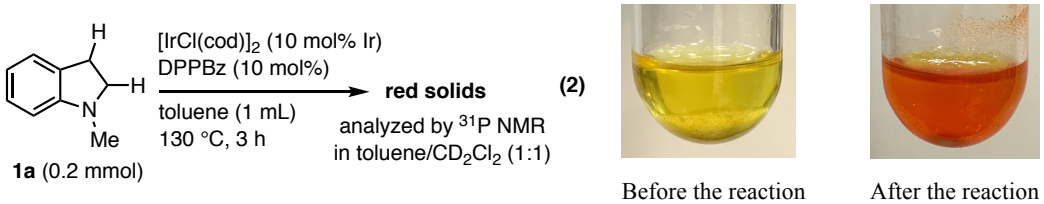

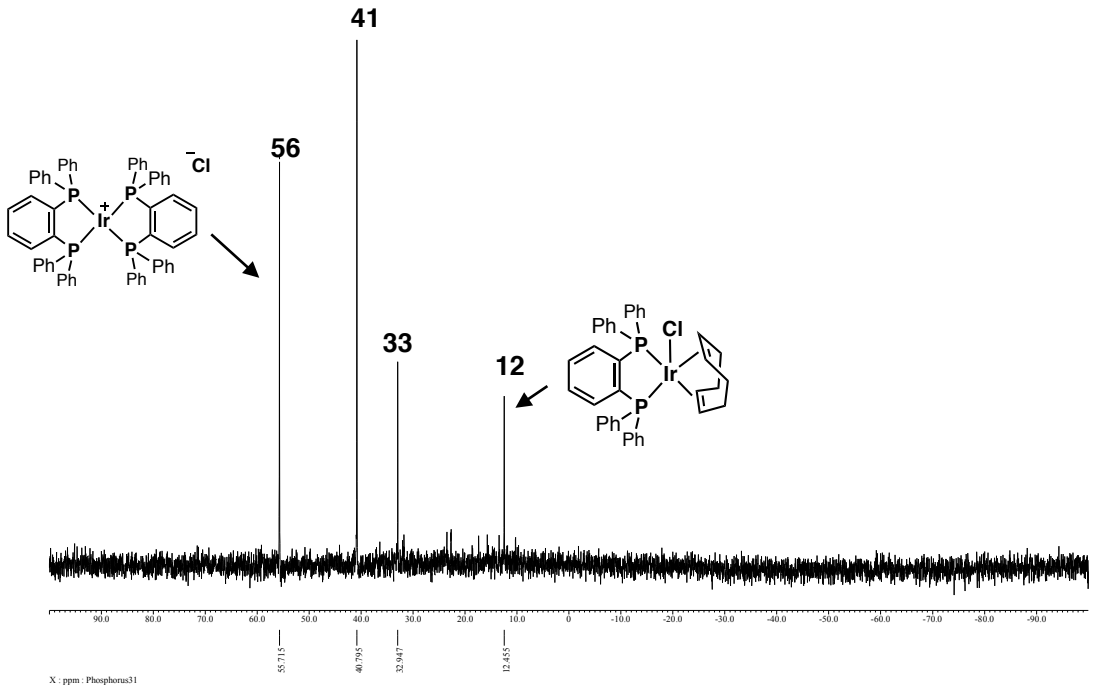

Figure 5. ^{31}P NMR Spectrum of the Reaction Mixture of [IrCl(cod)]$_2$, DPPBz and **1a** in toluene/CD_2Cl_2 (1:1)

The use of the polymer ligand PS-DPPBz is crucial for efficient dehydrogenation of **1a** (Table 1). The soluble counterpart of PS-DPPBz, 1,2-bis(diphenylphosphino)benzene (DPPBz, entry 3), induced only a little activity, indicating the critical importance of the polystyrene cross-linking. Introduction of sterically demanding substituents (*t*Bu) on the *P*-Ph groups (SciOPP, entry 4) of the soluble ligand DPPBz increased its catalytic activity, but the yield was much lower than

that with PS-DPPBz (16% vs 91%). DPPE, DEtPE and DCyPE (entries 7–9) with an ethylene linker between the two P atoms were also less effective. Larger bite-angle bisphosphines (Xantphos, entry 10), monophosphines (PPh_3, entry 13) and bipyridine-based ligands (dtbpy, entry 12) exhibited no catalytic activity.

Table 1. Ligand Effects on the Ir-Catalyzed Acceptorless Dehydrogenation of **1a**[a]

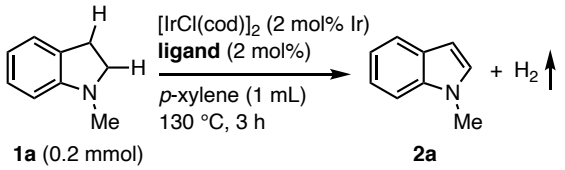

Entry	Ligand		**2a** [%, ^{1}H NMR]
1	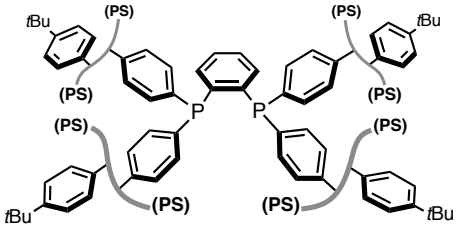	**PS-DPPBz**	**91**
2	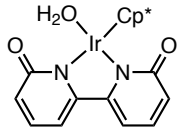	**cat.1**	47
	(w/o $[IrCl(cod)]_2$)		
3	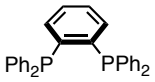	DPPBz	4
4	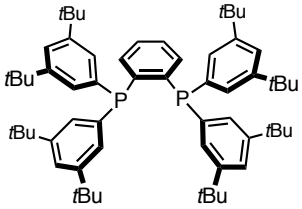	SciOPP	16
5	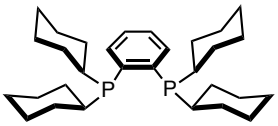	DCyPBz	0
6	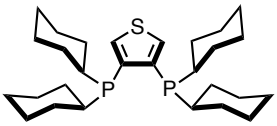	DCyPT	3
7	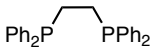	DPPE	3
8	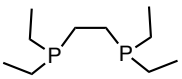	DEtPE	0

9	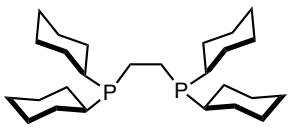	DCyPE	5
10	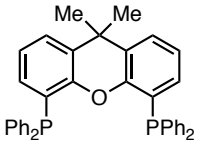	Xantphos	0
11	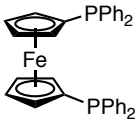	DPPF	0
12	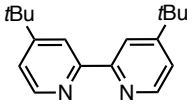	Dtbpy	0
13		PPh_3 (4 mol%)	0

[a]Conditions: **1a** (0.2 mmol), $[IrCl(cod)]_2$ (2 mol% Ir), ligand (2 mol%), p-xylene (1 mL), 130 °C, 3 h. Yield of **2a** was determined by ^{1}H NMR analysis of the crude product.

The solvent effects were also examined (Table 2). The catalyst showed most effective in *p*-xylene (entry 1). Toluene as solvent is also a good candidate, which promote the reaction in a slightly low yield (88%, entry 2). Ethers as solvents such as CPME Bu_2O, 1,4-dioxane and THF were also examined but resulted in much lower yield (entries 3–6). DMF can not be used as solvent for this reaction (entry 7)

Table 2. Solvent Effects on the Ir-Catalyzed Acceptorless Dehydrogenation of **1a**[a]

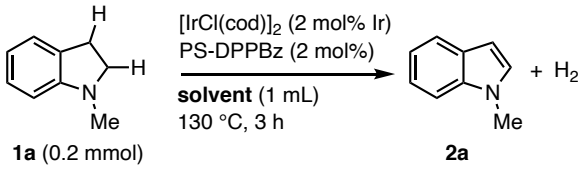

Entry	Solvent	Tem. [°C]	**2a** [%, ^{1}H NMR]
1	***p*-xylene**	**130**	**91**
2	toluene	130	88
3	CPME	130	52
4	nBu_2O	130	41
5	1,4-dioxane	110	15

6	THF	70	0
7	DMF	130	0

[a]Conditions: **1a** (0.2 mmol), $[IrCl(cod)]_2$ (2 mol% Ir), PS-DPPBz (2 mol%), solvent (1 mL), 130 °C, 3 h. Yield of **2a** was determined by ^{1}H NMR analysis of the crude product.

The effects of transition metal species in the Ir-catalyzed acceptorless dehydrogenation of **1a** were also investigated (Table 3). $[IrCl(cod)]_2$ shows higher reactivity (entry 1), while the yields of product were decreased to 49% and 36% when $[IrCl(cod)]_2$ was changed to $[IrCl(coe)_2]_2$ and $[IrCl(C_2H_4)_2]_2$, respectively (entries 2–3). In the replacement of anionic chloride in $[IrCl(cod)]_2$ with methoxyl group led to little reactivity. Cationic $[Ir(cod)_2]BF_4$ and $[IrCl_2Cp^*]$ induced no reactivity (entries 5–6).

Table 3. Metal Effects on the Ir-Catalyzed Acceptorless Dehydrogenation of **1a**

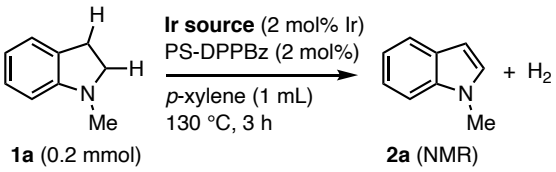

Entry	Metal	**2a** [%, ^{1}H NMR]
1	**$[IrCl(cod)]_2$**	**91**
2	$[IrCl(coe)_2]_2$	49
3	$[IrCl(C_2H_4)_2]_2$	36
4	$[Ir(OMe)(cod)]_2$	5
5	$[Ir(cod)_2]BF_4$	0
6	$[IrCl_2Cp^*]_2$ + NaO*t*Bu (5 mol%) (w/o PS-DPPBz)	0

Next, I examined the scope of *N*-substituted indolines with the (PS-DPPBz)-Ir system (4 mol% Ir, *p*-xylene, 130–160 °C, 10–48 h, Scheme 5). Not only electron-neutral (**2b**) and donating (**2c**) substituents but also electron-withdrawing chloro and nitro (**2d** and **2e**) substituents were tolerated in the carbon framework of the *N*-methylindoline scaffold. *cis*-1,2,3-Trimethylindoline (*cis*-**1f**) underwent efficient dehydrogenation, while its *trans* isomer did not participate in the dehydrogenation at all, indicating that the *cis* arrangement of the two vicinal hydrogen atoms was crucial for the dehydrogenation.

Importantly, various *N*-substituents were tolerated in the indoline scaffold (**2g-2p**). Even in the presence of β-hydrogen atoms in the *N*-alkyl substituent as in Et, *n*-Bu, *i*-

Bu and Cy groups, the dehydrogenation occurred at the indoline ring with exclusive site-selectivity. It is also noteworthy that branching was tolerated at the positions α or β to the N atom. Thus, this protocol is useful for the synthesis of *N*-alkylindoles since the direct *N*-alkylation of indole derivatives under basic conditions often suffers from competitive elimination reactions of the alkylating reagents.[10] Moreover, the reaction of **1k** bearing a 4-methoxybenzyl group at the N atom, which should be sensitive to the oxidation conditions, occurred cleanly to give **2k** in high yield, while the oxidation with stoichiometric DDQ (in THF at 40 °C for 12 h) produced **2k** in only 57% yield along with unidentified byproducts. A phenyl group on the N atom was also tolerated (**2m**).

The indoline (**1n**) with a strongly electron-withdrawing *N*-tosyl group underwent efficient dehydrogenation to give **2n** in 89% yield, whereas Fujita's catalyst **cat.1** did not promote the reaction. *N*-Trifluoromethylsulfonyl or *N*-acyl-substituted indolines were also suitable substrates (**1o** and **1p**) although the yields were moderate.

The (PS-DPPBz)-Ir catalyst system is also applicable to the acceptorless dehydrogenation of NH-free heterocycles (**1q-1ab**). The reaction of **1q** was conducted on a gram-scale with a reduced catalyst loading of 0.08 mol% (10 mmol scale, 94% NMR yield, TON 1175) with reasonable hydrogen gas release (~210 mL, 94% based on H_2). The reaction apparatus for the gram-scale reaction is depicted in Figure 6 and the GC analysis of evolved H_2 gas is shown in Figure 7. Two- or three-fold dehydrogenation occurred from tetrahydroquinoline-, tetrahydroisoquinoline-, tetrahydroquinoxaline- and piperazine-type substrates to give the corresponding *N*-heteroarenes. 2-Phenyl-2,3-dihydrobenzothiazole (**1ab**) also participated in this reaction.

Scheme 5. Scope of *N*-Heterocycles for Acceptorless Dehydrogenation

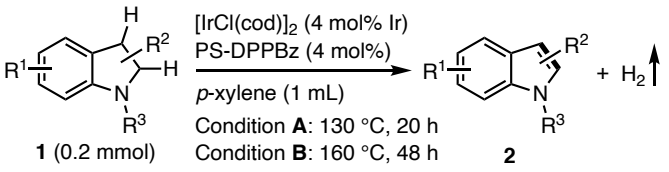

N-substituted indolines, isolated yield

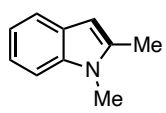

2b, 98% (**A**)

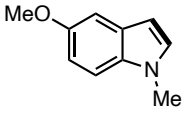

2c, 90% (**A**)

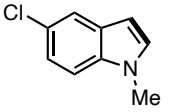

2d, 87% (**A**)

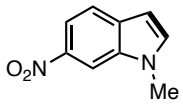

2e, 97% (**A**)

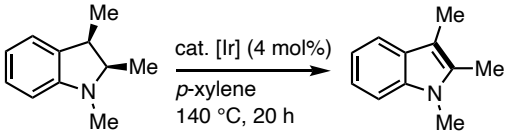

cis-**1f**

2f, 87%

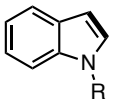

2g (R = Et), 91% (**A**)
2h (R = *n*-Bu), 93% (**A**)
2i (R = *i*-Bu), 95% (**A**)
2j (R = Bn), 94% (**A**)
2l (R = Cy), 92% (**A**)
2m (R = Ph), 91% (**A**)

2n (R = Ts), 89% (**B**)
2o (R = Tf), 41% (**B**)
2p (R = Ac), 46% (**B**)

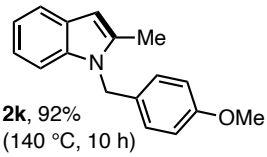

2k, 92%
(140 °C, 10 h)
cf. 57% with DDQ (1.2 eq)
(THF, 40 °C, 12 h)

NH-free heterocycles, isolated yield

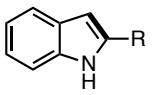

2q (R = H), 99% (**A**)
2r (R = Me), 98% (**A**)

2q, 94%[a]
10 mmol scale (1.2 g)
0.08 mol% [Ir]
p-xylene (0.5 mL)
160 °C, 60 h

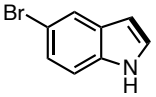

2s, 98% (**A**)

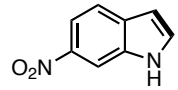

2t, 89% (**A**)

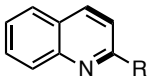

2u (R = H), 64% (**B**)
2v (R = Me), 93% (**B**)

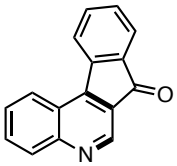

2w, 67% (**B**)

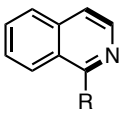

2x (R = H), 51% (**B**)
2y (R = Me), 93% (**B**)

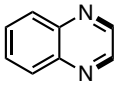

2z, 82% (**B**)

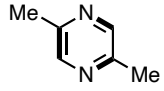

2aa, 47%[a] (**B**)

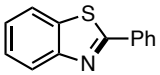

2ab, 81% (**A**)

Reaction conditions: **1** (0.2 mmol), $[IrCl(cod)]_2$ (4 mol% Ir), PS-DPPBz (4 mol%), *p*-xylene (1 mL), 130 °C, 20 h (condition **A**) or 160 °C, 48 h (condition **B**). Isolated yields are shown. [a]Yields are determined by ^{1}H NMR analysis of the crude product.

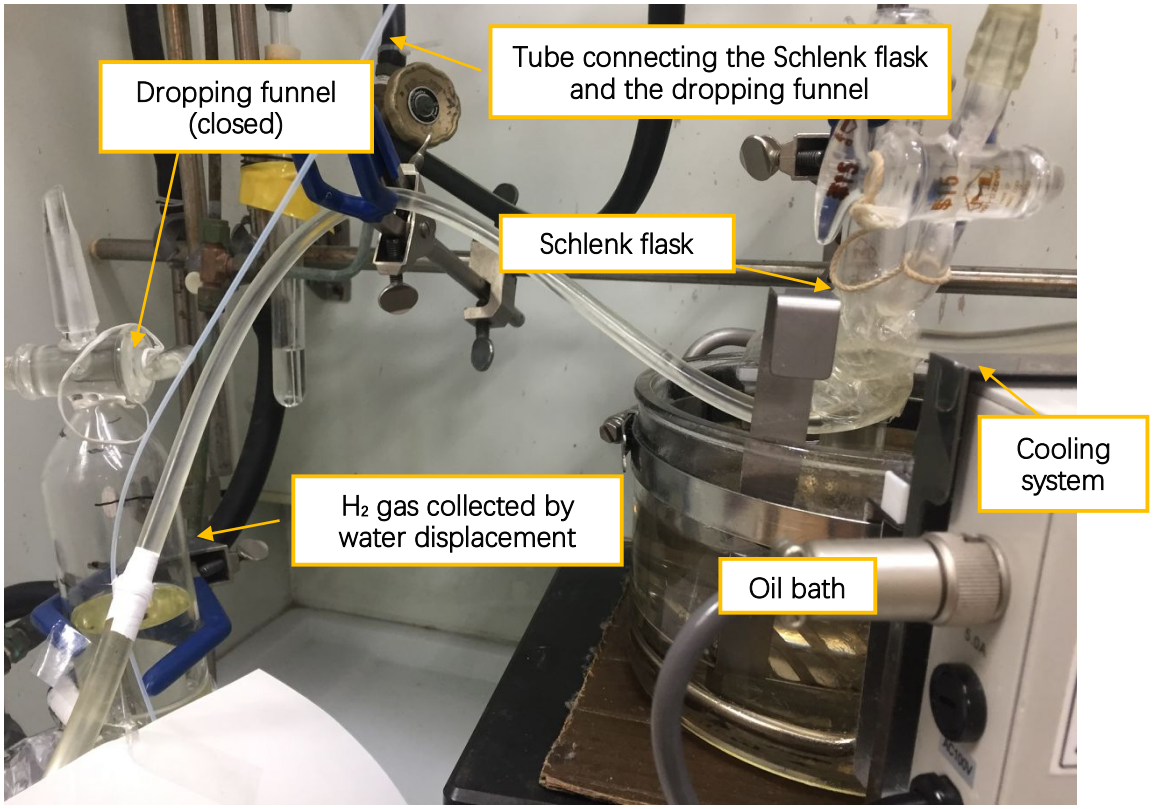

Figure 6. The Reaction Apparatus for the Gram-scale Reaction.

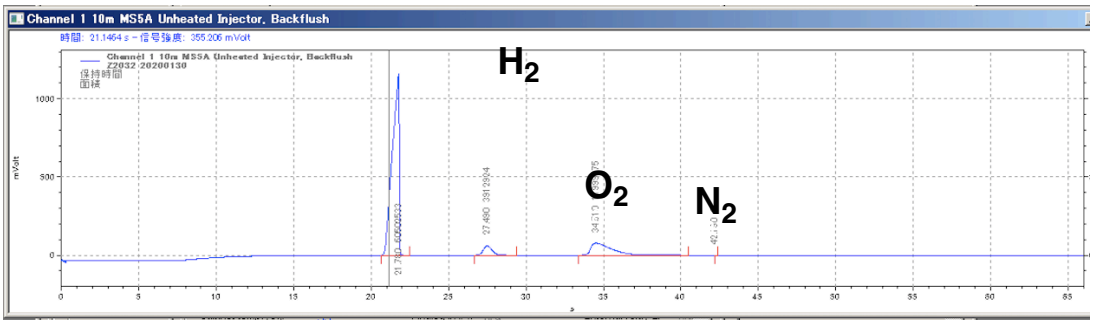

Figure 7. GC Analysis of Evolved H_2 Gas (contaminated with small amounts of O_2 and N_2 gas during the analysis operation).

To demonstrate the utility of this catalytic acceptorless dehydrogenation, I applied the protocol to the synthesis of pharmacologically active molecules having *N*-substituted indoline scaffolds. The dehydrogenation of indolines **1ac** and **1ad** proceeded smoothly to provide CDK4/cyclin D1 inhibitors **2ac** and **2ad**, respectively, in high yields (Scheme 6a,b). When the corresponding dehydrogenative transformations were conducted using a large excess of activated MnO_2, the yields were only moderate.[11] Compound **1ae**, having piperidine and pyridine moieties, was transformed to the precursor of enzastaurin (**2ae**)[14] in 37% yield (5 mol% Ir, 43% conv. of **1ae**, Scheme 6c).

Scheme 6. Synthesis of Pharmacologically Active Molecules

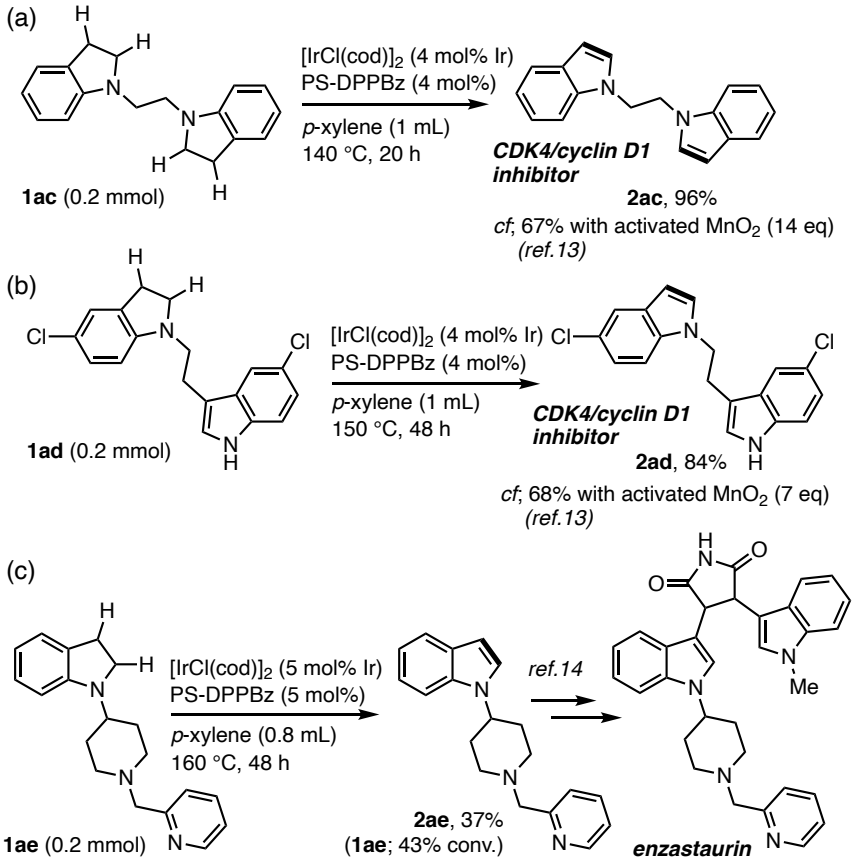

To gain insights into the mechanism, the reactions of deuterated *N*-methylindolines were conducted. The dehydrogenation of 2,2- and 3,3-di-deuterated *N*-methylindolines [2 mol% (PS-DPPBz)-Ir, 130 °C, for 2 h] proceeded at only slightly reduced rates compared to that of nondeuterated *N*-methylindoline (61% and 53% ^{1}H NMR yields vs. 78%, Scheme 7a–c). A deuteration effect in the reaction of 2,2,3,3-tetradeuterated *N*-methylindoline (3%, Scheme 7d) was much more significant than expected from the combination of the effects of the deuteration at the C2 and C3 positions. These results suggest that the rate of the catalytic reaction may be mainly affected by H_2 release from a putative iridium (di)hydride intermediate rather than by dissociations of two C(sp^3)–H bonds at the C2 and C3 positions of the *N*-substituted indolines.

Scheme 7. Deuterium Isotope Experiments[a]

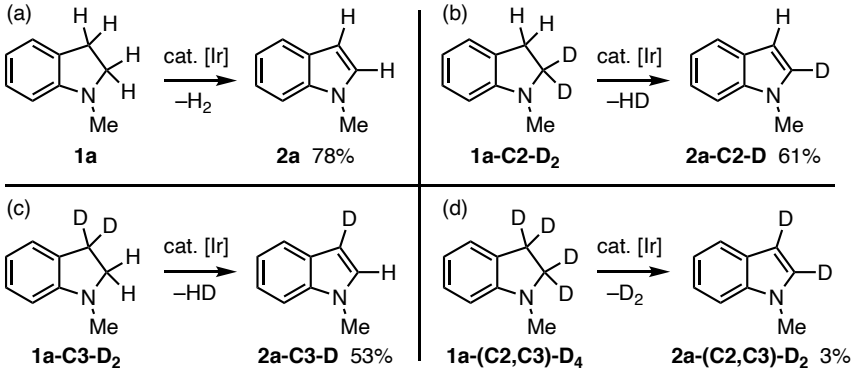

[a]Conditions: **1** (0.2 mmol), $[IrCl(cod)]_2$ (2 mol% Ir), PS-DPPBz (2 mol%), *p*-xylene (1 mL), 130 °C, 2 h. Yield was determined by ^{1}H NMR analysis of the crude product.

Based on the above results, I propose a reaction pathway for the acceptorless dehydrogenation of *N*-substituted indolines (**1**) (Scheme 8), which should be distinct from the well-established pathway for the acceptorless dehydrogenation of NH-free heterocycles, in which metal–ligand cooperation is essential for NH deprotonation and H_2 release from the catalyst as in Fujita's Cp*Ir(III) catalyst system.[13] The reaction starts from a coordination of the sp^3-hybridized N atom of **1** to bisphosphine-Ir(I) complex **A**. Oxidative addition of an *N*-adjacent C(sp^3)–H bond to the indoline-bound Ir(I) center in **B** gives Ir(III) monohydride **C**.[14,15] Subsequent β-hydrogen elimination provides dehydrogenated product **2** and Ir(III) dihydride species **D**.[18] The latter is in equilibrium with a hydride-bridged dimeric iridium complex (**D-dimer**) as an off-cycle species.[19] Finally, H_2 is released from **D** with the regeneration of **A**. This step is likely rate-determining on the basis of the experiments with the deuterated substrates.

According to the proposed reaction pathway, the ligand effect of PS-DPPBz can be ascribed to the controlled monochelation due to spatial isolation of the bisphosphine unit in the polymer matrix,[9] which suppresses formation of the inactive **D-dimer** species and hence facilitates the rate-determining H_2 releasing step.

Scheme 8. Plausible Reaction Pathway

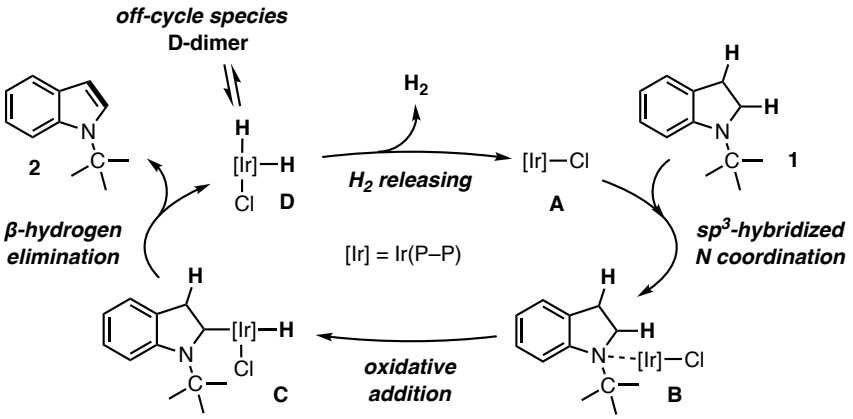

Based on the overall reaction mechanism, the reason for the observed different reactivities towards the dehydrogenation of *cis*-**1f** and *trans*-**1f** was proposed (Scheme 9). The oxidative addition of *N*-adjacent C–H bond in *cis* isomer to Ir(I) gives coordinatively saturated Ir(III) complex. Dissociation of cod as a η^2-ligand produces good σ acid Ir(III) with an empty *d* orbital. The coplanar Ir-C-C-H unit is prone to form two electron three center β-agostic interaction with a closed β-H to metal center. The back donation of *d* electron in metal center to σ* orbital of C–H bond breaks this bond and delivers desired product. In contrast, the *trans* isomer with the fixed configuration by heterocyclic ring gives a γ–agostic interaction with transition metal. For the moment I hypothesize that due to the high BDE of primary C–H and less strain in five membered ring intermediate, the weak back donation arising from the poor π-base Ir(III) unable to beak γ C-H bond.

Scheme 9. Plausible Pathway for the Dehydrogenation of *cis*-**1f** and *trans*-**1f**

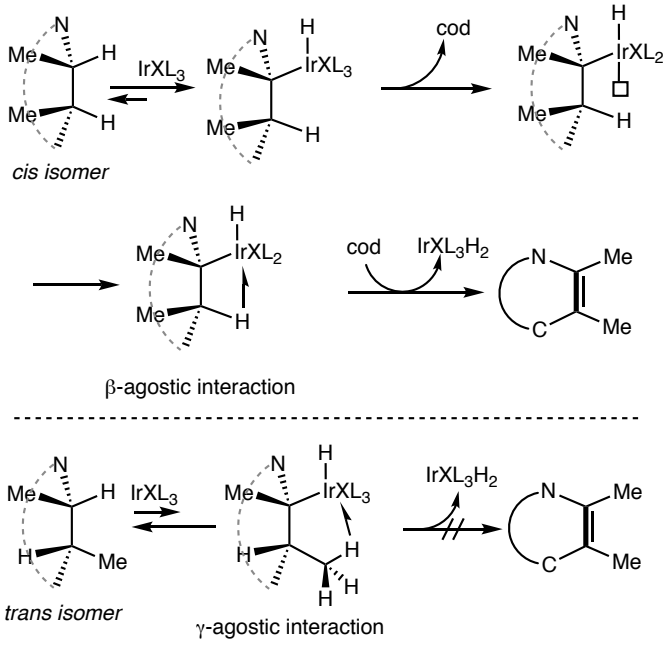

In view of the potential for organic hydride hydrogen storage, the development of efficient methods for reversible acceptorless dehydrogenation and hydrogenation with the same catalyst remains an important challenge.[5] Thus, the applicability of the (PS-DPPBz)-Ir system for hydrogenation of *N*-heteroarenes with molecular hydrogen, as the backward reaction of dehydrogenation, was examined. As illustrated in Scheme 10, a variety of *N*-substituted and unsubstituted indoles (**2a**, **2n** and **2q**) and six-membered heteroarenes (**2v**, **2x** and **2z**) were hydrogenated in high yields at 30 or 40 atm H_2 pressure.

Scheme 10. Hydrogenation of *N*-Heteroarenes

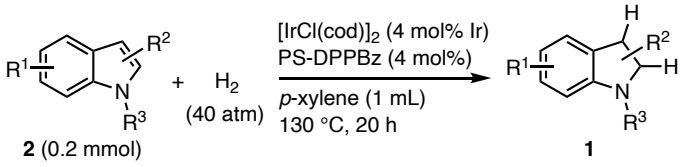

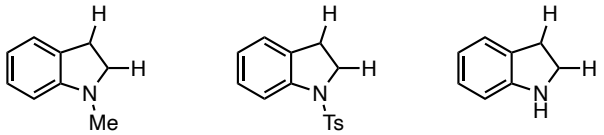

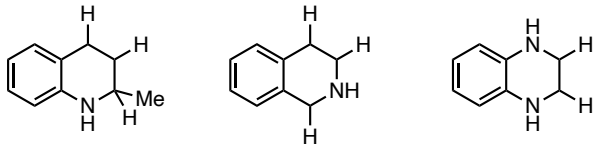

Conditions: **2** (0.2 mmol), $[IrCl(cod)]_2$ (4 mol% Ir), PS-DPPBz (4 mol%), H_2 (40 atm), *p*-xylene (1 mL), 130 °C, 40 h. Isolated yields are shown.

Conclusion

In summary, a polystyrene-cross-linking bisphosphine-Ir complex (PS-DPPBz)-Ir showed high activities for the acceptorless dehydrogenation of *N*-heterocycles. The protocol is applicable to the dehydrogenation of *N*-substituted indoline-type substrates, applicability to which has not been well explored with the reported catalytic systems. A catalytic reaction pathway involving oxidative addition of the *N*-adjacent C(sp^3)–H bond to the bisphosphine-Ir(I) species is proposed. The same Ir catalyst was applicable to backward hydrogenation of *N*-heteroarenes with molecular hydrogen.

Experimental Section

Instrumentation and Chemicals

NMR spectra were recorded on a JEOL ECXII, operating at 400 MHz for ^{1}H NMR, 100.5 MHz for ^{13}C NMR and 161.8 MHz for ^{31}P NMR. Chemical shift values were reported relative to Me_4Si (0 ppm) and CH_2Cl_2 (5.32 ppm) for ^{1}H NMR, the solvent resonance ($CDCl_3$, 77 ppm; CD_2Cl_2, 53.8 ppm) for ^{13}C NMR and H_3PO_4 (0 ppm) for ^{31}P NMR. Magic angle spinning (MAS) NMR spectra were recorded on a Brucker MSL-300 spectrometer, operating at 121.5 MHz for ^{31}P NMR (spinning rate 10 kHz). High-resolution mass spectra were recorded at the Instrumental Analysis Division, Global Facility Center, Creative Research Institution, Hokkaido University (JEOL JMS-T100GCv for EI-MS) and the GC–MS & NMR Laboratory, Research Faculty of Agriculture, Hokkaido University (JEOL JMS-T100GCv mass spectrometer for FD-MS). Melting points were determined on a micro melting point apparatus using micro cover glass (Yanaco MP-500D). TLC analyses were performed on commercial glass plates bearing 0.25-mm layer of Merck Silica gel $60F_{254}$. Silica gel (Kanto Chemical Co., Silica gel 60 N, spherical, neutral) was used for column chromatography. IR spectra were measured with a PerkinElmer Frontier instrument.

All reactions were carried out under nitrogen or argon atmosphere. Materials were obtained from commercial suppliers or prepared according to standard procedures unless otherwise noted. *p*-Xylene was purchased from Kanto Chemical Co., Inc., and degassed by freeze-pump-thaw cycle. PS-DPPBz and $[IrCl(cod)]_2$ were prepared according to the reported procedures.[9,18] Fujita's iridium catalyst **cat.1** (CAS: 1436571-06-0) was perphased from Kanto Chemical Co., Inc.

Synthesis of the Substrates

N-Heterocycles **1q–1s, 1u, 1v, 1x–1aa** are commercial available. Other substrates listed in Figure S1 are reported in the literature.

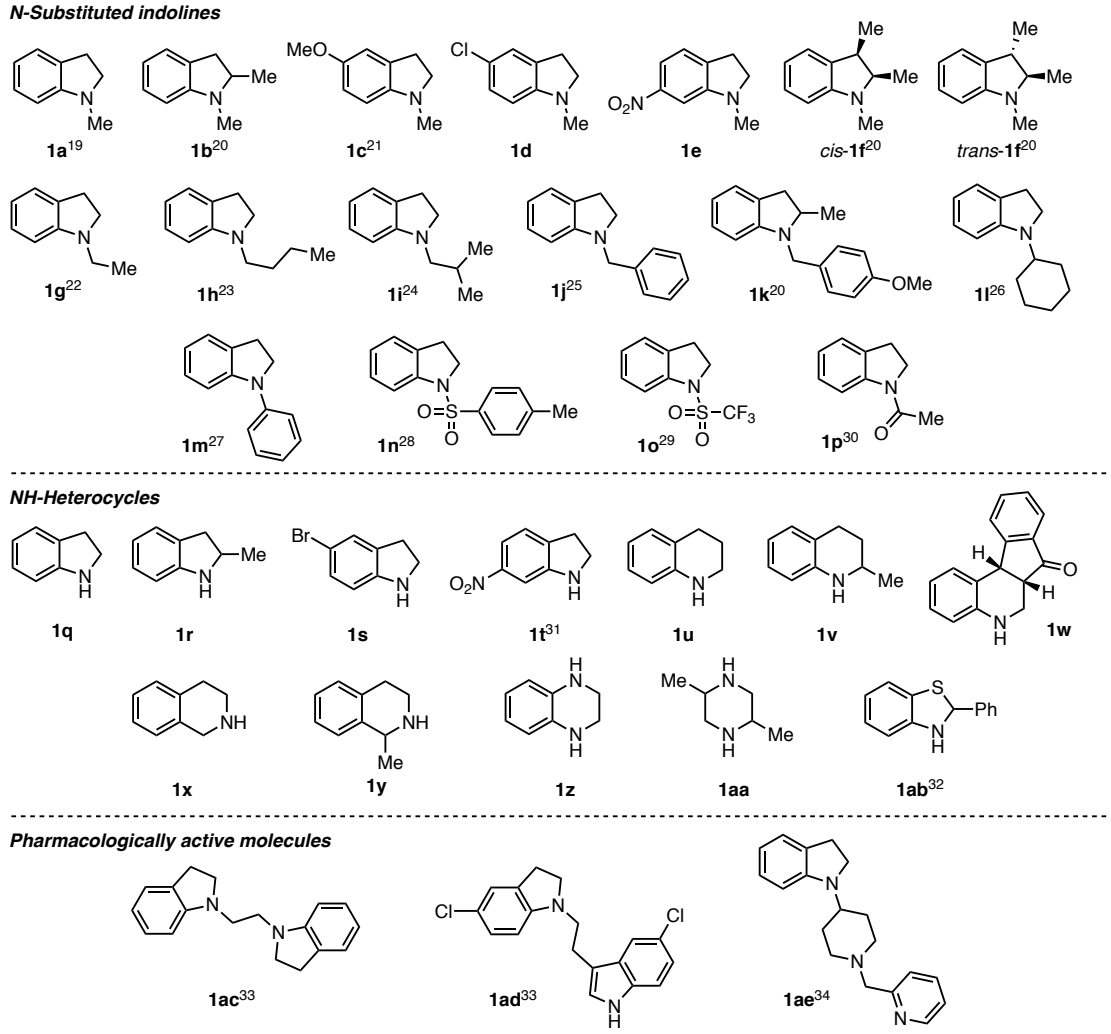

Figure 6. *N*-Heterocycle Substrates used in This Work.

5-Chloro-1-methylindoline (1d)

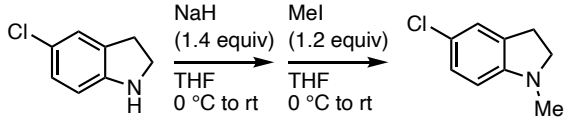

To a well-stirred solution of 5-chloroindoline (1.0 g, 7.0 mmol, 1.0 equiv) in THF (15 mL) at 0 °C was added NaH (55% in mineral oil, 426 mg, 9.8 mmol, 1.4 equiv). The reaction was warmed to room temperature and allowed to stir for 30 min. The flask was cooled again to 0 °C and MeI (1.2 g, 8.4 mmol, 1.2 equiv) was added dropwise. The reaction mixture was warmed to room temperature and allowed to stir until the reaction completed (monitored by TLC) and then quenched with saturated aqueous NH_4Cl at 0 °C. The mixture was extracted with Et_2O (3 x 20 mL). The organic layer was dried over anhydrous Na_2SO_4, filterd and concentrated under vacuum. The crude product was purified by column chromatography (using 10% EtOAc/hexane) to give **1d** (928 mg, 85% yield) as yellow oil. **^{1}H NMR** (400 MHz, $CDCl_3$): δ 2.72 (s, 3H), 2.90 (t, J = 8.2 Hz, 2H), 3.29 (t, J = 8.2 Hz, 2H), 6.33–6.37 (m, 1H), 6.99–7.03 (m, 2H). **^{13}C NMR** (100.5 MHz, $CDCl_3$): δ 28.46, 36.15, 56.16, 107.66, 122.23, 124.41, 126.89,

132.11, 152.01. **IR** (ATR): 717, 796, 871, 1094, 1196, 1268, 1419, 1491, 1604, 1671, 2812, 2951 cm^{-1}. **EI-HRMS** (*m/z*): $[M]^+$ Calcd for $C_9H_{10}NCl$, 167.04963. found. 167.05003.

1-Methyl-6-nitroindoline (1e)

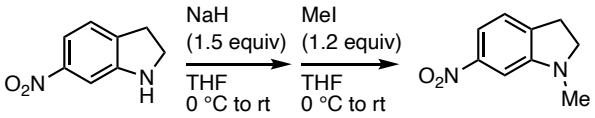

To a well-stirred solution of 6-nitroindoline (821 mg, 5.0 mmol, 1.0 equiv) in THF (15 mL) at 0 °C was added NaH (55% in mineral oil, 327 mg, 7.5 mmol, 1.5 equiv). The reaction mixture was warmed to room temperature and allowed to stir for 30 min. The flask was cooled again to 0 °C and MeI (852 mg, 6 mmol, 1.2 equiv) was added dropwise. The reaction mixture was warmed to room temperature and allowed to stir until the reaction completed (monitored by TLC) and then quenched with saturated aqueous NH_4Cl at 0 °C. The mixture was extracted with Et_2O (3 x 20 mL). The organic layer was dried over anhydrous Na_2SO_4, filtered and concentrated under vacuum. The crude product was purified by column chromatography (using 10% EtOAc/hexane) to give **1e** (766 mg, 86% yield) as red solids. **M.P.** 53.8–55.6 °C. **^{1}H NMR** (400 MHz, $CDCl_3$): δ 2.83 (s, 3H), 3.03 (t, J = 8.6 Hz, 2H), 3.46 (t, J = 8.6 Hz, 2H), 7.10 (d, J = 8.0 Hz, 1H), 7.16 (d, J = 1.6 Hz, 1H), 7.54 (dd, J = 7.8, 1.8 Hz, 1H). **^{13}C NMR** (100.5 MHz, $CDCl_3$): δ 28.56, 35.23, 55.75, 100.41, 113.47, 123.76, 137.92, 148.60, 154.09. **IR** (ATR): 735, 841, 1065, 1292, 1338, 1392, 1508, 1594, 1612, 2924 cm^{-1}. **EI-HRMS** (*m/z*): $[M+H]^+$ Calcd for $C_9H_{11}N_2O_2$, 179.08150. found. 179.08181.

***cis*-5,6,6a,11b-Tetrahydro-7*H*-indeno[2,1-*c*]quinolin-7-one (1w)**

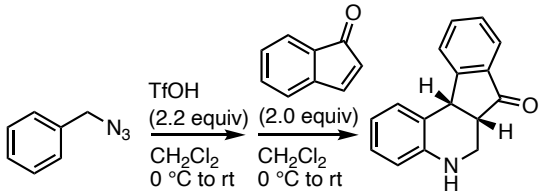

1w was prepared via hetero-Diels-Alder reaction according to Pearson's procedure.[19] To a solution of BnN_3 (282 mg, 2.1 mmol, 1.0 equiv.) in CH_2Cl_2 (15 mL) at 0 °C was added TfOH (698 mg, 4.7 mmol, 2.2 equiv) was added. The mixture was allowed to stir for 10 min at room temperature. Next, 1*H*-Inden-1-one (550 mg, 4.2 mmol, 2.0 equiv) was added at 0 °C. The reaction mixture was warmed to room temperature and allowed to stir until the reaction completed (monitored by TLC) and then quenched with saturated aqueous $NaHCO_3$. The mixture was extracted with EtOAc (3 x 100 mL). The organic layer was dried over anhydrous Na_2SO_4, filtered and concentrated under vacuum. The crude product was purified by column chromatography (using 10% EtOAc/hexane) to give **1w** (304 mg, 61% yield) as yellow solids. **M.P.** 162.3–164.4 °C. **^{1}H NMR** (400 MHz, $CDCl_3$): δ 3.20–3.25 (m, 1H), 3.32 (dd, J = 11.2, 5.2 Hz, 1H), 3.63 (br-s, 1H), 3.75 (dd, J = 11.2, 2.8 Hz, 1H), 4.66 (d, J =

8.4 Hz, 1H), 6.53 (dd, J = 8.0, 0.8 Hz, 1H), 6.86 (td, J = 7.6, 1.2 Hz, 1H), 7.02 (td, J = 7.6, 1.6 Hz, 1H), 7.34 (t, J = 7.6 Hz, 1H), 7.47–7.64 (m, 3H), 7.73 (d, J = 7.6 Hz, 1H). **^{13}C NMR** (100.5 MHz, $CDCl_3$): δ 40.23, 44.35, 50.27, 115.90, 119.62, 123.28, 124.44, 126.26, 127.24, 127.75, 129.20, 135.29, 135.63, 146.53, 156.52, 207.84. **IR** (ATR): 750, 793, 959, 1011, 1254, 1460, 1485, 1601, 1710, 3055, 3338 cm^{-1}. **EI-HRMS** (*m/z*): $[M+H]^+$ Calcd for $C_{16}H_{14}ON$, 236.10699. found. 236.10734.

Experimental Procedures

General Procedure for Scheme 3: In a nitrogen-filled glove box, $[IrCl(cod)]_2$ (1.34 mg, 0.002 mmol, 2 mol% Ir; prepared c = 0.01 mol/L *p*-xylene solution, 0.2 mL), PS-DPPBz (40 mg, 0.004 mmol, 2 mol%) and *p*-xylene (0.8 mL; total 1 mL) were placed successively in a 10-mL glass tube containing a magnetic stirring bar. After stirring at room temperature for 5 min, *N*-heterocycle substrate **1a** (0.2 mmol) was added. The tube was sealed with a screw top-hole caps with a Teflon®-coated sealing disk, and was removed from the glove box. The tube was connected with an empty balloon. The mixture was stirred at 130 °C for 3 h. After being cooled to room temperature, the mixture was filtered through a Celite pad (eluting with Et_2O). The volatiles were removed under reduced pressure, and an internal standard (1,1,2,2-tetrachloroethane) was added to determine the yield of 1-methyl-1*H*-indole **2a**.

General Procedure for Scheme 5: In a nitrogen-filled glove box, $[IrCl(cod)]_2$ (2.7 mg, 0.004 mmol, 4 mol% Ir), PS-DPPBz (80 mg, 0.008 mmol, 4 mol%) and *p*-xylene (1 mL) were placed successively in a 10-mL glass tube containing a magnetic stirring bar. After stirring at room temperature for 5 min, *N*-heterocycle substrate **1** (0.2 mmol) was added. The tube was sealed with a screw top-hole caps with a Teflon®-coated sealing disk, and was removed from the glove box. The tube was connected with an empty balloon. The mixture was stirred at 130 °C for 20 h. After being cooled to room temperature, the mixture was filtered through a Celite pad (eluting with Et_2O). The volatiles were removed under reduced pressure, and an internal standard (1,1,2,2-tetrachloroethane) was added to determine the yield of **2**. The crude material was purified by silica gel column chromatography to give the dehydrogenated product **2**.

General Procedure for Scheme 9: In a nitrogen-filled glove box, $[IrCl(cod)]_2$ (2.7 mg, 0.004 mmol, 4 mol% Ir), PS-DPPBz (80 mg, 0.008 mmol, 4 mol%) and *p*-xylene (1 mL) were placed successively in a 50 mL stainless steel Parr pressure reactor. After stirring at room temperature for 5 min, *N*-heterocycle substrate **2** (0.2 mmol) was added. The reactor was sealed, flushed with H_2 three times, and placed under 30 or 40 atm H_2 pressure. The solution was heated to 130 °C and stirred for 20 h. After being cooled to room temperature, the mixture was filtered through a Celite pad (eluting with Et_2O). The volatiles were removed under reduced pressure, and an internal standard (1,1,2,2-tetrachloroethane) was added to determine the yield of **1**. The crude material was purified by silica gel column chromatography to give the hydrogenated product **1**.

Gram-Scale Reaction of 1q: The reaction apparatus is shown in Figure 6. In a two-necked Schlenk flask, $[IrCl(cod)]_2$ (2.7 mg, 0.004 mmol, 0.08 mol% Ir), PS-DPPBz (80 mg, 0.008 mmol, 0.08 mol%) and *p*-xylene (0.5 mL) were placed successively after the flask was evacuated and backfilled with argon three times. After stirring at room temperature for 5 min, indoline **1q** (1.2 g, 10 mmol) was added. The mixture was stirred at 160 °C for 60 h. An internal standard (1,1,2,2-tetrachloroethane) was added to determine the yield of **2q** (94%). The volume of evolved H_2 gas was measured by a gas burette, and the molar amount of H_2 was calculated using the ideal gas law (210 mL, 94%). H_2 gas evolution was confirmed by GC analysis (Figure 7).

Characterization of Products

1-Methyl-1*H*-indole (2a)

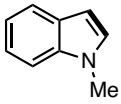

[4 mol% Ir, 130 °C, 20 h] The product **2a** (25.9 mg, 99% yield) was isolated by silica gel column chromatography with hexane/EtOAc (90:10). Colorless oil. **^{1}H NMR** (400 MHz, $CDCl_3$): δ 3.70 (s, 3H), 6.46 (d, J = 3.2 Hz, 1H), 6.99 (d, J = 3.2 Hz, 1H), 7.06–7.13 (m, 1H), 7.17–7.23 (m, 1H), 7.28 (dd, J = 8.0, 0.8 Hz, 1H), 7.62 (d, J = 8.0 Hz, 1H). **^{13}C NMR** (100.5 MHz, $CDCl_3$): δ 32.68, 100.77, 109.11, 119.17, 120.77, 121.38, 128.37, 128.72, 136.57.

1,2-Dimethyl-1*H*-indole (2b)

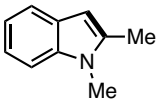

[4 mol% Ir, 130 °C, 20 h] The product **2b** (28.4 mg, 98% yield) was isolated by silica gel column chromatography with hexane/EtOAc (90:10). Light yellow oil. **^{1}H NMR** (400 MHz, $CDCl_3$): δ 2.40 (s, 3H), 3.63 (s, 3H), 6.23 (s, 1H), 7.05 (t, J = 8.0 Hz, 1H), 7.14 (td, J = 7.6, 0.8 Hz, 1H), 7.22 (t, J = 8.6 Hz, 1H), 7.51 (d, J = 8.0 Hz, 1H). **^{13}C NMR** (100.5 MHz, $CDCl_3$): δ 13.32, 29.91, 100.05, 109.25, 119.75, 120.13, 120.94, 128.45, 137.34, 137.81

5-Methoxy-1-methyl-1*H*-indole (2c)

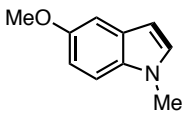

[4 mol% Ir, 130 °C, 20 h] The product **2c** (28.9 mg, 90% yield) was isolated by silica gel column chromatography with hexane/EtOAc (95:5). White solid. **^{1}H NMR** (400

MHz, $CDCl_3$): δ 3.74 (s, 3H), 3.84 (s, 3H), 6.39 (dd, J = 3.2, 0.8 Hz, 1H), 6.88 (dd, J = 8.8, 2.4 Hz, 1H), 7.00 (d, J = 2.8 Hz, 1H), 7.08 (d, J = 2.4 Hz, 1H), 7.19 (d, J = 8.4 Hz, 1H). **^{13}C NMR** (100.5 MHz, $CDCl_3$): δ 33.03, 55.92, 100.39, 102.47, 109.98, 111.89, 128.79, 129.37, 132.13, 154.01.

5-Chloro-1-methyl-1*H*-indole (2d)

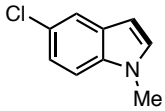

[4 mol% Ir, 130 °C, 20 h] The product **2d** (28.8 mg, 87% yield) was isolated by silica gel column chromatography with hexane/EtOAc (95:5). Colorless oil. **^{1}H NMR** (400 MHz, $CDCl_3$): δ 3.73 (s, 3H), 6.40 (d, J = 4.0 Hz, 1H), 7.03 (d, J = 2.8 Hz, 1H), 7.13–7.22 (m, 2H), 7.57 (d, J = 2.0 Hz, 1H). **^{13}C NMR** (100.5 MHz, $CDCl_3$): δ 32.94, 100.50, 110.16, 120.11, 121.69, 124.99, 129.34, 130.07, 135.03.

1-Methyl-6-nitro-1*H*-indole (2e)

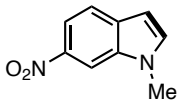

[4 mol% Ir, 130 °C, 20 h] The product **2e** (34.1 mg, 97% yield) was isolated by silica gel column chromatography with hexane/EtOAc (95:5). Yellow solid. **^{1}H NMR** (400 MHz, $CDCl_3$): δ 3.89 (s, 3H), 6.58 (d, J = 3.2 Hz, 1H), 7.34 (d, J = 2.8 Hz, 1H), 7.64 (d, J = 9.2 Hz, 1H), 8.00 (dd, J = 8.8, 2.4 Hz, 1H), 8.31 (d, J = 2.0 Hz, 1H). **^{13}C NMR** (100.5 MHz, $CDCl_3$): δ 33.25, 102.08, 106.33, 114.80, 120.66, 133.21, 134.54, 135.20, 142.86.

1,2-Dimethyl-1*H*-indole (2f)

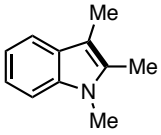

[4 mol% Ir, 140 °C, 20 h, *cis*-**1f**] The product **2f** (27.7 mg, 87% yield) was isolated by silica gel column chromatography with hexane/EtOAc (90:10). Light yellow oil. **^{1}H NMR** (400 MHz, $CDCl_3$): δ 2.23 (s, 3H), 2.29 (s, 3H), 3.55 (s, 3H), 7.01–7.25 (m, 3H), 7.47 (t, J = 6.6 Hz, 1H). **^{13}C NMR** (100.5 MHz, $CDCl_3$): δ 8.75, 10.03, 29.33, 106.04, 108.27, 117.80, 118.44, 120.36, 128.27, 132.54, 136.35.

1-Ethyl-1*H*-indole (2g)

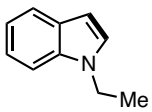

[4 mol% Ir, 130 °C, 20 h] The product **2g** (26.4 mg, 91% yield) was isolated by silica gel column chromatography with hexane/EtOAc (95:5). Colorless liquid. **^{1}H NMR**

(400 MHz, $CDCl_3$): δ 1.42 (t, J = 7.4 Hz, 3H), 4.12 (q, J = 7.2 Hz, 2H), 6.48 (dd, J = 3.2, 0.8 Hz, 1H), 7.05–7.12 (m, 2H), 7.16–7.22 (m, 1H), 7.32 (d, J = 8.0 Hz, 1H), 7.62 (d, J = 8.0 Hz, 1H). **^{13}C NMR** (100.5 MHz, $CDCl_3$): δ 15.40, 40.85 100.90, 109.20, 119.12, 120.90, 121.24, 126.93, 128.54, 135.59.

1-Butyl-1*H*-indole (2h)

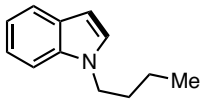

[4 mol% Ir, 130 °C, 20 h] The product **2h** (32.2 mg, 93% yield) was isolated by silica gel column chromatography with hexane/EtOAc (95:5). Yellow oil. **^{1}H NMR** (400 MHz, $CDCl_3$): δ 0.93 (t, J = 7.6 Hz, 3H), 1.19–1.39 (m, 2H), 1.76–1.85 (m, 2H), 4.10 (t, J = 7.0 Hz, 2H), 6.48 (d, J = 3.2 Hz, 1H), 7.06–7.12 (m, 2H), 7.17–7.23 (m, 1H), 7.33 (d, J = 8.0 Hz, 1H), 7.62 (d, J = 8.0 Hz, 1H). **^{13}C NMR** (100.5 MHz, $CDCl_3$): δ 13.69, 20.16, 32.29, 46.07, 100.74, 109.34, 119.09, 120.88, 121.22, 127.77, 128.49, 135.89.

1-Isobutyl-1*H*-indole (2i)

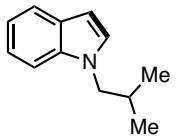

[4 mol% Ir, 130 °C, 20 h] The product **2i** (32.9 mg, 95% yield) was isolated by silica gel column chromatography with hexane/EtOAc (95:5). Colorless oil. **^{1}H NMR** (400 MHz, $CDCl_3$): δ 0.92 (d, J = 6.4 Hz, 6H), 2.13–2.27 (m, 1H), 3.90 (d, J = 7.2 Hz, 2H), 6.48 (d, J = 3.2 Hz, 1H), 7.04–7.12 (m, 2H), 7.16–7.22 (m, 1H), 7.33 (d, J = 8.0 Hz, 1H), 7.63 (d, J = 7.6 Hz, 1H). **^{13}C NMR** (100.5 MHz, $CDCl_3$): δ 20.31 (2C), 29.49, 54.12, 100.66, 109.56, 119.08, 120.85, 121.21, 128.39, 128.47, 136.17.

1-Benzyl-1*H*-indole (2j)

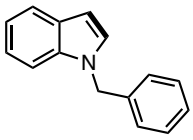

[4 mol% Ir, 130 °C, 20 h] The product **2j** (39.0 mg, 94% yield) was isolated by silica gel column chromatography with hexane/EtOAc (95:5). Yellow solid. **^{1}H NMR** (400 MHz, $CDCl_3$): δ 5.31 (s, 2H), 6.55 (d, J = 2.8 Hz, 1H), 7.07–7.19 (m, 5H), 7.21–7.31 (m, 4H), 7.65 (d, J = 8.0 Hz, 1H). **^{13}C NMR** (100.5 MHz, $CDCl_3$): δ 50.03, 101.63, 109.65, 119.48, 120.93, 121.64, 126.71 (2C), 127.54, 128.23, 128.65, 128.72 (2C), 136.24, 137.50.

1-(4-Methoxybenzyl)-2-methyl-1*H*-indole (2k)

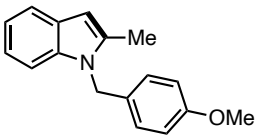

[4 mol% Ir, 140 °C, 10 h] The product **2k** (46.2 mg, 92% yield) was isolated by silica gel column chromatography with hexane/EtOAc (95:5). Yellow oil. **^{1}H NMR** (400 MHz, $CDCl_3$): δ 2.34 (s, 3H), 3.70 (s, 3H), 5.19 (s, 2H), 6.30 (s, 1H), 6.76 (d, J = 8.8 Hz, 2H), 6.88 (d, J = 8.4 Hz, 2H), 7.03–7.12 (m, 2H), 7.19 (d, J = 7.6 Hz, 1H), 7.52–7.56 (m, 1H). **^{13}C NMR** (100.5 MHz, $CDCl_3$): δ 12.73, 45.80, 55.15, 100.28, 109.15, 114.02 (2C), 119.37, 119.62, 120.61, 127.14 (2C), 128.07, 129.84, 136.62, 137.04, 158.68.

1-Cyclohexyl-1*H*-indole (2l)

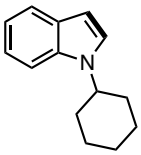

[4 mol% Ir, 130 °C, 20 h] The product **2l** (36.6 mg, 92% yield) was isolated by silica gel column chromatography with hexane/EtOAc (95:5). Colorless oil. **^{1}H NMR** (400 MHz, $CDCl_3$): δ 1.17–1.37 (m, 1H), 1.43–1.56 (m, 2H), 1.64–1.83 (m, 3H), 1.89–1.98 (m, 2H), 2.09–2.18 (m, 2H), 4.21 (tt, J = 12.0, 3.6 Hz, 1H), 6.50 (d, J = 3.2 Hz, 1H), 7.05–7.12 (m, 1H), 7.16–7.24 (m, 2H), 7.38 (d, J = 8.0 Hz, 1H), 7.63 (d, J = 8.0 Hz, 1H). **^{13}C NMR** (100.5 MHz, $CDCl_3$): δ 25.62, 25.93 (2C), 33.48 (2C), 55.00, 100.90, 109.38, 119.15, 120.89, 121.02, 124.00, 128.37, 135.44.

1-Phenyl-1*H*-indole (2m)

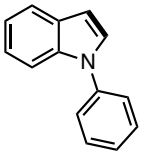

[4 mol% Ir, 130 °C, 20 h] The product **2m** (35.2 mg, 91% yield) was isolated by silica gel column chromatography with hexane/EtOAc (95:5). White solid. **^{1}H NMR** (400 MHz, $CDCl_3$): δ 6.67 (d, J = 3.2 Hz, 1H), 7.13–7.24 (m, 2H), 7.29–7.36 (m, 2H), 7.46–7.51 (m, 4H), 7.56 (d, J = 7.6 Hz, 1H), 7.68 (d, J = 7.2 Hz, 1H). **^{13}C NMR** (100.5 MHz, $CDCl_3$): δ 103.53, 110.47, 120.32, 121.09, 122.31, 124.31 (2C), 126.38, 127.91, 129.26, 129.56 (2C), 135.77, 139.76.

1-Tosyl-1*H*-indole (2n)

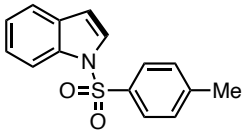

[4 mol% Ir, 160 °C, 48 h] The product **2n** (48.3 mg, 89% yield) was isolated by silica gel column chromatography with hexane/EtOAc (95:5). Light red solid. **^{1}H NMR** (400 MHz, $CDCl_3$): δ 2.31 (s, 3H), 6.64 (dd, J = 3.6, 0.8 Hz, 1H), 7.17–7.25 (m, 3H), 7.30 (t, J = 7.8 Hz, 1H), 7.51 (d, J = 8.0 Hz, 1H), 7.56 (d, J = 4.0 Hz, 1H), 7.75 (d, J = 8.4 Hz, 2H), 7.99 (dd, J = 8.4, 0.8 Hz, 1H). **^{13}C NMR** (100.5 MHz, $CDCl_3$): δ 21.65, 109.13, 113.62, 121.47, 123.37, 124.65, 126.43, 126.91 (2C), 129.97 (2C), 130.83, 134.89, 135.34, 145.03.

1-((Trifluoromethyl)sulfonyl)-1*H*-indole (2o)

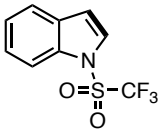

[4 mol% Ir, 160 °C, 48 h] The product **2o** (20.4 mg, 41% yield) was isolated by silica gel column chromatography with hexane/EtOAc (95:5). Colorless oil. **^{1}H NMR** (400 MHz, $CDCl_3$): δ 6.80 (d, J = 3.6 Hz, 1H), 7.32–7.41 (m, 3H), 7.61 (dt, J = 7.8, 1.2 Hz, 1H), 7.91 (d, J = 8.4 Hz, 1H). **^{13}C NMR** (100.5 MHz, $CDCl_3$): δ 111.60, 113.67, 119.56 (q, J = 324 Hz), 121.86, 124.86, 125.76, 126.18, 130.65, 135.31.

1-(1*H*-Indol-1-yl)ethan-1-one (2p)

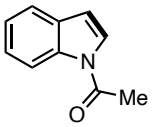

[4 mol% Ir, 160 °C, 48 h] The product **2p** (14.6 mg, 46% yield) was isolated by silica gel column chromatography with hexane/EtOAc (90:10). Yellow solid. **^{1}H NMR** (400 MHz, $CDCl_3$): δ 2.65 (s, 3H), 6.65 (dd, J = 7.6, 0.8 Hz, 1H), 7.27–7.31 (m, 1H), 7.36 (td, J = 6.8, 1.2 Hz, 1H), 7.43 (d, J = 3.6 Hz, 1H), 7.57 (d, J = 8.0 Hz, 1H), 8.45 (d, J = 7.6 Hz, 1H). **^{13}C NMR** (100.5 MHz, $CDCl_3$): δ 24.02, 109.18, 116.53, 120.82, 123.65, 125.12, 125.21, 130.19, 135.51, 168.66.

1*H*-Indole (2q)

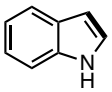

[2 mol% Ir, 130 °C, 20 h] The product **2q** (23.2 mg, 99% yield) was isolated by silica gel column chromatography with hexane/EtOAc (95:5). White solid. **^{1}H NMR** (400 MHz, $CDCl_3$): δ 6.54 (s, 1H), 7.09–7.22 (m, 3H), 7.35 (dd, J = 8.4, 0.8 Hz, 1H), 7.65 (d, J = 8.0 Hz, 1H), 8.01 (br, 1H). **^{13}C NMR** (100.5 MHz, $CDCl_3$): δ 102.51, 110.99, 119.75, 120.68, 121.93, 124.12, 127.75, 135.68.

2-Methyl-1*H*-indole (2r)

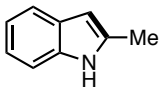

[4 mol% Ir, 130 °C, 20 h] The product **2r** (25.7 mg, 98% yield) was isolated by silica gel column chromatography with hexane/EtOAc (95:5). Yellow solid. **^{1}H NMR** (400 MHz, $CDCl_3$): δ 2.41 (s, 3H), 6.21 (s, 1H), 7.04–7.14 (m, 2H), 7.25 (t, J = 7.4 Hz, 1H), 7.51 (d, J = 7.2 Hz, 1H), 7.76 (br, 1H). **^{13}C NMR** (100.5 MHz, $CDCl_3$): δ 13.67, 100.31, 110.16, 119.57 (2C, overlapping), 120.86, 128.98, 135.02, 135.96.

5-Bromo-1*H*-indole (2s)

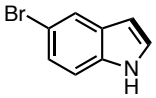

[4 mol% Ir, 130 °C, 20 h] The product **2s** (38.4 mg, 98% yield) was isolated by silica gel column chromatography with hexane/EtOAc (95:5). Yellow solid. **^{1}H NMR** (400 MHz, $CDCl_3$): δ 6.50 (t, J = 2.6 Hz, 1H), 7.20 (t, J = 3.0 Hz, 1H), 7.23–7.30 (m, 2H), 7.77 (s, 1H), 8.16 (br, 1H). **^{13}C NMR** (100.5 MHz, $CDCl_3$): δ 102.28, 112.39, 112.98, 123.18, 124.81, 125.32, 129.57, 134.33.

6-Nitro-1*H*-indole (2t)

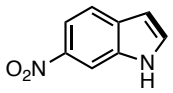

[4 mol% Ir, 130 °C, 20 h] The product **2t** (28.8 mg, 89% yield) was isolated by silica gel column chromatography with hexane/EtOAc (90:10). Yellow solid. **^{1}H NMR** (400 MHz, $CDCl_3$): δ 6.65–6.69 (m, 1H), 7.53 (t, J = 2.8 Hz, 1H), 7.69 (d, J = 8.4 Hz, 1H), 8.04 (dd, J = 8.8, 2.4 Hz, 1H), 8.41 (s, 1H), 8.75 (br, 1H). **^{13}C NMR** (100.5 MHz, $CDCl_3$): δ 103.60, 108.05, 115.38, 120.61, 130.03, 132.78, 134.21, 143.25.

Quinoline (2u)

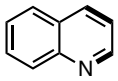

[4 mol% Ir, 160 °C, 48 h] The product **2u** (16.5 mg, 64% yield) was isolated by silica gel column chromatography with hexane/EtOAc (90:10). Colorless oil. **^{1}H NMR** (400 MHz, $CDCl_3$): δ 7.30–7.37 (m, 1H), 7.51 (t, J = 7.6 Hz, 1H), 7.69 (t, J = 7.6 Hz, 1H), 7.76 (d, J = 8.4 Hz, 1H), 8.10 (t, J = 8.6 Hz, 2H), 8.90 (d, J = 4.4 Hz, 1H). **^{13}C NMR** (100.5 MHz, $CDCl_3$): δ 120.87, 126.33, 127.60, 128.07, 129.25 (2C, overlapping), 135.83, 148.08, 150.23.

2-Methylquinoline (2v)

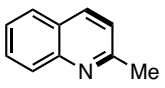

[4 mol% Ir, 160 °C, 48 h] The product **2v** (26.6 mg, 93% yield) was isolated by silica gel column chromatography with hexane/EtOAc (90:10). Colorless oil. **^{1}H NMR** (400 MHz, $CDCl_3$): δ 2.73 (s, 3H), 7.22–7.25 (m, 1H), 7.45 (t, J = 7.4 Hz, 1H), 7.66 (t, J = 7.8 Hz, 1H), 7.73 (d, J = 8.4 Hz, 1H), 7.96–8.05 (m, 2H). **^{13}C NMR** (100.5 MHz, $CDCl_3$): δ 25.26, 121.84, 125.50, 126.31, 127.34, 128.47, 129.26, 135.99, 147.71, 158.82.

7*H*-Indeno[2,1-*c*]quinolin-7-one (2w)

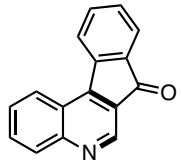

[4 mol% Ir, 160 °C, 48 h] The product **2w** (31.6 mg, 67% yield) was isolated by silica gel column chromatography with hexane/EtOAc (90:10). Yellow solid. **^{1}H NMR** (400 MHz, $CDCl_3$): δ 7.49 (t, J = 7.2 Hz, 1H), 7.63 (td, J = 7.6, 1.2 Hz, 1H), 7.67–7.73 (m, 1H), 7.77 (d, J = 7.2 Hz, 1H), 7.82–7.89 (m, 1H), 8.12 (d, J = 7.2 Hz, 1H), 8.17 (d, J = 8.0 Hz, 1H), 8.47 (d, J = 8.4 Hz, 1H), 9.15 (s, 1H). **^{13}C NMR** (100.5 MHz, $CDCl_3$): δ 123.61, 124.53, 124.83, 124.89, 124.98, 128.23, 131.12, 132.16, 133.96, 134.71, 142.49, 144.84, 151.14, 152.58, 193.05.

Isoquinoline (2x)

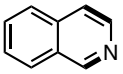

[4 mol% Ir, 160 °C, 48 h] The product **2x** (13.2 mg, 51% yield) was isolated by silica gel column chromatography with hexane/EtOAc (90:10). Colorless oil. **^{1}H NMR** (400 MHz, $CDCl_3$): δ 7.56–7.72 (m, 3H), 7.82 (d, J = 8.4 Hz, 1H), 7.97 (d, J = 8.4 Hz, 1H), 8.53 (d, J = 6.0 Hz, 1H), 9.26 (s, 1H). **^{13}C NMR** (100.5 MHz, $CDCl_3$): δ 120.39, 126.41, 127.17, 127.56, 128.60, 130.27, 135.69, 142.98, 152.50.

1-Methylisoquinoline (2y)

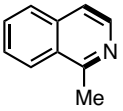

[4 mol% Ir, 160 °C, 48 h] The product **2y** (26.6 mg, 93% yield) was isolated by silica gel column chromatography with hexane/EtOAc (90:10). Yellow liquid. **^{1}H NMR** (400 MHz, $CDCl_3$): δ 2.97 (s, 3H), 7.51 (d, J = 6.0 Hz, 1H), 7.60 (t, J = 7.8 Hz, 1H), 7.68 (t, J = 7.6 Hz, 1H), 7.81 (d, J = 7.8 Hz, 1H), 8.12 (d, J = 7.6 Hz, 1H), 8.40 (d, J = 4.4 Hz, 1H). **^{13}C NMR** (100.5 MHz, $CDCl_3$): δ 22.40, 119.22, 125.57, 126.97, 127.14, 127.43, 129.87, 135.81, 141.77, 158.55.

Quinoxaline (2z)

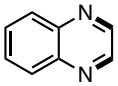

[4 mol% Ir, 160 °C, 48 h] The product **2z** (21.3 mg, 82% yield) was isolated by silica gel column chromatography with hexane/EtOAc (90:10). Light yellow solid. **^{1}H NMR** (400 MHz, $CDCl_3$): δ 7.69–7.82 (m, 2H), 8.04–8.16 (m, 2H), 8.86 (s, 2H). **^{13}C NMR** (100.5 MHz, $CDCl_3$): δ 129.40 (2C), 129.96 (2C), 142.90 (2C), 144.88 (2C).

2,5-Dimethylpyrazine (2aa)

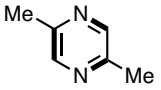

[4 mol% Ir, 160 °C, 48 h] 47% yield (based on ^{1}H NMR analysis of the crude product). **^{1}H NMR** (400 MHz, $CDCl_3$): δ 8.71 (s, 2H), 2.90 (s, 6H).

2-Phenylbenzo[*d*]thiazole (2ab)

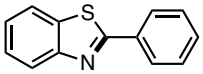

[4 mol% Ir, 130 °C, 20 h] The product **2ab** (34.2 mg, 81% yield) was isolated by silica gel column chromatography with hexane/EtOAc (90:10). Yellow solid. **^{1}H NMR** (400 MHz, $CDCl_3$): δ 7.39 (td, J = 8.0, 1.2 Hz, 1H), 7.47–7.52 (m, 4H), 7.91 (d, J = 7.6 Hz, 1H), 8.05–8.13 (m, 3H). **^{13}C NMR** (100.5 MHz, $CDCl_3$): δ 121.60, 123.20, 125.17, 126.30, 127.53 (2C), 129.00 (2C), 130.96, 133.58, 135.03, 154.10, 168.06.

1,2-Di(1*H*-indol-1-yl)ethane (2ac)

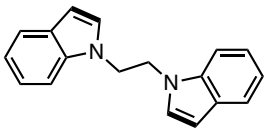

[4 mol% Ir, 140 °C, 20 h] The product **2ac** (50.1 mg, 96% yield) was isolated by silica gel column chromatography with hexane/EtOAc (90:10). Yellow solid. **^{1}H NMR** (400 MHz, $CDCl_3$): δ 4.46 (s, 4H), 6.38 (d, J = 3.2 Hz, 2H), 6.57 (d, J = 3.2 Hz, 2H), 7.09–7.25 (m, 6H), 7.62 (d, J = 7.6 Hz, 2H). **^{13}C NMR** (100.5 MHz, $CDCl_3$): δ 46.15 (2C), 101.76 (2C), 108.70 (2C), 119.62 (2C), 121.18 (2C), 121.73 (2C), 127.96 (2C), 128.80 (2C), 135.46 (2C).

5-Chloro-3-(2-(5-chloro-1*H*-indol-1-yl)ethyl)-1*H*-indole (2ad)

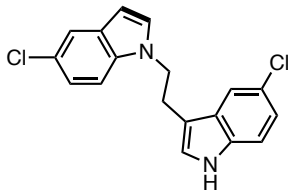

[4 mol% Ir, 150 °C, 48 h] The product **2ad** (43.8 mg, 84% yield) was isolated by silica gel column chromatography with CH_2Cl_2/Et_2O (50:1). Yellow solid. **^{1}H NMR** (400 MHz, DMSO-d_6) δ 3.15 (t, J = 7.2 Hz, 2H), 4.42 (t, J = 7.2 Hz, 2H), 6.37 (d, J = 3.2 Hz, 1H), 7.02–7.12 (m, 3H), 7.33 (d, J = 8.0 Hz, 1H), 7.40 (d, J = 3.2 Hz, 1H), 7.48 (d, J = 8.4 Hz, 1H), 7.54 (d, J = 2.0 Hz, 1H), 7.56 (d, J = 2.0 Hz, 1H), 11.03 (br, 1H). **^{13}C NMR** (101 MHz, DMSO-d_6) δ 25.62, 46.51, 100.19, 110.91, 111.41, 112.88, 117.67, 119.50, 120.78, 120.93, 123.14, 123.53, 125.14, 128.23, 129.19, 130.43, 134.17, 134.54.

1-(1-(Pyridin-2-ylmethyl)piperidin-4-yl)-1*H*-indole (2ae)

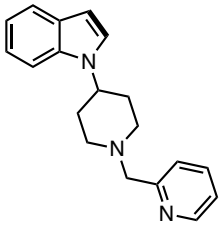

[5 mol% Ir, 160 °C, 48 h] The product **2ae** (21.6 mg, 37% yield; 43% conversion of **1ae**) was isolated by silica gel column chromatography with hexane/EtOAc (90:10). Yellow solid. **^{1}H NMR** (400 MHz, $CDCl_3$): δ 2.03–2.20 (m, 4H), 2.33 (td, J = 11.2, 2.4 Hz, 2H), 3.09 (d, J = 12.0 Hz, 2H), 3.74 (s, 2H), 4.22–4.32 (m, 1H), 6.52 (d, J = 3.2 Hz, 1H), 7.09 (t, J = 7.2 Hz, 1H), 7.16–7.28 (m, 3H), 7.38 (d, J = 8.0 Hz, 1H), 7.44 (d, J = 7.6 Hz, 1H), 7.63 (d, J = 7.6 Hz, 1H), 7.68 (td, J = 8.0, 1.6 Hz, 1H), 8.60 (d, J = 4.8 Hz, 1H). **^{13}C NMR** (100.5 MHz, $CDCl_3$): δ 32.45 (2C), 53.30, 53.39 (2C), 64.56, 101.32, 109.23, 119.32, 120.97, 121.19, 122.10, 123.19, 123.99, 128.44, 135.50, 136.44, 149.36, 158.51.

1-Methylindoline (1a)

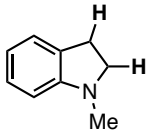

[4 mol% Ir, 130 °C, 20 h, 40 atm H_2] The product **1a** (26.1 mg, 98% yield) was isolated by silica gel column chromatography with hexane/EtOAc (95:5). Yellow oil. **^{1}H NMR** (400 MHz, $CDCl_3$): δ 2.74 (s, 3H), 2.93 (t, J = 8.0 Hz, 2H), 3.27 (t, J = 8.4 Hz, 2H), 6.48 (d, J = 7.6 Hz, 1H), 6.66 (t, J = 7.0 Hz, 1H), 7.06–7.09 (m, 2H). **^{13}C NMR** (100.5 MHz, $CDCl_3$): δ 28.67, 36.21, 56.09, 107.15, 117.68, 124.19, 127.24, 130.22, 153.32.

1-Tosylindoline (1n)

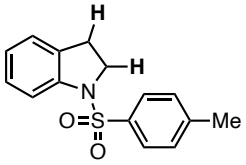

[4 mol% Ir, 130 °C, 40 h, 30 atm H_2] The product **1n** (52.0 mg, 95% yield) was isolated by silica gel column chromatography with hexane/EtOAc (95:5). White solid. **^{1}H NMR** (400 MHz, $CDCl_3$): δ 2.37 (s, 3H), 2.88 (t, J = 8.4 Hz, 2H), 3.91 (t, J = 8.4 Hz, 2H), 6.97 (td, J = 7.2, 0.8 Hz, 1H), 7.07 (d, J = 7.6 Hz, 1H), 7.16–7.25 (m, 3H), 7.62–7.70 (m, 3H). **^{13}C NMR** (100.5 MHz, $CDCl_3$): δ 21.51, 27.83, 49.89, 114.96, 123.66, 125.05, 127.29 (2C), 127.67, 129.61 (2C), 131.71, 133.88, 141.93, 144.01.

Indoline (1q)

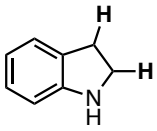

[4 mol% Ir, 130 °C, 20 h, 40 atm H_2] The product **1q** (19.3 mg, 81% yield) was isolated by silica gel column chromatography with hexane/EtOAc (95:5). Colorless oil. **^{1}H NMR** (400 MHz, $CDCl_3$): δ 2.98 (t, J = 8.0 Hz, 2H), 3.48 (t, J = 8.4 Hz, 2H), 3.63 (br, 1H), 6.60 (d, J = 8.0 Hz, 1H), 6.68 (t, J = 7.2 Hz, 1H), 6.99 (t, J = 7.4 Hz, 1H), 7.09 (d, J = 7.2 Hz, 1H). **^{13}C NMR** (100.5 MHz, $CDCl_3$): δ 29.65, 47.15, 109.29, 118.46, 124.44, 127.02, 129.15, 151.42.

2-Methyl-1,2,3,4-tetrahydroquinoline (1v)

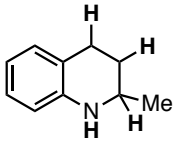

[4 mol% Ir, 130 °C, 20 h, 40 atm H_2] The product **1v** (28.2 mg, 96% yield) was isolated by silica gel column chromatography with hexane/EtOAc (95:5). Colorless oil. **^{1}H NMR** (400 MHz, $CDCl_3$): δ 1.15 (d, J = 6.4 Hz, 3H), 1.48–1.62 (m, 1H), 1.83–1.93 (m, 1H), 2.63–2.87 (m, 2H), 3.28–3.39 (m, 1H), 3.62 (br-s, 1H), 6.42 (d, J = 8.0 Hz, 1H), 6.54–6.64 (m, 1H), 6.88–6.96 (m, 2H). **^{13}C NMR** (100.5 MHz, $CDCl_3$): δ 22.42, 26.44, 29.95, 46.95, 113.86, 116.78, 120.87, 126.50, 129.10, 144.61.

1,2,3,4-Tetrahydroisoquinoline (1x)

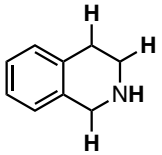

[4 mol% Ir, 130 °C, 20 h, 40 atm H_2] The product **1x** (23.1 mg, 87% yield) was isolated by silica gel column chromatography with hexane/EtOAc (95:5). Colorless oil. **^{1}H**

NMR (400 MHz, $CDCl_3$): δ 2.78 (t, J = 5.8 Hz, 2H), 3.12 (t, J = 5.8 Hz, 2H), 4.00 (s, 2H), 6.96–7.02 (t, J = 4.4 Hz, 1H), 7.05–7.15 (m, 3H). **^{13}C NMR** (100.5 MHz, $CDCl_3$): δ 29.12, 43.83, 48.25, 125.61, 125.89, 126.12, 129.23, 134.71, 135.92.

1,2,3,4-Tetrahydroquinoxaline (1z)

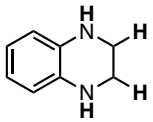

[4 mol% Ir, 130 °C, 20 h, 40 atm H_2] The product **1z** (24.7 mg, 92% yield) was isolated by silica gel column chromatography with hexane/EtOAc (90:10). Colorless oil. **^{1}H NMR** (400 MHz, $CDCl_3$): δ 3.42 (s, 4H), 3.64 (br, 2H), 6.46–6.52 (m, 2H), 6.55–6.61 (m, 2H). **^{13}C NMR** (100.5 MHz, $CDCl_3$): δ 41.32 (2C), 114.65 (2C), 118.70 (2C), 133.63 (2C).

References

(1) (a) Kaushik, N. K.; Kaushik, N.; Attri, P.; Kumar, N.; Kim, C. H.; Verma, A. K.; Choi, E. H. Biomedical Importance of Indoles. *Molecules* **2013**, *18*, 6620–6662. (b) Vitaku, E.; Smith, D. T.; Njardarson, J. T. Analysis of the Structural Diversity, Substitution Patterns, and Frequency of Nitrogen Heterocycles among U.S. FDA Approved Pharmaceuticals. *J. Med. Chem.* **2014**, *57*, 10257–10274.

(2) (a) Dobereiner, G. E.; Crabtree, R. H. Dehydrogenation as a Substrate-Activating Strategy in Homogeneous Transition-Metal Catalysis. *Chem. Rev*. **2010**, *110*, 681–703. (b) Choi, J.; MacArthur, A. H. R.; Brookhart, M.; Goldman, A. S. Dehydrogenation and Related Reactions Catalyzed by Iridium Pincer Complexes. *Chem. Rev.* **2011**, *111*, 1761–1779.

(3) For the homogeneous catalysis, see: (a) Yamaguchi, R.; Ikeda, C.; Takahashi, Y.; Fujita, K. Homogeneous Catalytic System for Reversible Dehydrogenation-Hydrogenation Reactions of Nitrogen Heterocycles with Reversible Interconversion of Catalytic Species. *J. Am. Chem. Soc.* **2009**, *131*, 8410–8412. (b) Muthaiah, S.; Hong, S. H. Acceptorless and Base-Free Dehydrogenation of Alcohols and Amines using Ruthenium-Hydride Complexes. *Adv. Synth. Catal*. **2012**, *354*, 3045–3053. (c) Wu, J.; Talwar, D.; Johnston, S.; Yan, M.; Xiao, J. Acceptorless Dehydrogenation of Nitrogen Heterocycles with a Versatile Iridium Catalyst. *Angew. Chem., Int. Ed.* **2013**, *52*, 6983–6987. (d) Fujita, K.; Tanaka, Y.; Kobayashi, M.; Yamaguchi, R. Homogeneous Perdehydrogenation and Perhydrogenation of Fused Bicyclic N-Heterocycles Catalyzed by Iridium Complexes Bearing a Functional Bipyridonate Ligand. *J. Am. Chem. Soc.* **2014**, *136*, 4829–4832. (e) Chakraborty, S.; Brennessel, W. W.; Jones, W. D. A Molecular Iron Catalyst for the Acceptorless Dehydrogenation and Hydrogenation of *N*-Heterocycles. *J. Am. Chem. Soc.* **2014**, *136*, 8564–8567. (f) Manas, M. G.; Sharninghausen, L. S.; Lin, E.; Crabtree, R. H. Iridium Catalyzed Reversible

Dehydrogenation–Hydrogenation of Quinoline Derivatives under Mild Conditions. *J. Organomet. Chem*. **2015**, *792*, 184–189. (g) Xu, R.; Chakraborty, S.; Yuan, H.; Jones, W. D. Acceptorless, Reversible Dehydrogenation and Hydrogenation of *N*-Heterocycles with a Cobalt Pincer Catalyst. *ACS Catal.* **2015**, *5*, 6350–6354. (h) Fujita, K.; Wada, T.; Shiraishi, T. Reversible Interconversion between 2,5-Dimethylpyrazine and 2,5-Dimethylpiperazine by Iridium-Catalyzed Hydrogenation/Dehydrogenation for Efficient Hydrogen Storage. *Angew. Chem., Int. Ed.* **2017**, *56*, 10886–10889. (i) Vivancos, Á.; Beller, M.; Albrecht, M. NHC-Based Iridium Catalysts for Hydrogenation and Dehydrogenation of *N*-Heteroarenes in Water under Mild Conditions. *ACS Catal.* **2018**, *8*, 17–21.

(4) For the selected heterogeneous catalysis, see: (a) Mikami, Y.; Ebata, K.; Mitsudome, T.; Mizugaki, T.; Jitsukawa, K.; Kaneda, K. Reversible Dehydrogenation-Hydrogenation of Tetrahydroquinoline-Quinoline Using a Supported Copper Nanoparticle Catalyst. *Heterocycles* **2011**, *2*, 1371–1377. (b) Moromi, S. K.; Siddiki, S. M. A. H.; Kon, K.; Toyao, T.; Shimizu, K. Acceptorless Dehydrogenation of *N*-Heterocycles by Supported Pt Catalysts. *Catal. Today*. **2017**, *281*, 507–511. (c) Deraedt, C.; Ye, R.; Ralston, W. T.; Toste, F. D.; Somorjai, G. A. Dendrimer-Stabilized Metal Nanoparticles as Efficient Catalysts for Reversible Dehydrogenation/Hydrogenation of *N*-Heterocycles. *J. Am. Chem. Soc.* **2017**, *139*, 18084–18092. (d) Jaiswal, G.; Landge, V. G.; Jagadeesan, D.; Balaraman, E. Iron-Based Nanocatalyst for the Acceptorless Dehydrogenation Reactions. *Nat. Commun.* **2017**, *8*, 2147.

(5) (a) Sartbaeva, A.; Kuznersov, V. L.; Wells, S. A.; Edward, P. P. Hydrogen Nexus in a Sustainable Energy Future. *Energy Environ. Sci*. **2008**, *1*, 79–85. (b) Eberle, U.; Felderhoff, M.; Schüth, F. Chemical and Physical Solution for Hydrogen Storage. *Angew. Chem., Int. Ed.* **2009**, *48*, 6608–6630. (c) Armaroli, N.; Balzani, V. The Hydrogen Issue. *ChemSusChem*, **2011**, *4*, 21–36. (d) Preuster, P.; Papp, C.; Wasserscheid, P. Liquid Organic Hydrogen Carriers (LOHCs): Toward a Hydrogen-free Hydrogen Economy. *Acc. Chem. Res.* **2017**, *50*, 74–85.

(6) (a) Kato, S.; Saga, Y.; Kojima, M.; Fuse, H.; Matsunaga, S.; Fukatsu, A.; Kondo, M.; Masaoka, S.; Kanai, M. Hybrid Catalysis Enabling Room-Temperature Hydrogen Gas Release from *N*-Heterocycles and Tetrahydronaphthalenes. *J. Am. Chem. Soc.* **2017**, *139*, 2204–2207. (b) He, K.-H.; Tan, F.-F.; Zhou, C.-Z.; Zhou, G.-J.; Yang, X.-L.; Li, Y. Acceptorless Dehydrogenation of *N*-Heterocycles by Merging Visible Light Photoredox Catalysis and Cobalt Catalysis. *Angew. Chem., Int. Ed.* **2017**, *56*, 3080–3084. For a highlight review, see: (c) Yin, Q.; Oestreich, M. Photocatalysis Enabling Acceptorless Dehydrogenation of Benzofused Saturated Rings at Room Temperature. *Angew. Chem., Int. Ed.* **2017**, *56*, 7716–7718.

(7) Maier, A. F. G.; Tussing, S.; Schneider, T.; Flörke, U.; Qu, Z.-W.; Grimme, S.; Paradies, J. Frustrated Lewis Pair Catalyzed Dehydrogenative Oxidation of Indolines and Other Heterocycles. *Angew. Chem., Int. Ed.* **2016**, *55*, 12219–12223.

(8) (a) Wendlandt, A. E.; Stahl, S. S. Bioinspired Aerobic Oxidation of Secondary Amines and Nitrogen Heterocycles with a Bifunctinal Quinone Catalyst. *J. Am. Chem. Soc.* **2014**, *136*, 506–512. (b) Wendlandt, A. E.; Stahl, S. S. Modular *o*-Quinone Catalyst System for Dehydrogenation of Tetrahydroquinolines under Ambient Conditions. *J. Am. Chem. Soc.* **2014**, *136*, 11910−11913. (c) Wendlandt, A. E.; Stahl, S. S. Quinone-Catalyzed Selective Oxidation of Organic Molecules. *Angew. Chem., Int. Ed.* **2015**, *54*, 14638−14658. (d) Li, B.; Wendlandt, A. E.; Stahl, S. S. Replacement of Stoichiometric DDQ with a Low Potential *o*-Quinone Catalyst Enabling Aerobic Dehydrogenation of Tertiary Indolines in Pharmaceutical Intermediates. *Org. Lett.* **2019**, *21*, 1176–1181.

(9) (a) Iwai, T.; Harada, T.; Shimada, H.; Asano, K.; Sawamura, M. A Polystyrene-Cross-Linking Bisphosphine: Controlled Metal Monochelation and Ligand-Enabled First-Row Transition Metal Catalysis. *ACS Catal*. **2017**, *7*, 1681–1692. (b) Yamazaki, Y.; Arima, N.; Iwai, T.; Sawamura, M. Heterogeneous Nickel-Catalyzed Cross-Coupling between Aryl Chlorides and Alkyllithiums Using a Polystyrene-Cross-Linking Bisphosphine Ligand. *Adv. Synth. Catal.* **2019**, *361*, 2250–2254. (c) Nishizawa, A.; Takahira, T.; Yasui, K.; Fujimoto, H.; Iwai, T.; Sawamura, M.; Chatani, N.; Tobisu, M. Nickel-Catalyzed Decarboxylation of Aryl Carbamates for Converting Phenols into Aromatic Amines. *J. Am. Chem. Soc.* **2019**, *141*, 7261–7265.

(10) (a) Ling, L.; Cao, J.; Hu, J.; Zhang, H. Copper-Catalyzed *N*-Alkylation of Indoles by *N*-Tosylhydrazones. *RSC Adv.* **2017**, *7*, 27974–27980. (b) Merschaert, A.; Boquel, P.; Van Hoeck, J.-P.; Gorissen, H.; Borghese, A.; Bonnier, B.; Mockel, A.; Napora, F. Novel Approaches towards the LTD_4/E_4 Antagonist, LY290154. *Org. Process Res. Dev.* **2006**, *10*, 776–783. (c) Singh, P.; Verma, P.; Yadav, B.; Komath, S. S. Synthesis and Evaluation of Indole-Based New Scaffolds for Antimicrobial Activities-Identification of Promising Candidates. *Bioorg. Med. Chem. Lett*. **2011**, *21*, 3367–3372.

(11) Aubry, C.; Wilson, A. J.; Emmerson, D.; Murphy, E.; Chan, Y. Y.; Dickens, M. P.; García, M. D.; Jenkins, P. R.; Mahale, S.; Chaudhuri, B. Fascaplysin-Inspired Diindolyls as Selective Inhibitors of CDK4/Cyclin D1. *Bioorg. Med. Chem.* **2009**, *17*, 6073–6084.

(12) Wang, M.; Xu, L.; Gao, M.; Miller, K. D.; Sledge, G. W.; Zheng, Q.-H. [^{11}C]Enzastaurin, The First Design and Radiosynthesis of a New Potential PET Agent for Imaging of Protein Kinase C. *Bioorg. Med. Chem. Lett*. **2011**, *21*, 1649–1653.

(13) (a) Li, H.; Jiang, J.; Lu, G.; Huang, F.; Wang, Z.-X. On the “Reverse Gear” Mechanism of the Reversible Dehydrogenation/Hydrogeantion of a Nitrogen Heterocycle Catalyzed by a Cp*Ir Complex: A Computational Study. *Organometallics* **2011**, *30*, 3131–3141. (b) Fujita, K. Development and Application of New Iridium Catalysts for Efficient Dehydrogenation Reactions of Organic Molecules. *Bull. Chem. Soc. Jpn.* **2019**, *92*, 344–351.

(14) Selected examples of direct transformations of *N*-adjacent C(sp^3)–H bonds. For Rh or Ir catalysis, see: (a) Chatani, N.; Asaumi, T.; Ikeda, T.; Yorimitsu, S.; Ishii, Y.; Kakiuchi, F.; Murai, S. Carbonylation at sp^3 C−H Bonds Adjacent to a Nitrogen Atom in Alkylamines Catalyzed by Rhodium Complexes. *J. Am. Chem. Soc.* **2000**, *122*, 12882–12883. (b) Sakaguchi, S.; Kubo, T.; Ishii, Y. A Three-Component Coupling Reaction of Aldehydes, Amines, and Alkynes. *Angew. Chem., Int. Ed.* **2001**, *40*, 2534–2536. (c) DeBoef, B.; Pastine, S. J.; Sames, D. Cross-Coupling of sp^3 C−H Bonds and Alkenes: Catalytic Cyclization of Alkene−Amide Substrates. *J. Am. Chem. Soc.* **2004**, *126*, 6556–6557. (d) Tsuchikama, K.; Kasagawa, M.; Endo, K.; Shibata, T. Cationic Ir(I)-Catalyzed sp^3 C–H Bond Alkenylation of Amides with Alkynes. *Org. Lett.* **2009**, *11*, 1821–1823. (e) Pan, S.; Endo, K.; Shibata, T. Ir(I)-Catalyzed Enantioselective Secondary sp^3 C–H Bond Activation of 2-(Alkylamino)pyridines with Alkenes. *Org. Lett.* **2011**, *13*, 4692–4695. (f) Kawamorita, S.; Miyazaki, T.; Iwai, T; Sawamura, M. Rh-Catalyzed Borylation of *N*-Adjacent C(sp^3)–H Bonds with a Silica-Supported Triarylphosphine Ligand. *J. Am. Chem. Soc.* **2012**, *134*, 12924–12927. (g) Lahm, G.; Opatz, T. Unique Regioselectivity in the C(sp^3)–H α-Alkylation of Amines: The Benzoxazole Moiety as a Removable Directing Group. *Org. Lett.* **2014**, *16*, 4201–4203. (h) Tahara, Y.; Michino, M.; Ito, M.; Kanyiva, K. S.; Shibata, T. Enantioselective sp^3 C–H Alkylation of t-Butyrolactam by a Chiral Ir(I) Catalyst for the Synthesis of 4-Substituted Amino Acids. *Chem. Commun.* **2015**, *51*, 16660–16663. (i) Tran, A. T.; Yu, J.-Q. Practical Alkoxythiocarbonyl Auxiliaries for Iridium(I)-Catalyzed C–H Alkylation of Azacycles. *Angew. Chem., Int. Ed.* **2017**, *56*, 10530–10534. (j) Torigoe, T.; Ohmura, T.; Suginome, M. Asymmetric Cycloisomerization of *o*-Alkenyl-*N*-Methylanilines to Indolines by Iridium-Catalyzed C(sp^3)–H Addition to Carbon–Carbon Double Bonds. *Angew. Chem., Int. Ed.* **2017**, *56*, 14272–14276. (k) Reyes, R. L.; Sato, M.; Iwai, T.; Sawamura, M. Asymmetric Synthesis of α-Aminoboronates via Rhodium-Catalyzed Enantioselective C(sp^3)–H Borylation. *J. Am. Chem. Soc.* **2020**, *142*, 589–597. For Ru catalysis, see: (l) Chatani, N.; Asaumi, T.; Yorimitsu, S.; Ikeda, T.; Kakiuchi, F.; Murai, S. $Ru_3(CO)_{12}$-Catalyzed Coupling Reaction of sp^3 C–H Bonds Adjacent to a Nitrogen Atom in Alkylamines with Alkenes. *J. Am. Chem. Soc.* **2001**, *123*, 10935–10941. (m) Schinkel, M.; Wang, L.; Bielefeld, K.; Ackermann, L. Ruthenium(II)-Catalyzed C(sp^3)–H α-Alkylation of Pyrrolidines. *Org. Lett.* **2014**, *16*, 1876–1879. For Pd catalysis, see: (n) Jain, P.; Verma, P.; Xia, G.; Yu, J.-Q. Enantioselective Amine α-Functionalization via Palladium-catalysed C–H Arylation of Thioamides. *Nat. Chem.* **2017**, *9*, 140–144 and references cited therein.

(15) For a related review on the direct transformation of *N*-adjacent C(sp^3)–H bonds in heterocycles, see: Campos, K. R. Direct sp^3 C–H bond Activation Adjacent to Nitrogen in Heterocycles. *Chem. Soc. Rev.* **2007**, *36*, 1069–1084.

(16) For a related paper from our group on bisphosphine-iridium(III) dihydride species, which was utilized in transfer hydrogenation of alkenes with 1,4-dioxane as hydrogen donor: see: Zhang, D.; Iwai, T.; Sawamura, M. Iridium-Catalyzed Alkene-Selective Transfer Hydrogenation with 1,4-Dioxane as Hydrogen Donor. *Org. Lett.* **2019**, *21*, 5867–5872.
(17) Tani, K.; Iseki, A.; Yamagata, T. Efficient Transfer Hydrogenation of Alkynes and Alkenes with Methanol Catalysed by Hydrido(methoxo)iridium(III) Complexes. *Chem. Commun.* **1999**, 1821–1882.
(18) Walter, R.; Kirchner, S.; Franz, R. Method for Producing $[IrCl(cod)]_2$. U.S. Patent 6,399,804, 2002. *Chem. Commun.* **1999**, 1821–1882.
(19) Kojima, M.; Kanai, M. Tris(pentafluorophenyl)borane-Catalyzed Acceptorless Dehydrogenation of *N*-Heterocycles. *Angew. Chem., Int. Ed.* **2016**, *55*, 12224–12227.
(20) Maier, A. F. G.; Tussing, S.; Schneider, T.; Flörke, U.; Qu, Z.-W.; Grimme, S.; Paradies, J. Frustrated Lewis Pair Catalyzed Dehydrogenative Oxidation of Indolines and Other Heterocycles. *Angew. Chem., Int. Ed.* **2016**, *55*, 12219–12223.
(21) Jiang, X.; Wang, C.; Wei, Y.; Xue, D.; Liu, Z.; Xiao, J. A General Mehod for N-Methylation of Amines and Nitro Compounds with Dimethylsulfoxide. *Chem. Eur. J.* **2014**, *20*, 58–63.
(22) Gui, J.; Xie, H.; Jiang, H.; Zeng, W. Visible-Light-Mediated Sulfonylimination of Tertiary Amines with Sulfonylazides Involving C_{sp3}–C_{sp3} Bond Cleavage. *Org. Lett.* **2019**, *21*, 2804–2807.
(23) Wechsler, D.; Davis, B.; Jessop, P. G. The Dehydrogenation of Combined Organic and Inorganic Hydrogen-Storage Carriers. *Can. J. Chem.* **2010**, *88*, 548 555.
(26) Tomaszewski, M, J.; Warkentin, J.; Werstiuk, N. H. Free-Radical Chemistry of Imines. *Aust. J. Chem*. **1995**, *48*, 291–321.

(27) Jia, W.-L.; Westerveld, N.; Wong, K. M.; Morsch, T.; Hakkennes, M.; Naksomboon, K.; Fernández-Ibáñez, M. Á. Selective C–H Olefination of Indolines (C5) and Tetrahydroquinolines (C6) by Pd/S, O-Ligand Catalysis. *Org. Lett.* **2019**, *21*, 9339–9342.
(28) Sato, S.; Sakamoto, T.; Miyazawa, E.; Kikugawa, Y. One-Pot Reductive Amination of Aldehydes and Ketones with α-Picoline-Borane in Methanol, in Water, and in Neat Conditions. *Tetrahedron* **2004**, *60*, 7899–7906.
(29) Joe, C. L.; Doyle, A. G. Direct Acylation of $C(sp^3)$–H Bonds Enabled by Nickel and Photoredox Catalysis. *Angew. Chem., Int. Ed.* **2016**, *55*, 4040–4043.
(30) Ortgies, S.; Breder, A. Selenium-Catalyzed Oxidative $C(sp^2)$–H Amination of Alkenes Exemplified in the Expedient Synthesis of (Aza-)Indoles. *Org. Lett.* **2015**, *17*,2748–2751.
(31) Li, J.-J.; Mei, T.-S.; Yu, J.-Q. Synthesis of Indolines and Tetrahydroisoquinolines

from Arylethylamines by Pd^{II}-Catalyzed C–H Activation Reactions. *Angew. Chem., Int. Ed.* **2008**, *47*, 6452–6455.

(32)Ertugrul, B.; Kilic, H.; Lafzi, F.; Saracoglu, N. Access to C5-Alkylated Indolines/Indoles via Michael-Type Friedel-Crafts Alkylation Using Aryl-Nitroolefins. *J. Org. Chem.* **2018**, *83*, 9018–9038.

(33)Yang, J.; Zhou, S.; Ji, Li.; Zhang, C.; Yu, S.; Li, Z.; Meng, X. Synthesis and Structure-Activity Relationship of 4-Azaheterocycle Benzenesulfonamide Derivatives as New Microtubule-Targeting Agents. *Bioorg. Med. Chem. Lett*. **2014**, *24*, 5055–5058.

(34)Zhu, C.; Akiyama, T. Benzothiazoline: Highly Efficient Reducing Agent for the Enantioselective Organocatalytic Transfer Hydrogenation of Ketimines. *Org. Lett.* **2009**, *11*, 4180–4183.

(35) Aubry, C.; Wilson, A. J.; Emmerson, D.; Murphy, E.; Chan, Y. Y.; Dickens, M. P.; García, M. D.; Jenkins, P. R.; Mahale, S.; Chaudhuri, B. Fascaplysin-Inspired Diindolyls as Selective Inhibitors of CDK4/Cyclin D1. *Bioorg. Med. Chem.* **2009**, *17*, 6073–6084.

(35)Wang, M.; Xu, L.; Gao, M.; Miller, K. D.; Sledge, G. W.; Zheng, Q.-H. [^{11}C]Enzastaurin, The First Design and Radiosynthesis of a New Potential PET Agent for Imaging of Protein Kinase C. *Bioorg. Med. Chem. Lett*. **2011**, *21*, 1649–1653.

Publication List

1. *"Ir-Catalyzed Reversible Acceptorless Dehydrogenation/Hydrogenation of N-Substituted and Unsubstituted Heterocycles Enabled by a Polymer-Cross-Linking Bisphosphine"*

   Zhang, D.; Iwai, T.;* Sawamura, M.* *Org. Lett*. **2020***, 22,* 5240.

2. *"Iridium-Catalyzed Alkene-Selective Transfer Hydrogenation with 1,4-Dioxane as Hydrogen Donor"*

   Zhang, D.; Iwai, T.;* Sawamura, M.* *Org. Lett.* **2019**, *21*, 5867.

Acknowledgement

The studies described in this thesis have been carried out under the direction of Professor Masaya Sawamura at Department of Chemistry, Faculty of Science and Institute for Chemical Reaction Design and Discovery (WPI-ICReDD) from October 2015 to March 2021.

The author wishes to express his grateful acknowledgement to Professor Masaya Sawamura for giving opportunities to study in his laboratory and for his kind guidance, constant encouragement, and valuable discussion. The training in this lab will inspired the author to explore the realm of catalyst design in the future. He is deeply grateful to Lecturer Tomohiro Iwai for his practical guidance, helpful discussions and considerable suggestions. He would also like to express his appreciation to Professor Hirohisa Ohmiya, Associate Professor Yohei Shimizu, Assistant Professor Ronald Lazo Reyes, Assistant Professor Fernand Arteage Arteaga, Assistant Professor Kosuke Higashida for their kind discussion, advices and supports. He also expresses his thanks to all the members of Sawamura group for their kind discussions.

The kind suggestions from Professor Kenji Tanino, Prof. Hajime Ito, Professor Takanori Suzuki and Associate Professor Atsushi Minami helped the author upgrade the thesis.

Financial support from JSPS, Research Fellowship of Japan Society for the Promotion of Science for Young Scientists, was indispensable, and author deeply appreciates this support.

Finally, he would like to express his gratitude for his family for warm encouragement and continuous assistance.

Deliang Zhang
Graduate School of Chemical Sciences and Engineering